The MPI Semiconductor Laboratory

within the MPG Advanced Study Group (ASG)
within the Center of Free Electron Laser Science

Tracking and Imaging Detectors

in Heaven and on Earth

Prepared by

1. MPI-HLL (MPE and MPP)
   Lothar Strüder, Rainer Richter, Matteo Porro, Florian Schopper, Gabi Schächner, Danilo Miessner, Martina Schnecke, Thomas Lauf, Gerhard Schaller, Norbert Meidinger, Sven Herrmann, Laci Andricek, Gerhard Fuchs, Johannes Treis, Nils Kimmel, Robert Andritschke, Zdenka Albrechtskirchinger, Valentin Fedl, Giulio de Vita, Georg Weidenspointner, Andreas Wassatsch, Hans-Günther Moser, Admir Ramic, Gerhard Fuchs
   Daniel Pietschner, Johannes Elbs, Olaf Hälker, Toboas Panzner, Stefanie Ebermayer, Sebastian Hasinger, Florian Aschauer, Alexander Bähr

2. PNSensor and PNDetector
   Heike Soltau, Robert Hartmann, Peter Lechner, Peter Holl, Atakan Simsek Rouven Eckhart, Adrian Niculae, Klaus Heinzinger, Bianca Schweinfest, Andreas Liebel, Alois Bechtele, Uwe Weichert, Olga Jaritschin, Udo Weber Gerhard Lutz, Sebastian Ihle, Markus Lang, Dieter Schlosser Christian Reich, Christian Thamm, Kathrin Hermenau, Markus Kufner Adrian Niculae, Christian Sandow, Laure Mungenast, Barbara Titze, Melanie Schulze, Samantha Jeschke, Theresa Hildebrand, Petra Majewski, Andreas Liebel, Daniela Soffa

University of Leicester, Universität Tübingen, Universität Heidelberg, Universität Nürnberg-Erlangen, Universität Darmstadt, Universität Siegen Politecnico di Milano, DESY Hamburg, FZ Jülich, CEA, INAF, IKI, ESO, ESTEC, Penn State University, MIT, CfA, XFEL

MPI für Kernphysik, Sonnensystemforschung, medizinische Forschung, Quantenoptik, Biochemie, Metallforschung, Plasmaphysik, CFEL

OUTLINE

High speed, monolithic, large format detectors are being - or will be - used from 30 meV to 5 MeV for spectroscopic and intensity imaging of radiation

- SSDs
- SDDs
- pnCCDs
- DEPFET APS
  - gatable DEPFETs
  - RNDR DePFETs
  - BIB DePFETs

Conclusion, Summar

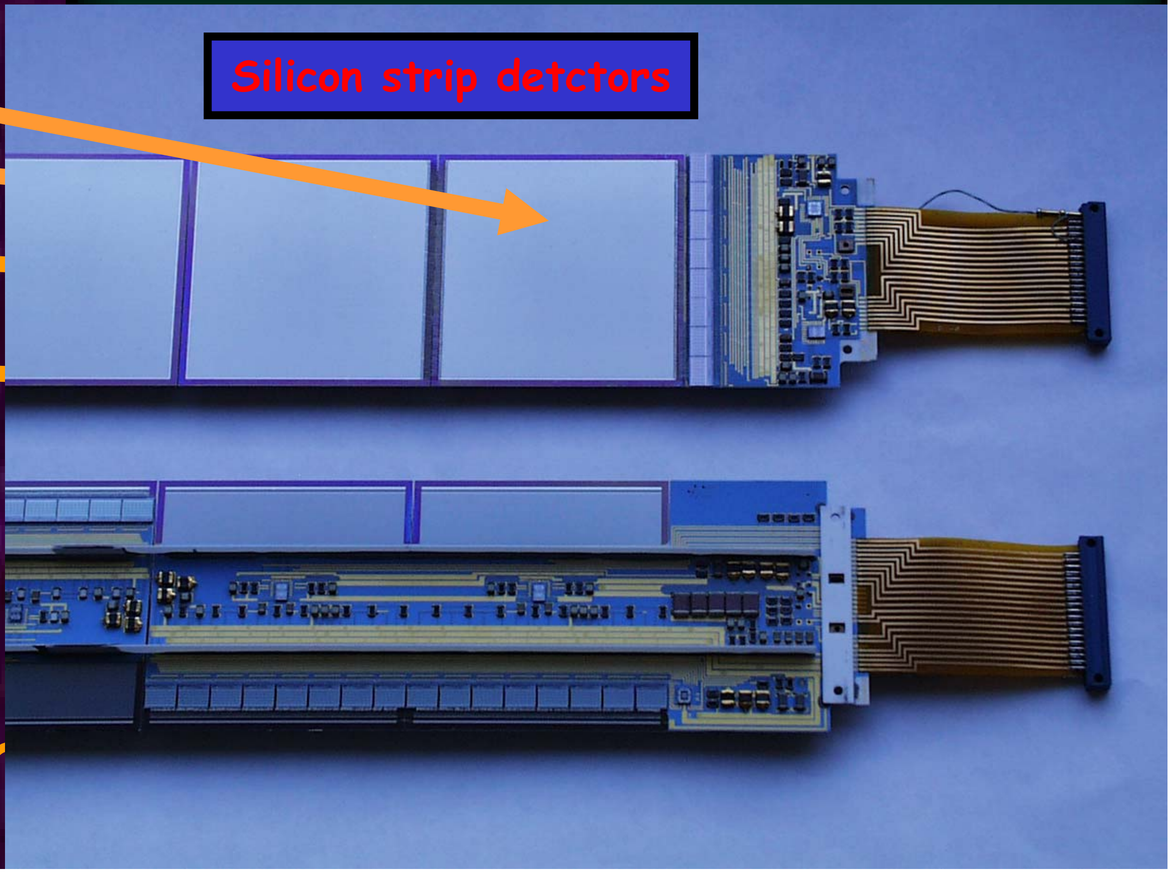

Infrared astronomy
Optical astronomy
X-ray astronomy
Gamma ray astronomy
Planetary science
Adaptive optics

Imaging at synchrotrons and
X-ray Free Electron Lasers
(FLASH, LCLS, SCSS, XFEL)
Solid state research
Beam monitoring

Quality assurance & control
X-ray fluorescence analysis (XRF)
environmental control
art and jewelery analysis
Microbeam analysis (SEM, TEM)
Wavelength dispersive spectroscopy (WDX)

Semiconductors as detector and electronics material

1. **Semiconductors: $E_{Gap} \approx 1 - 2$ eV**
   → small leakage currents
   → low noise, operation @ r.t.

2. **Pair creation energy: w = 2 – 5 eV**
   → large number of signal charges per energy deposit in detector

3. **Density: $\rho = 2 - 5$ g cm^{-3}**
   → high energy loss per unit length
   → low range of δ - electrons

This leads to:

good energy resolution
high spatial resolution
high quantum and detection efficiency
good mechanical regidity and thermal conductivity

Semiconductors equally offer:

fixed space charges
high mobility of charge carriers

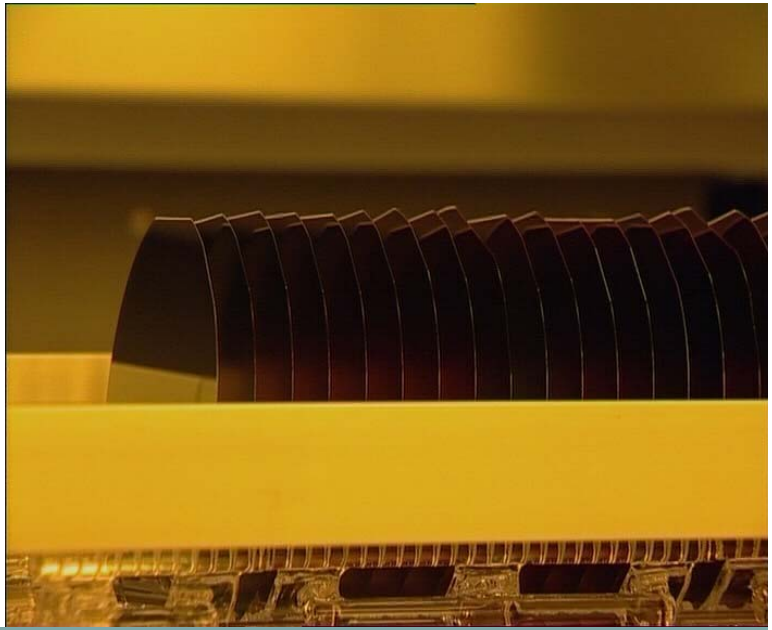

Detector and electronics simulation and layout

1. The detector idea: simulation of electrical properties

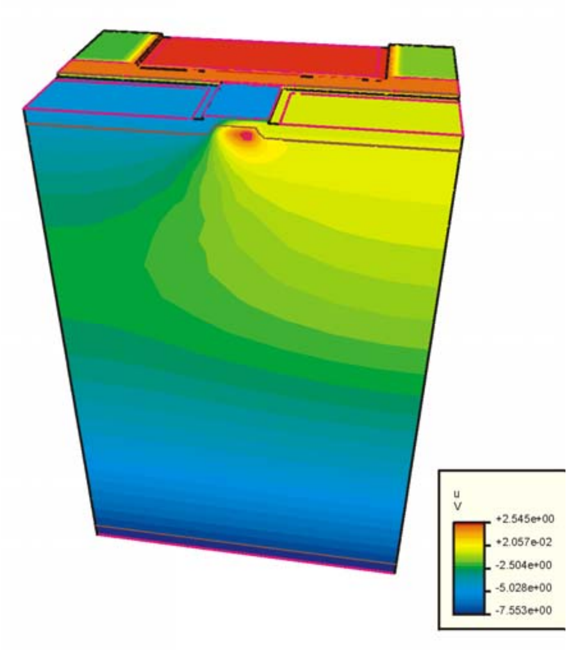

2. Simulation of the production process

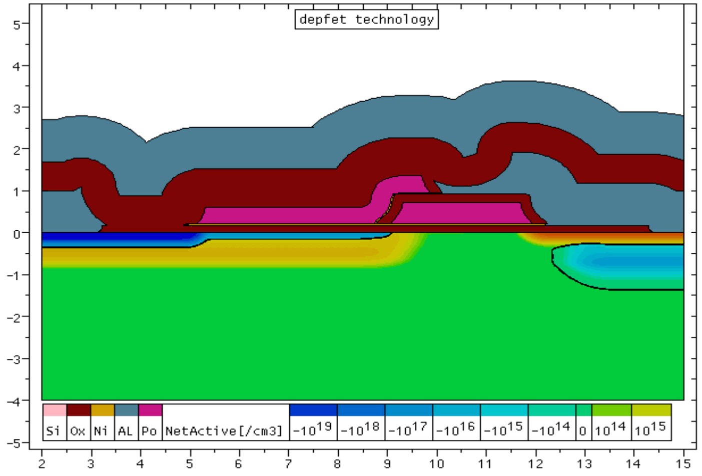

3. Design and layout of the entire detetor system, including signal processing and DAQ

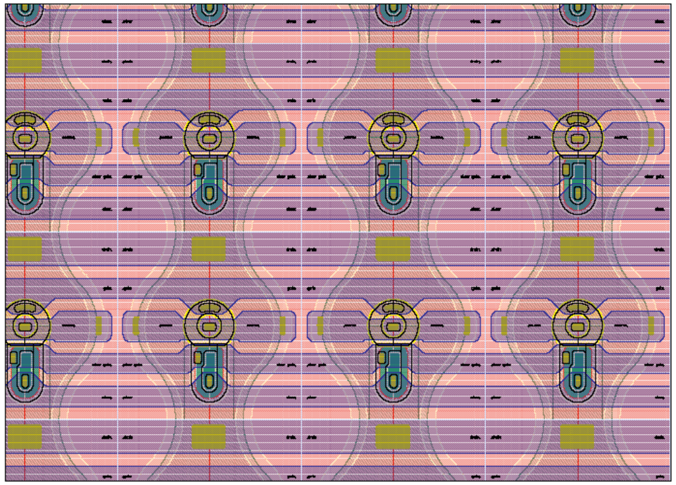

The location

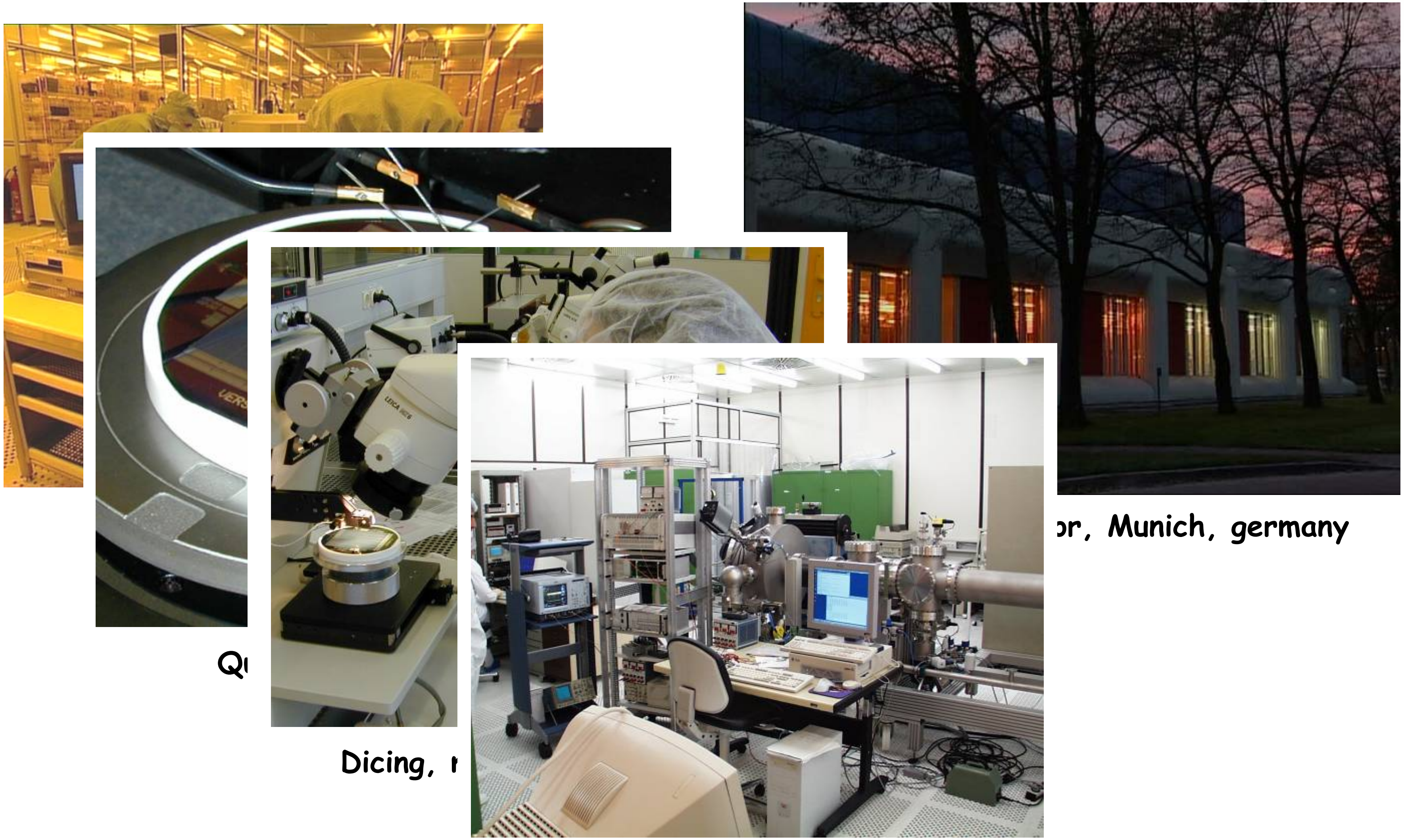

or, Munich, germany

Q

Dicing,

Device tests and operation

Ionization in Silicon

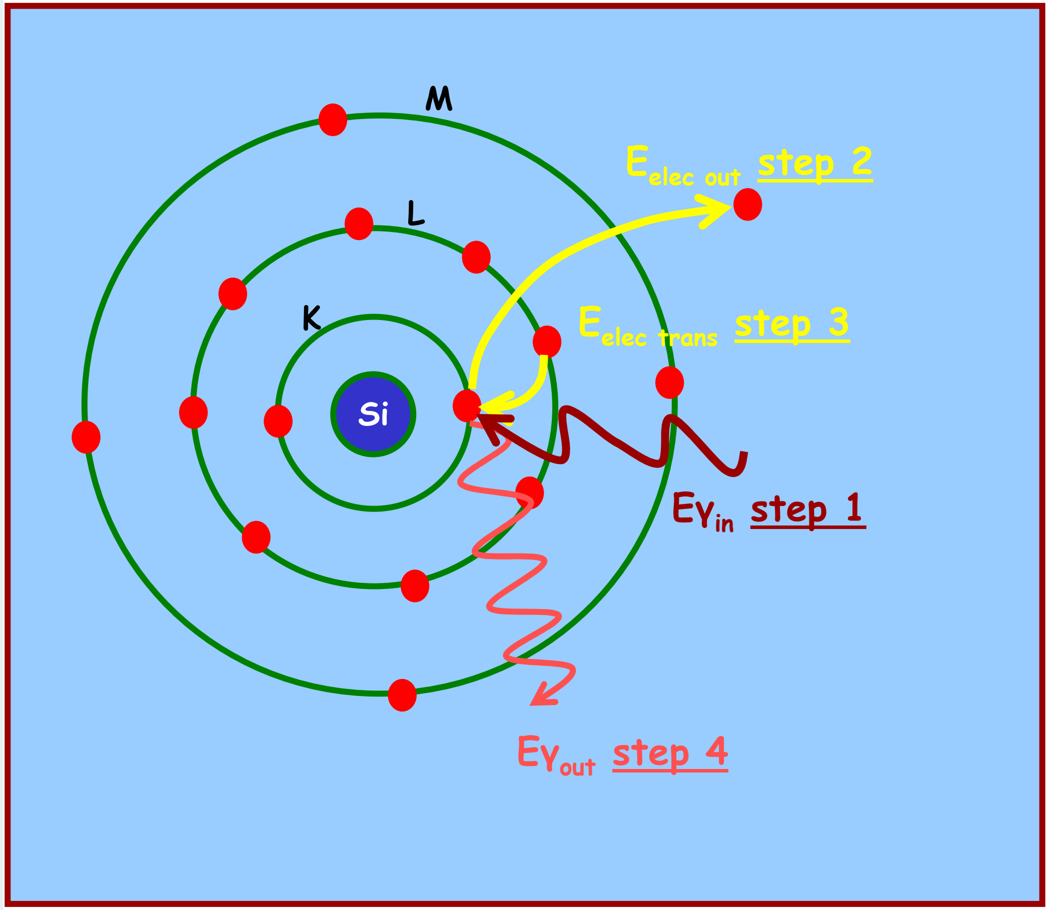

step 1: X-ray hits Si atom with energy $E_{\gamma in}$

step 2: If $E_{\gamma\ in} > E_{K\alpha}$
$E_{elec\ out} = E_{\gamma in} - E_{K\alpha}$

step 3: L shell electron is captured by K shell

step 4: X-ray is emitted with
$E_{\gamma\ out} = E_{K\alpha} - E_{L\alpha}$
$= 1.83\ \text{keV} – 0.1\ \text{keV}$
$= 1.73\ \text{keV}$

step 5: \`radiationless´ Auger process not considered

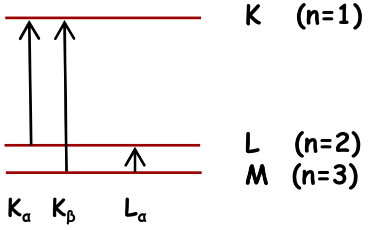

optical photons do M-shell ionization down to the band gap energy $E_G = 1.12$ eV
this results in a high QE up to $\lambda = 1.100$ nm !!!

Radiation detection with silicon detectors

direct detection through V – C ionization	NIR: up to	λ ≤ 1.15 µm
	Optical:	300 nm up to 650 nm
	UV, VUV:	50 nm up to 300 nm
	X-rays:	50 nm down to 0.3 Å
	Gamma rays*	5 keV to 5 MeV
impurity ionization (e.g. BIB detectors)	IR: up to	λ ≤ 50 µm

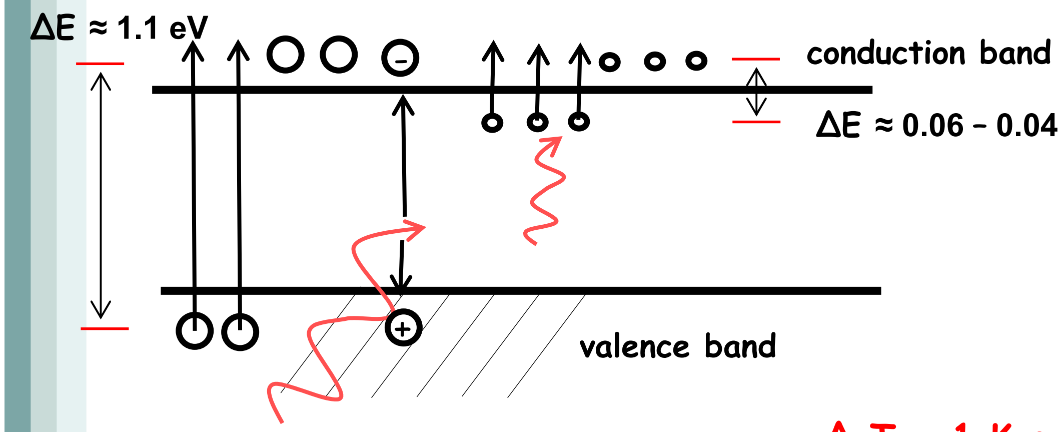

ΔE ≈ 0.06 – 0.04 eV (e.g. : P, As or Sb
[form substitutional donors in Si])

Δ T = 1 K corresponds to an energy kT of E = 86 µeV
@ 7 K E_{th} ≈ 0.6 meV

$$\boxed{\lambda = \frac{hc}{E} = \frac{1.24\mu m}{E(eV)}}$$

➡ for λ ≈ 30 µm E ≈ 42 meV

* through visible light if coupled to a scintillator

Limitations

- energy resolution
  limited by

$$ENC_{el} = \sqrt{\alpha \frac{2kT}{g_m} C_{tot}^2 A_1 \frac{1}{\tau} + 2\pi a_f C_{tot}^2 A_2 + q I_L A_3 \tau}$$

  - electronic noise
    - detector design, integrated electronics
    - cooling
    - fast operation
    - repetitive readout
  - Fano noise, ultimate statistical limit

$$ENC_{fano} = \sqrt{\frac{F \cdot E_X}{w}}$$

  - total noise

$$ENC_{tot}^2 = ENC_{el}^2 + ENC_{fano}^2$$

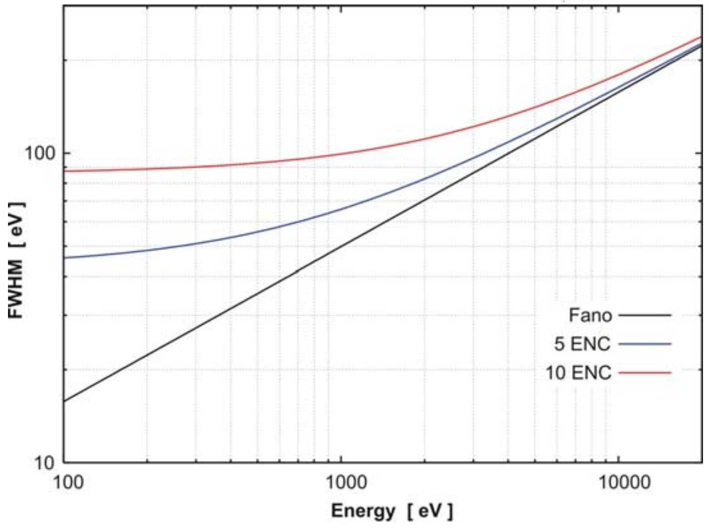

FWHM values (@ 5.9 keV)

- different electronic noise levels
- Fano limit

Limitations

spectral performance

- low energy background, composed of
  - lines (escape, fluorescence)
  - continuum

- continuum caused by signal charge loss
  - detector edge → collimation
  - insensitive regions → layout
  - split events → reconstruction
  - trapping → base material, technology
  - **entrance window dead layer**

    unavoidable insensitive layer: undepleted Si, metal

    ↳ minimize layer thickness

    ↳ terminate surface with 'reflector'

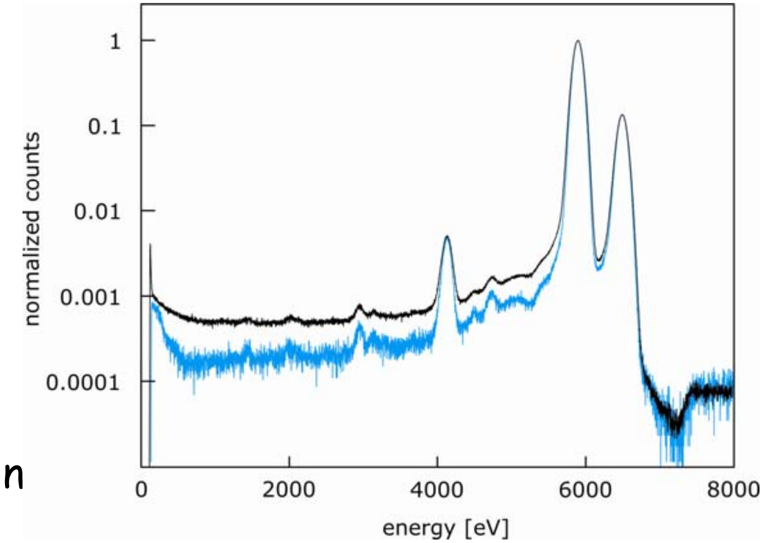

effect of entrance window termination

P/B ≈ 1.500

P/B ≈ 6.000

P/B = peak to background ratio

= amplitude ratio of Mn-Kα line and mean background at 1 ± 0.2 keV

Limitations

time resolution

- required to allocate events in different detector components

  e.g. Compton camera, (anti)coincidence

- limited by
  - drift & diffusion dynamics

    e.g. electron package, 10 nsec drift

    $\sigma_x = (2 \cdot kT/q \cdot \mu \cdot t_{drift})^{\frac{1}{2}} \approx 8\ \mu m$

    $\sigma_t = \sigma_x / v_{drift} \approx 0.2$ nsec

  - signal/noise ratio

- measured:

  self-triggering linear SDD

  using hole signal as start trigger for drift time

  time jitter 1.5 nsec @ 30.000 el. signal

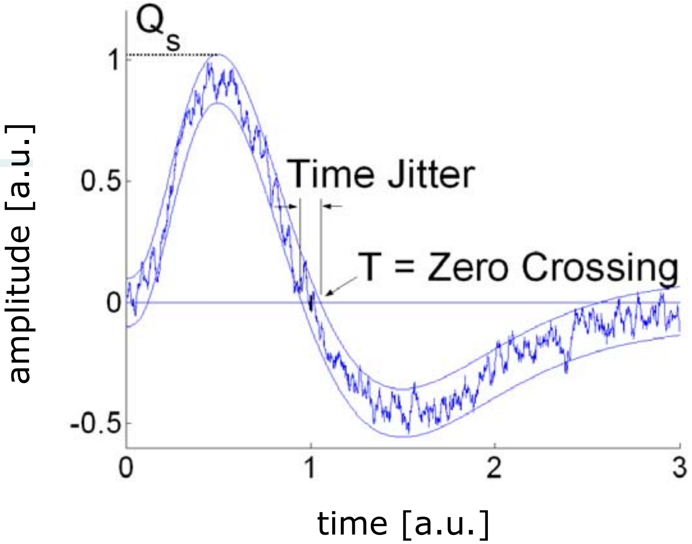

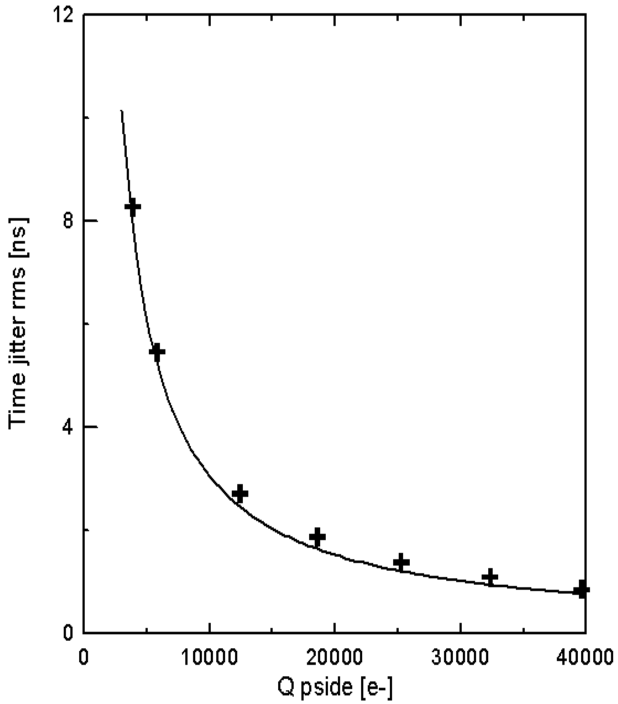

Limitations

♦ position resolution

- depending on specific application
- example

  pixel sensor for X-ray imaging spectroscopy

pixel size	75 μm
el. noise	5 el. r.m.s
signal charge	1.000 el.

  use of multiple pixel hits

  ↳ position resolution « pixel size

  e.g. 0.5 μm r.m.s @ pixel border

  13 μm r.m.s. @ pixel center
- limited by el. noise
- tradeoff

  energy vs. position resolution

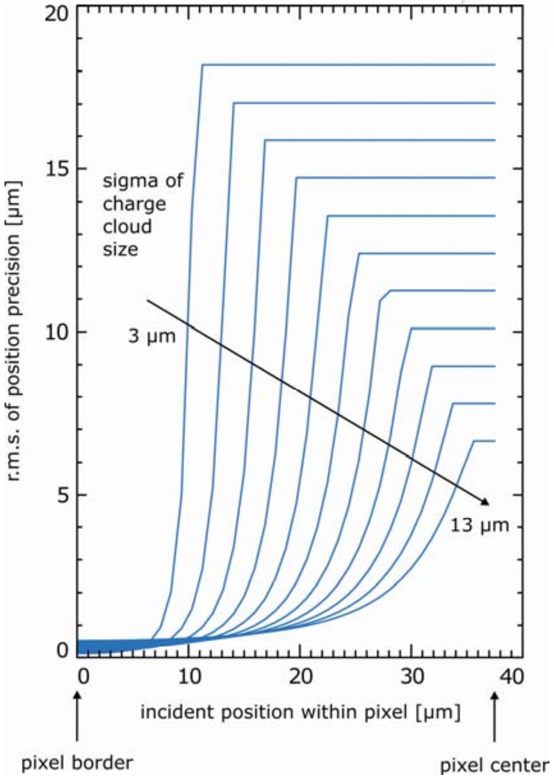

position precision of pixelated detector
1dim model

- pixel size	75 µm
- signal charge	1.000 el.
- el. noise	5 el. r.m.s.

Single photon counting position precision (@ 5 keV)

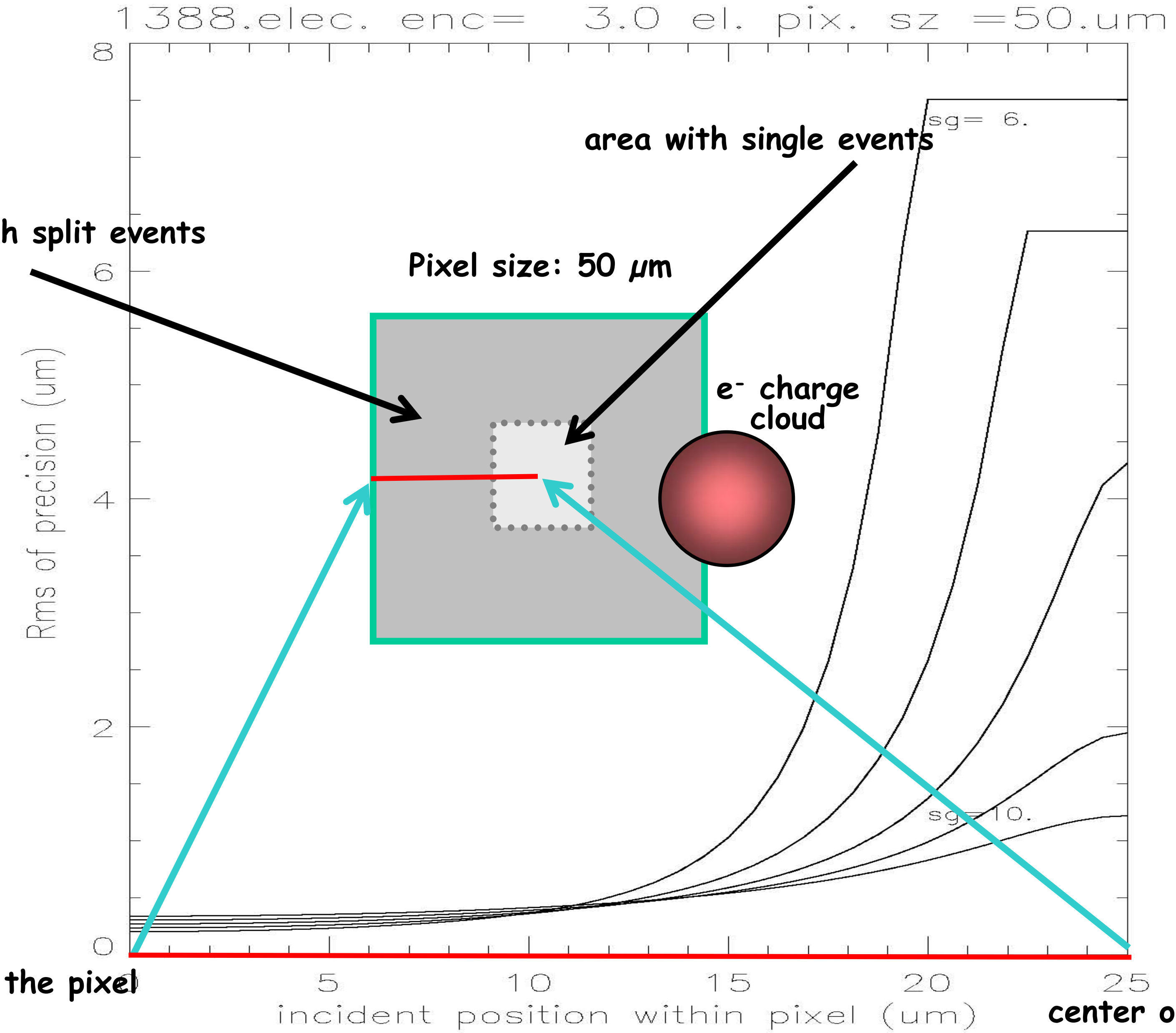

area with single events

area with split events

Pixel size: 50 µm

e⁻ charge cloud

edge of the pixel

center of the pixel

The charge spread function

Injected charge:
4.5 keV, i.e.
1.250 electrons

➡

The charge spread depends on:

- charge collection time
- pixel size
- number of charges
- operating temp.

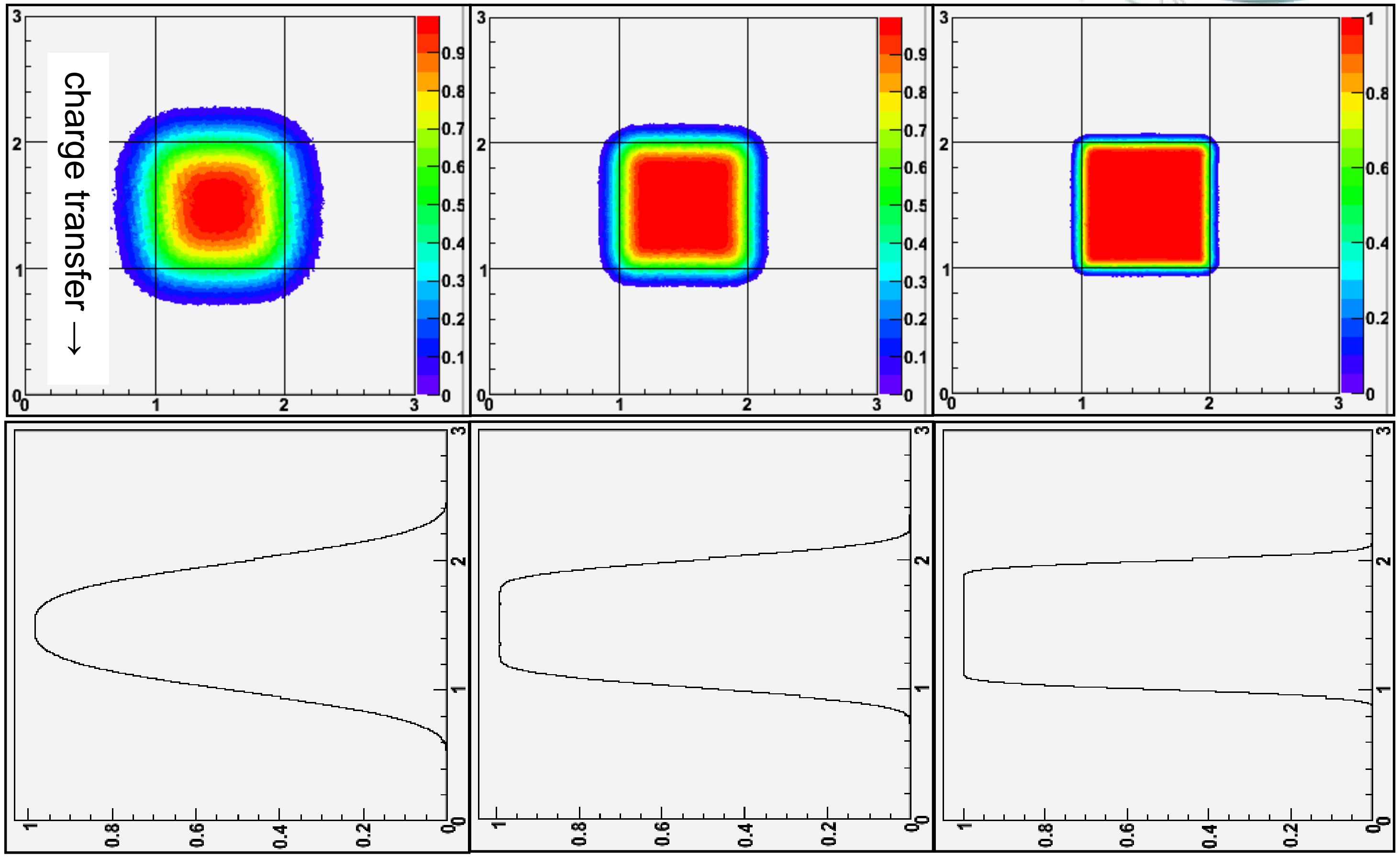

51µm pixel $\sigma_{transfer}$ = 8.5µm   75µm pixel $\sigma_{transfer}$ = 7.0µm   150µm pixel $\sigma_{transfer}$ = 6.4µm

For more than 1.500.000 signal charges a pixel size of less than 150 µm is not adequate

electron dynamics

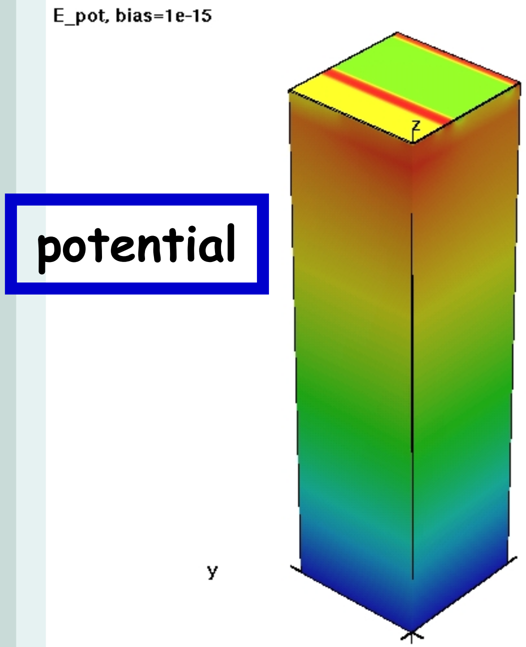

potential

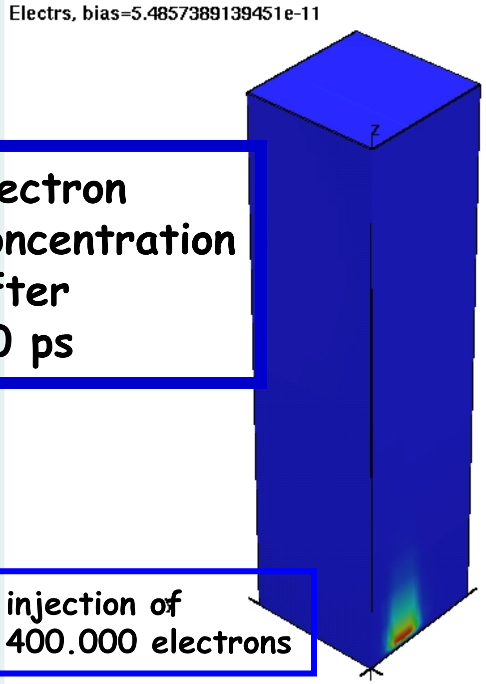

electron concentration after 50 ps

injection of 400.000 electrons

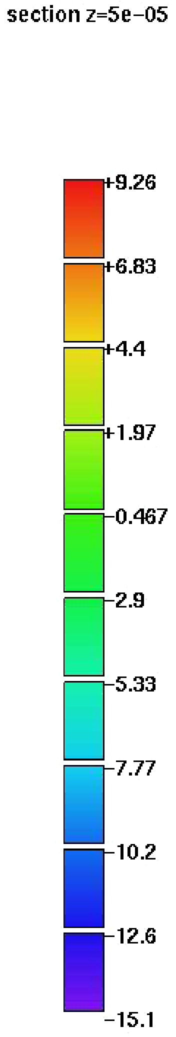

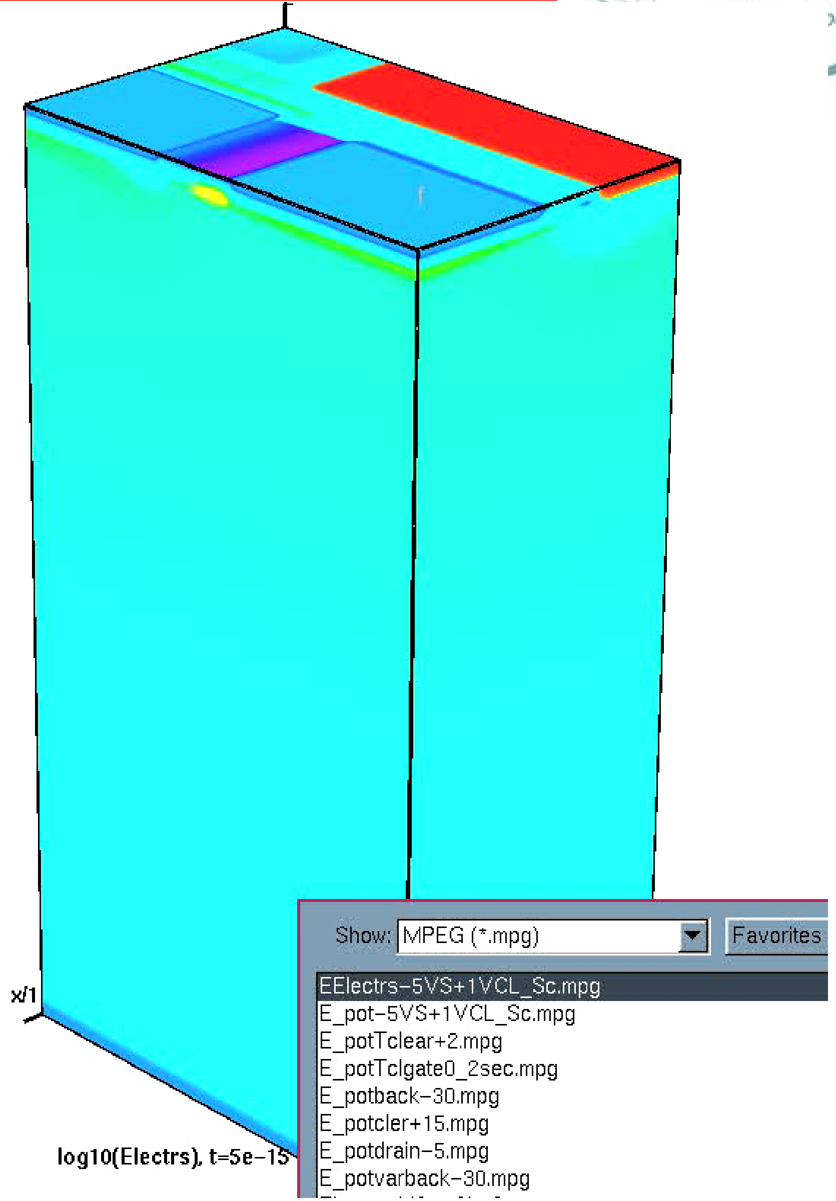

EElectrs-5VS+1VCL_Sc.mpg
E_pot-5VS+1VCL_Sc.mpg
E_potTclear+2.mpg
E_potTclgate0_2sec.mpg
E_potback-30.mpg
E_potcler+15.mpg
E_potdrain-5.mpg
E_potvarback-30.mpg

Limitations

energy range

- m.i. particles no problem
- photons
  Si is 'transparent'
  - at high energies » 10 keV
    absorption ~ Z^5/E^3
  - in the IR
    photon energy < E_{gap}

↳ transmission without interaction

Si is a good absorber
  - in the optical
  - in the UV
  - at X-rays from 100 eV to 15 keV

↳ loss of signal charges in the entrance window dead layer

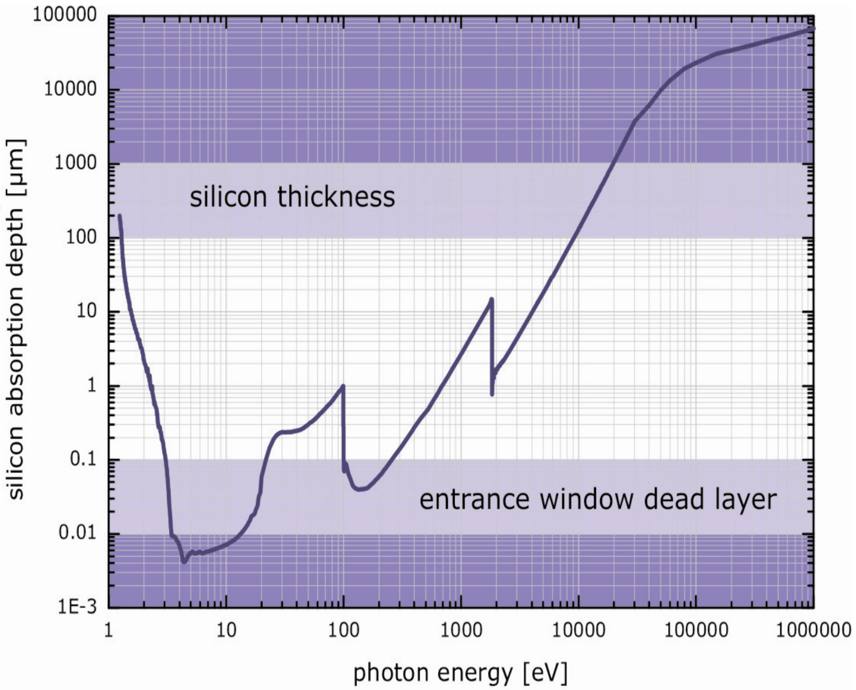

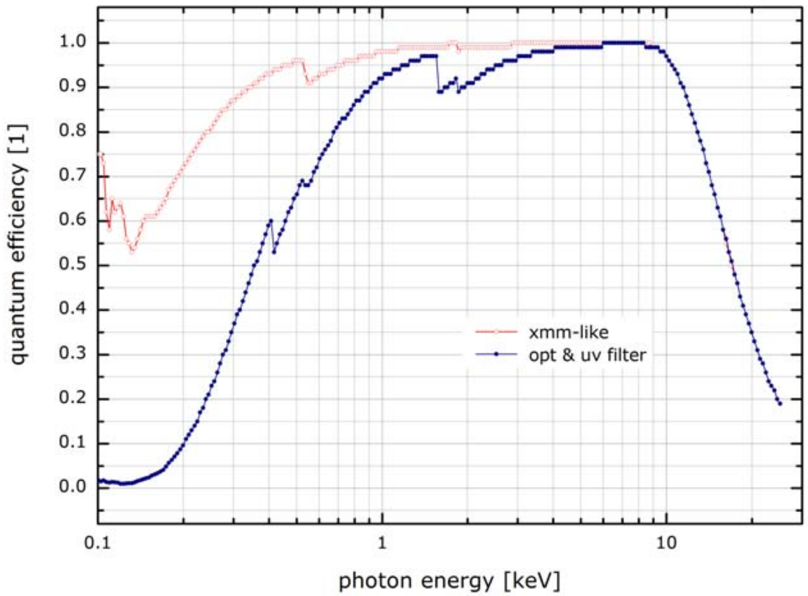

Photon conversion in signal electrons

Internal quantum efficiency

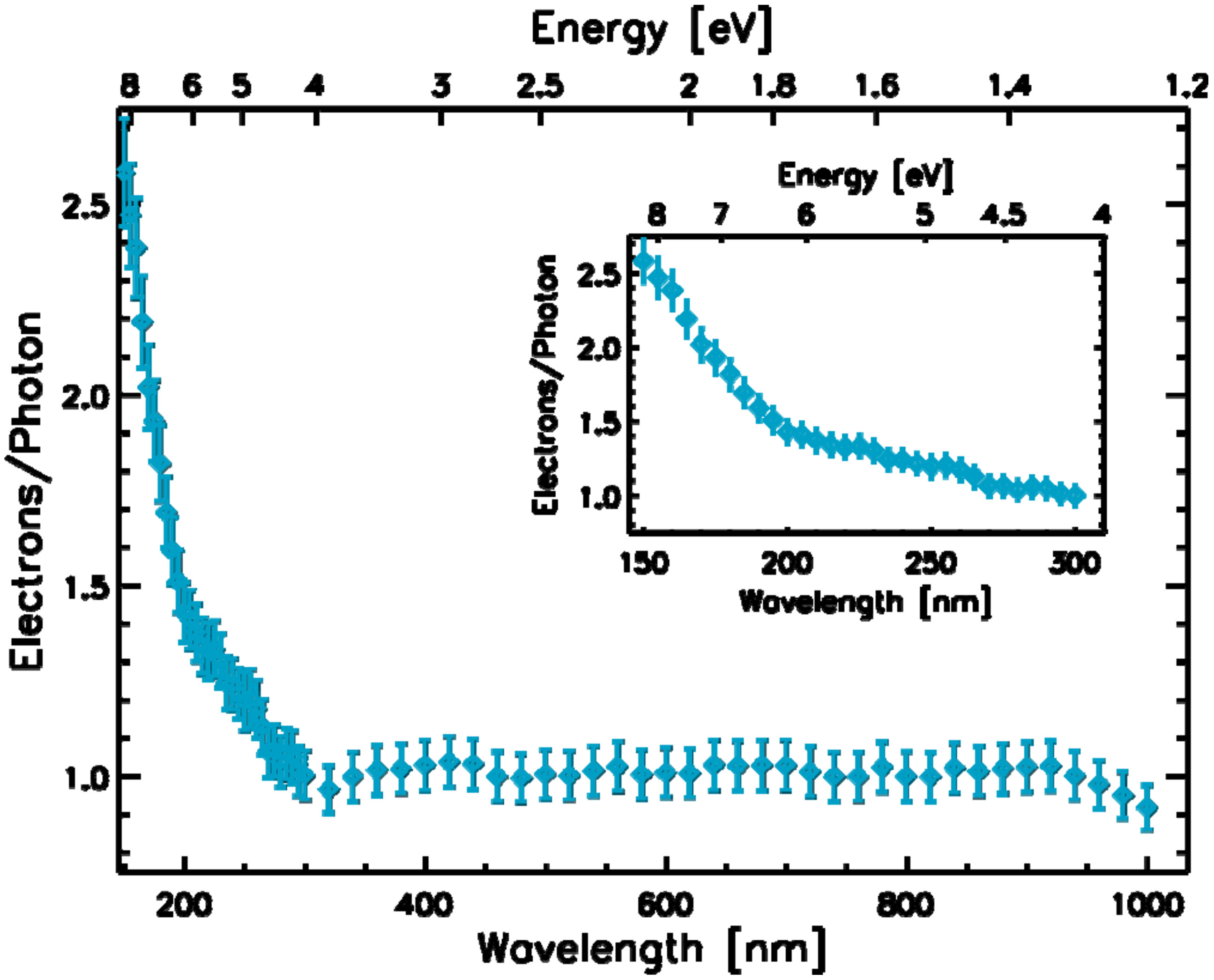

Sensitivity vs. different ARC

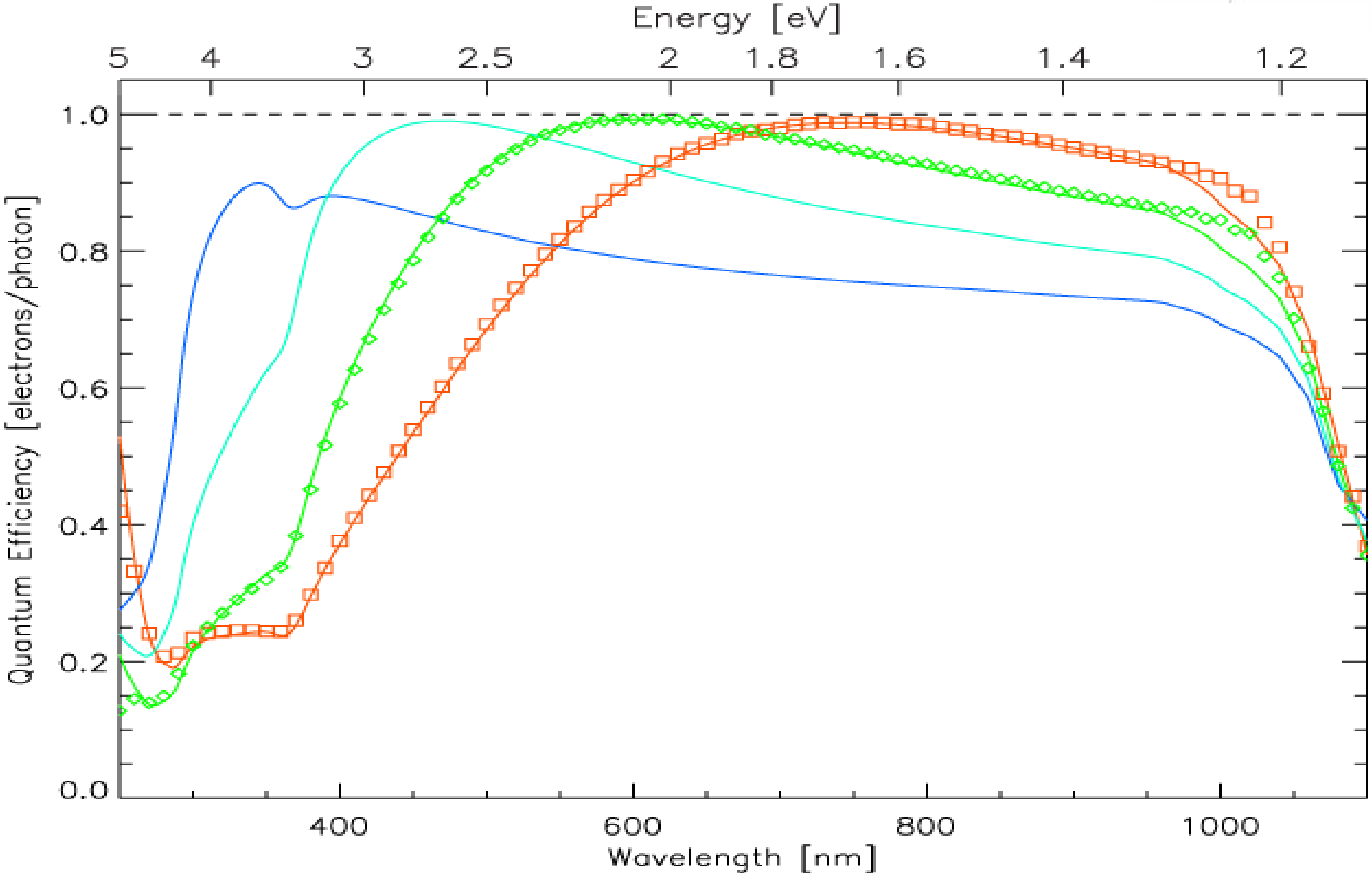

Semiconductor Physics, basics

Tetrahedron bond to closest neighbors, covalent bonds
(Diamond lattice structure)

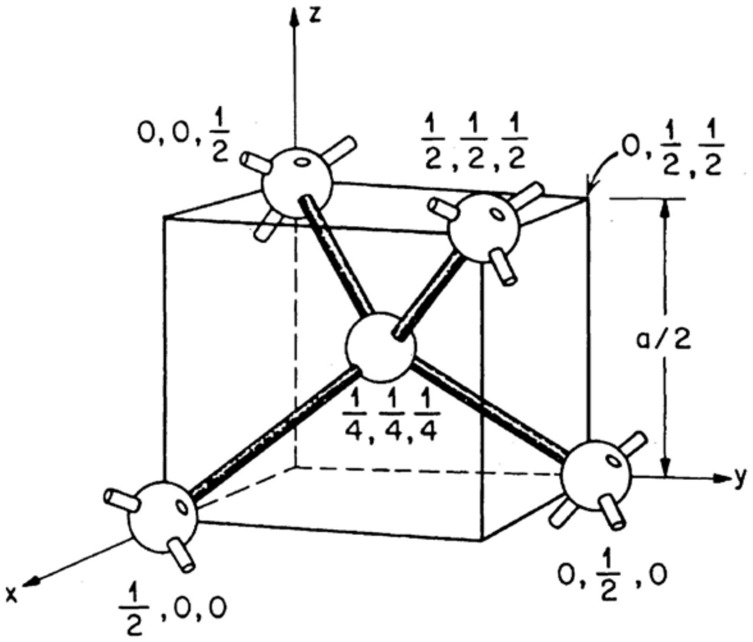

(a)

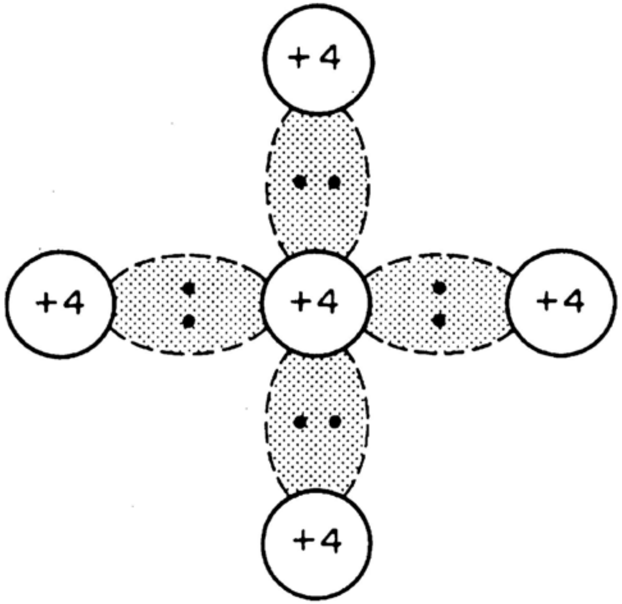

(b)

The silicon lattice

n-type **p-type**

Bond picture

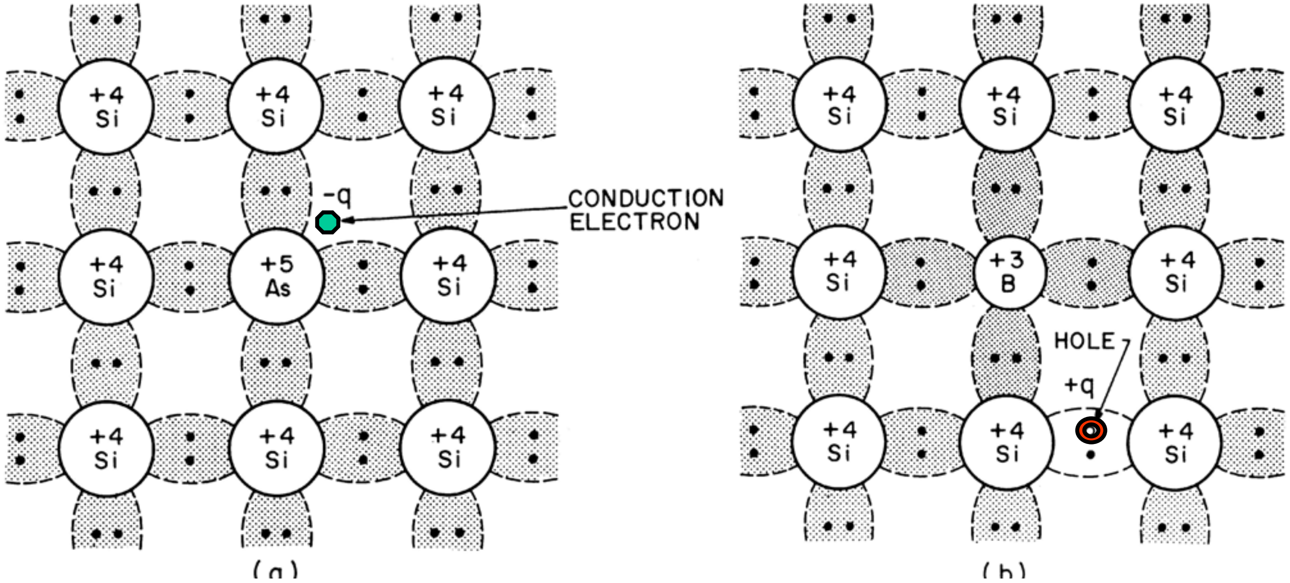

Band representation

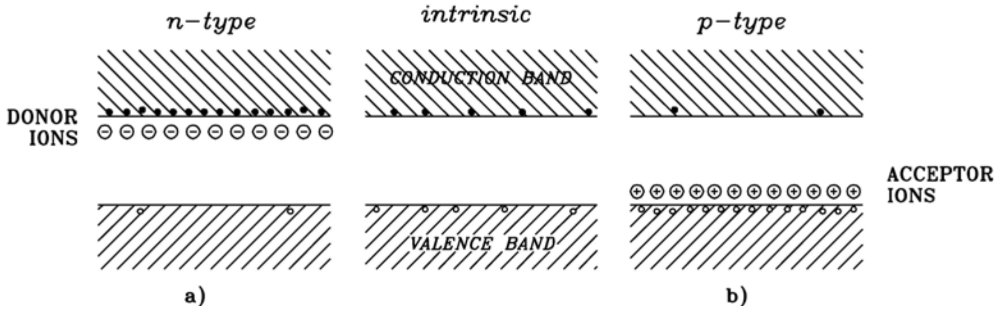

Band structure

indirect and direct semiconductors

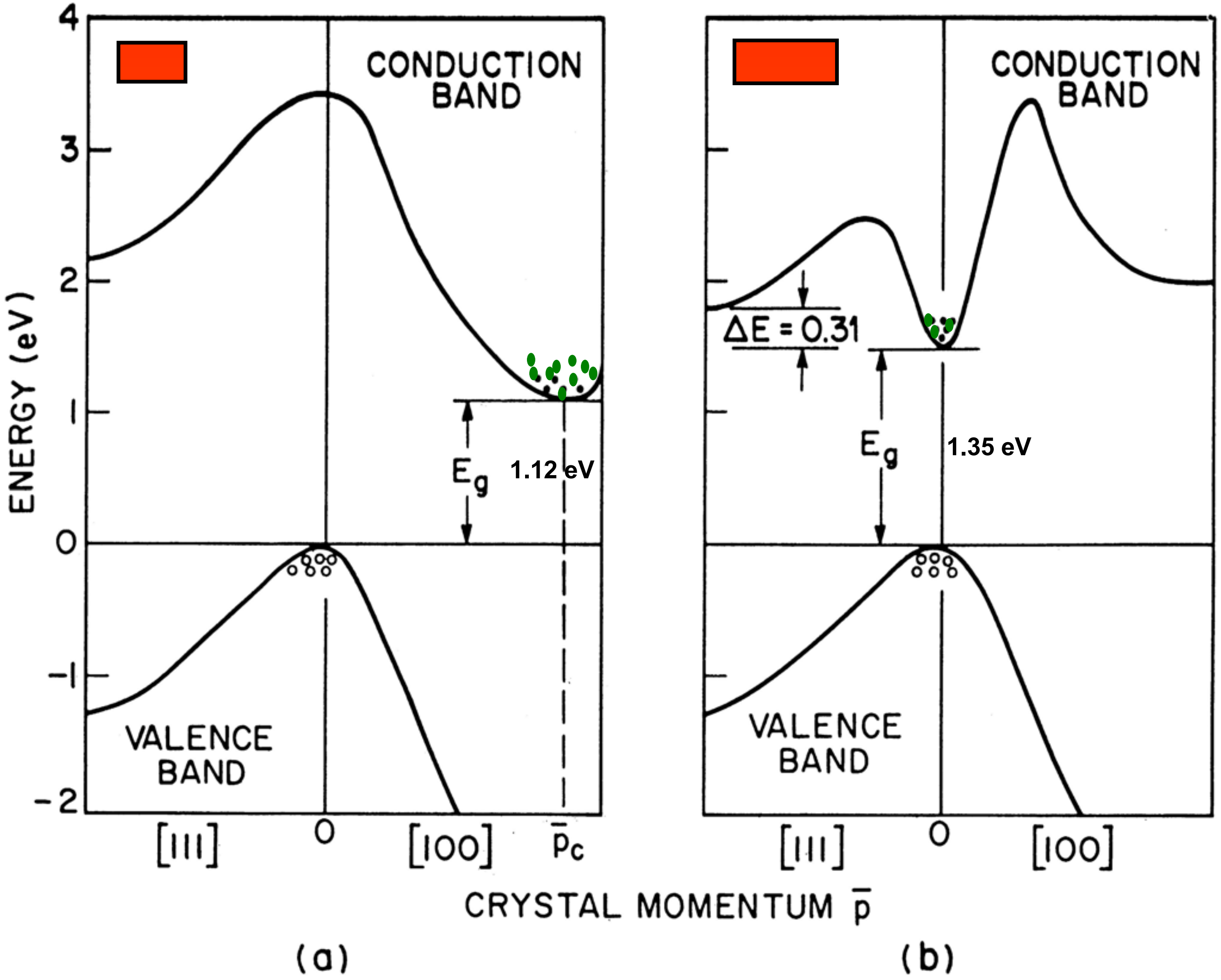

Carrier transport

Drift (acceleration between random collisions)

$$\vec{v}_n = -\frac{q\cdot \tau_c}{m_n}\mathcal{E} = -\mu_n\mathcal{E}$$

$$\vec{v}_p = \frac{q\cdot \tau_c}{m_n}\mathcal{E} = \mu_p\mathcal{E}$$

Diffusion

$$\vec{F}_n = -D_n\nabla n$$

$$\vec{F}_p = -D_p\nabla p$$

Current density (drift and diffusion)

$$\vec{J}_n = q\mu_n n\mathcal{E} + qD_n\nabla n$$

$$\vec{J}_p = q\mu_p p\mathcal{E} - qD_p\nabla p$$

Einstein equation

$$D_n = \frac{kT}{q}\mu_n$$

$$D_p = \frac{kT}{q}\mu_p$$

Inside magnetic field

$$\tan\theta_p = \mu_p^{\mathrm{H}}\mathcal{B}$$

$$\tan\theta_n = \mu_n^{\mathrm{H}}\mathcal{B}$$

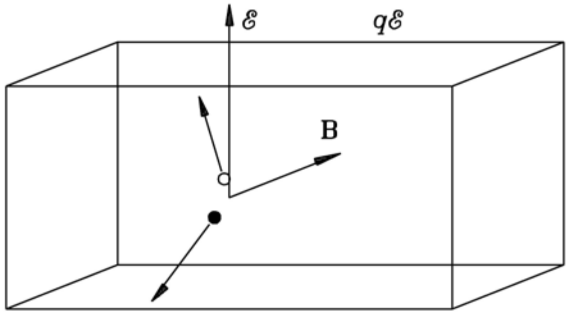

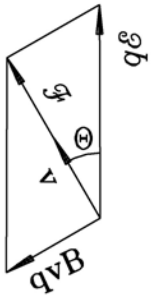

Continuity equations

Simultaneous consideration of

- Generation
- Recombination
- Drift
- Diffusion

$$\frac{\partial n}{\partial t} = \mu_n n \nabla \mathcal{E} + D_n \nabla^2 n + G_n - R_n$$

$$\frac{\partial p}{\partial t} = -\mu_p p \nabla \mathcal{E} + D_p \nabla^2 p + G_p - R_p$$

Drift due to electric field derived from Poisson Equation

$$\nabla \mathcal{E} = \frac{\rho}{\epsilon\epsilon_0} \quad , \quad \text{with } \rho = q(p - n + N_{\mathrm{D}} - N_{\mathrm{A}})$$

Numerical simulation: simultaneous solution of diffusion and Poisson equation with boundary conditions

Charge carrier generation

Thermal generation

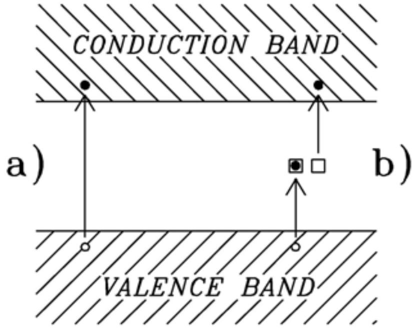

By photons

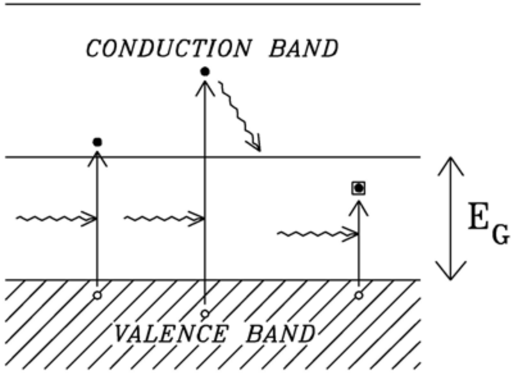

By charged particles (Bethe-Bloch)

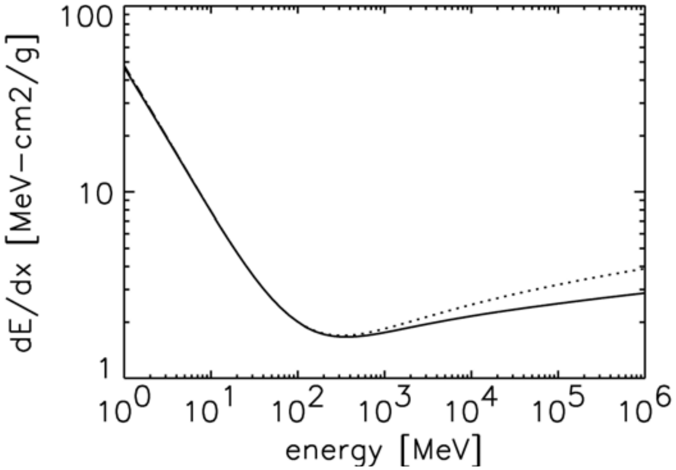

Charge multiplication

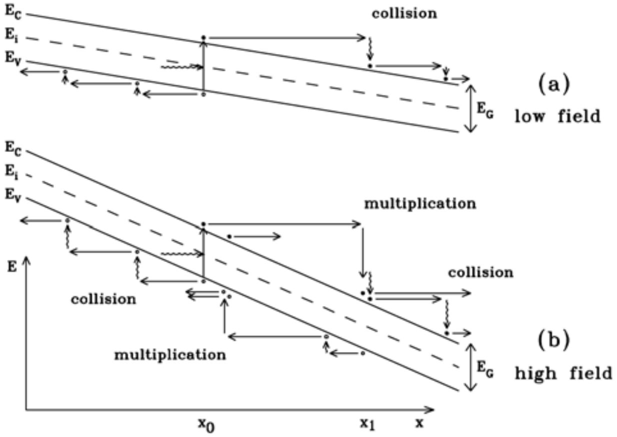

BASIC STRUCTURES
p-n junction

- **Connection between n-type and p-type semiconductor:**

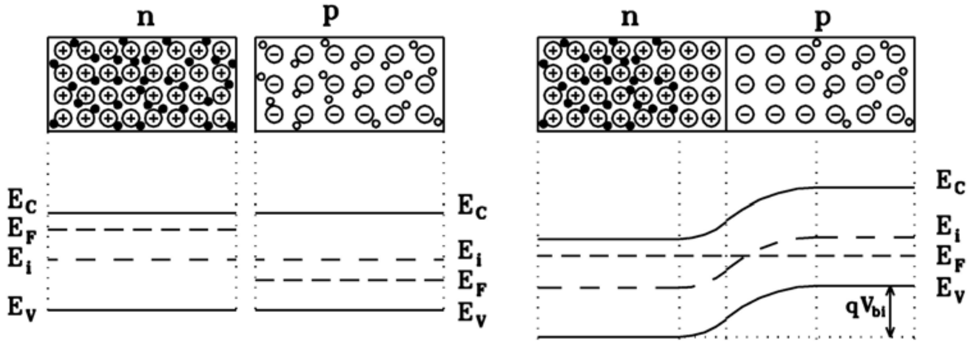

(a)

(b)

**Approximation:
abrupt change from
neutral semiconductor
to space charge region**

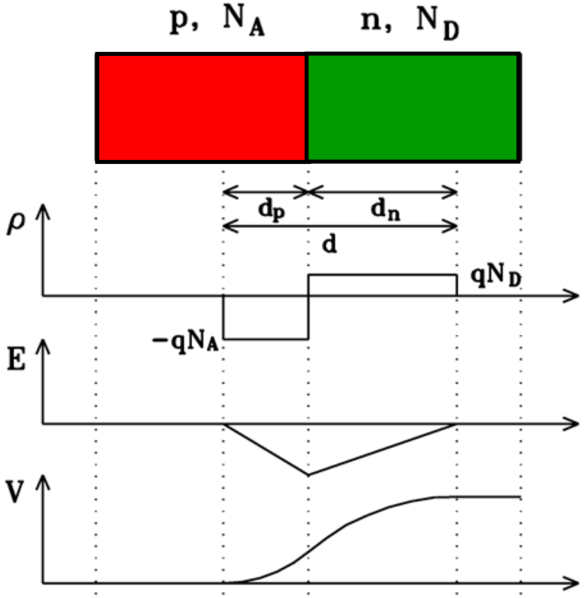

p-n junction – no bias

- Thermal equilibrium
  - Constant Fermi level
  - Drift current equal diffusion current
  - Built in voltage

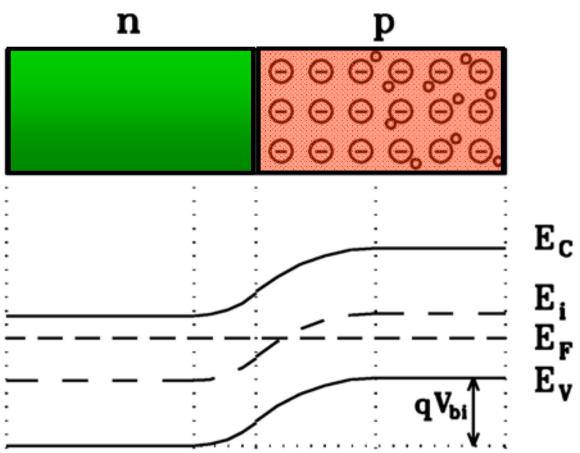

Shallow dopands
majority carriers

$$n_n = N_D = n_i \, e^{\frac{E_F - E_i^n}{kT}}$$

$$p_p = N_A = n_i \, e^{\frac{E_i^p - E_F}{kT}}$$

$$N_A \cdot N_D = n_i^2 \, e^{\frac{E_i^p - E_i^n}{kT}}$$

Built in voltage

$$\begin{aligned} V_{bi} &= \tfrac{1}{q}(E_i^p - E_i^n) = \tfrac{kT}{q} \ln \tfrac{N_A N_D}{n_i^2} \\ &= 0.0259 \ \ln \tfrac{10^{16} \cdot 10^{12}}{(1.45 \times 10^{10})^2} = 0.458 \, \mathrm{V} \end{aligned}$$

Example: high doped n (10^{16}) on low doped p(10^{12})

p-n junction – under bias

Application of an exteral voltage

- Change extent of space charge region

$$d = \sqrt{\frac{2\epsilon\epsilon_0(N_\mathrm{A}+N_\mathrm{D})}{qN_\mathrm{A}N_\mathrm{D}}(V_\mathrm{bi}-V)}$$

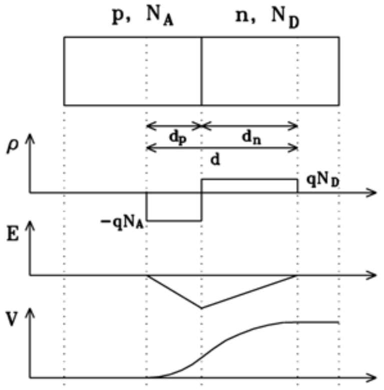

- Non-equilibrium: Fermi level not defined
- Drift current not equal diffusion current
- Diffusion of minority carriers into (out of) space charge region

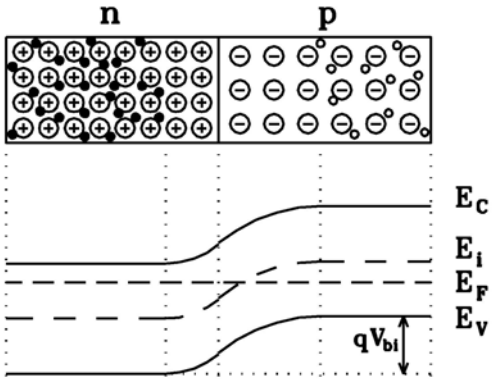

$$J = (J_{\mathrm{s}_n} + J_{\mathrm{s}_p})\left(\mathrm{e}^{\frac{qV}{kT}} - 1\right) = J_\mathrm{s}\left(\mathrm{e}^{\frac{qV}{kT}} - 1\right)$$

$$J_\mathrm{s} = q\left(\frac{n_{p0}D_n}{\sqrt{D_n\tau_{\mathrm{r}n}}} + \frac{p_{n0}D_p}{\sqrt{D_p\tau_{\mathrm{r}p}}}\right)$$

MOS (Metal-Insulator-Semiconductor) Structure

◆ Bond picture (p-type semiconductor)

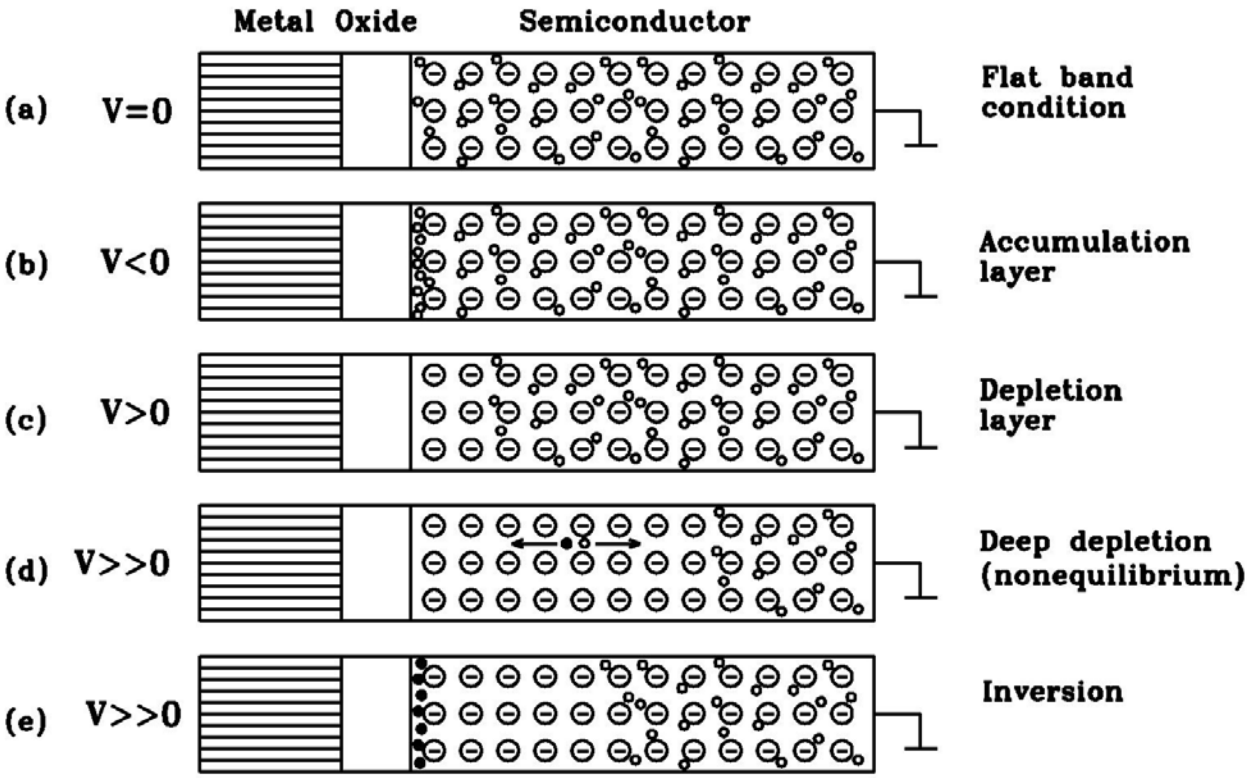

CCD

Transistor

Basic structure in MOS transistor and in MOS CCDs

Basis: Die in Sperrrichtung gepolte Diode

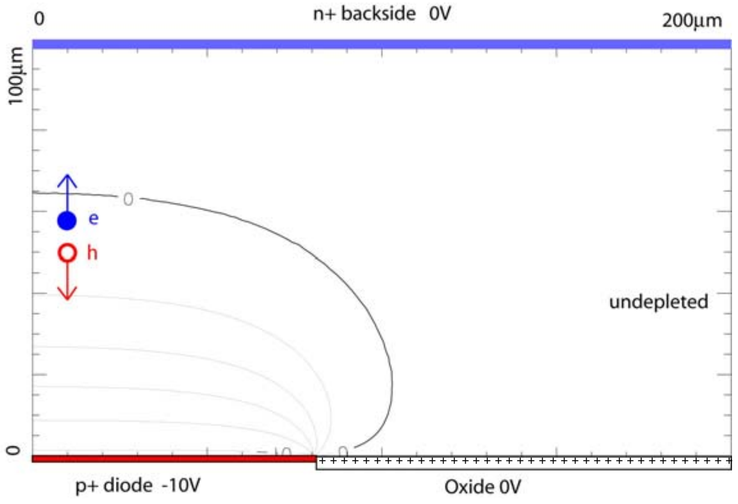

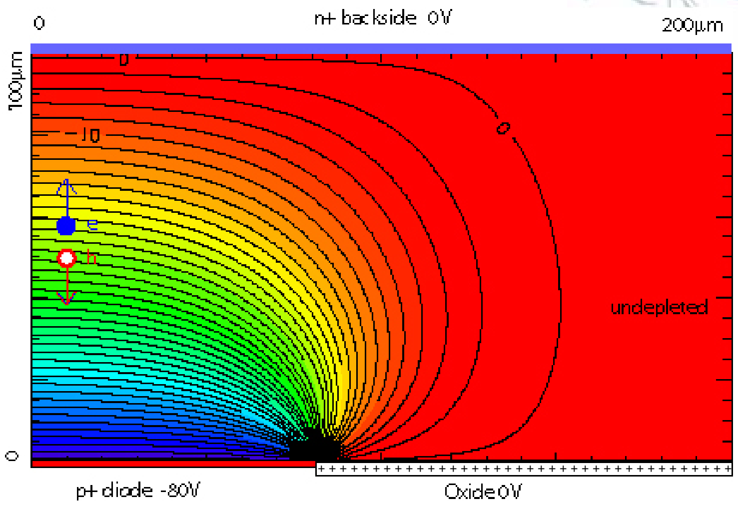

Depletionsverhalten von Dioden

$$d = \sqrt{\frac{2\epsilon\epsilon_0(N_\mathrm{A} + N_\mathrm{D})}{qN_\mathrm{A}N_\mathrm{D}}(V_\mathrm{bi} - V)}$$

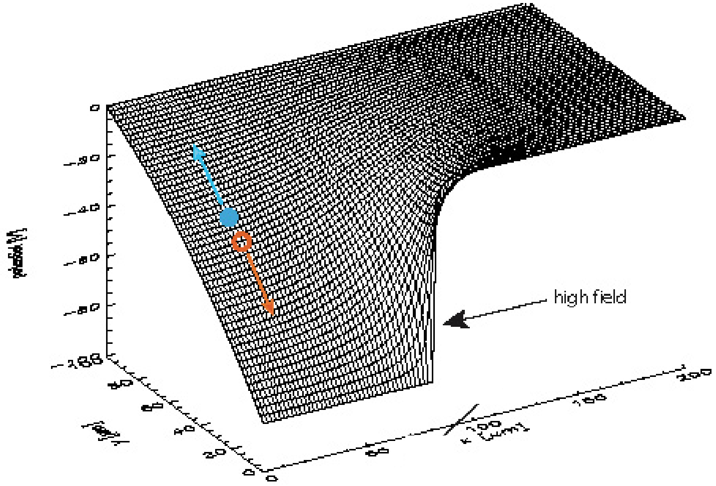

Detector Structures

◆ diode

- material silicon
  germanium
  compound semiconductors
  (CdTe, CZT, …)

- geometry
  size 5 mm² … several cm²
  thickness 300, 500 µm, 1 mm

- applications
  X-ray spectroscopy
  γ-ray spectroscopy

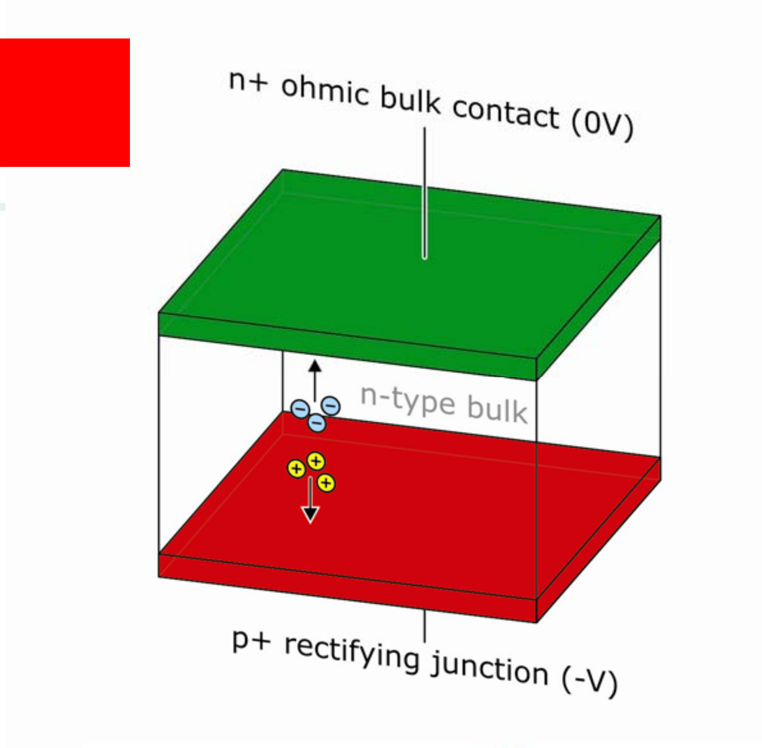

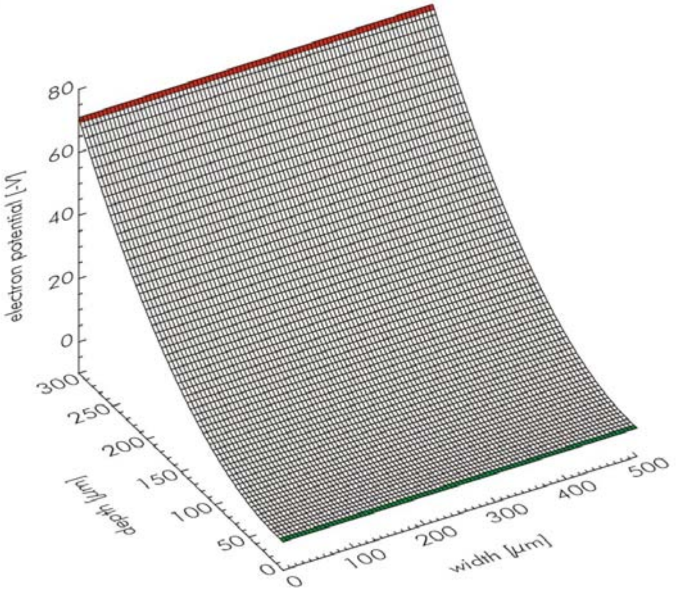

Detector Structures

structured diode: single-sided strip detector

- material silicon
  germanium
  compound semiconductors
  (GaAs, CdTe, CZT, …)
  diamond

- geometry
  - size wafer size
    typ. 6 x 6 cm^2
    10 x 10 cm^2
  - thickness 300, 500 µm
  - strip width/pitch it depends …
    10 µm … 1 mm
  - position accuracy down to few µm

- applications
  - particle tracking

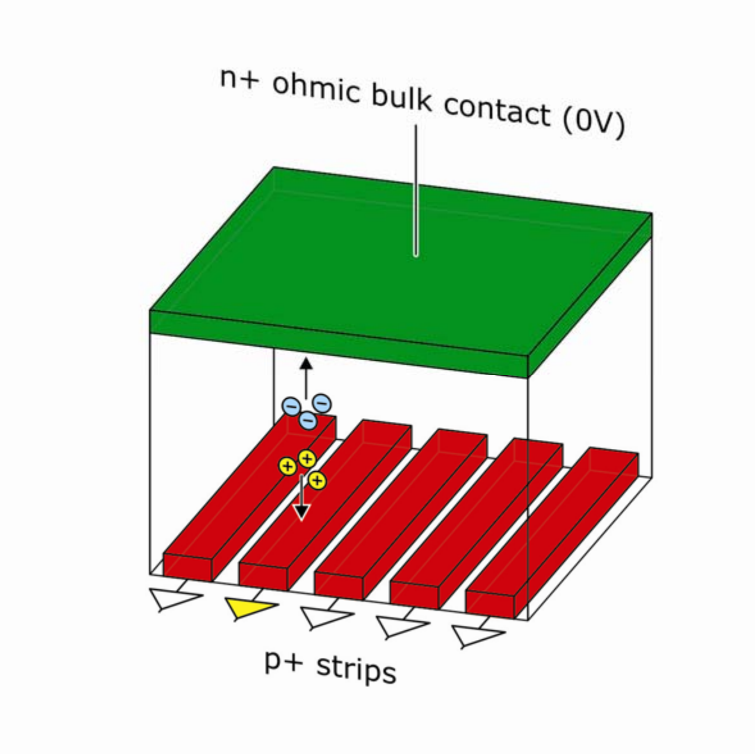

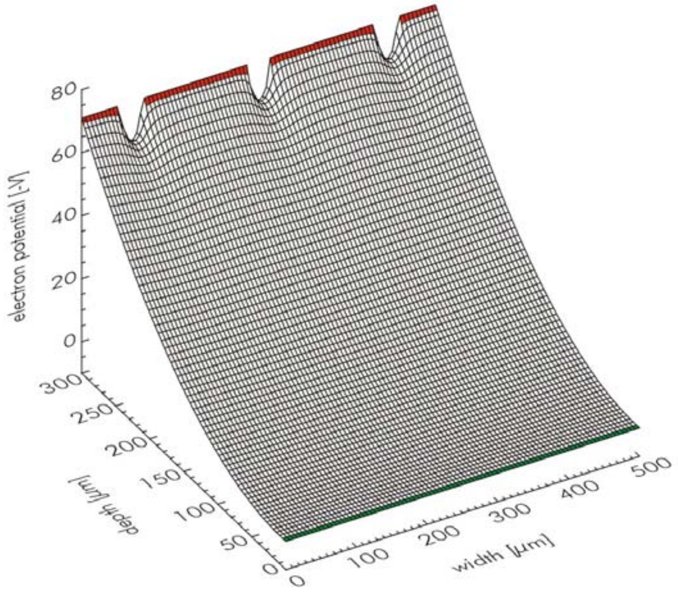

Detector Structures

structured diode: double-sided strip detector

- material silicon
  - germanium
  - compound semiconductors (GaAs, CdTe, CZT, …)
  - diamond
- geometry
  - size wafer size
    - typ. 6 x 6 cm²
    - 10 x 10 cm²
  - thickness 300, 500 µm
  - strip width/pitch it depends …
    - 10 µm … 1 mm
  - position accuracy down to few µm
- applications
  - particle tracking

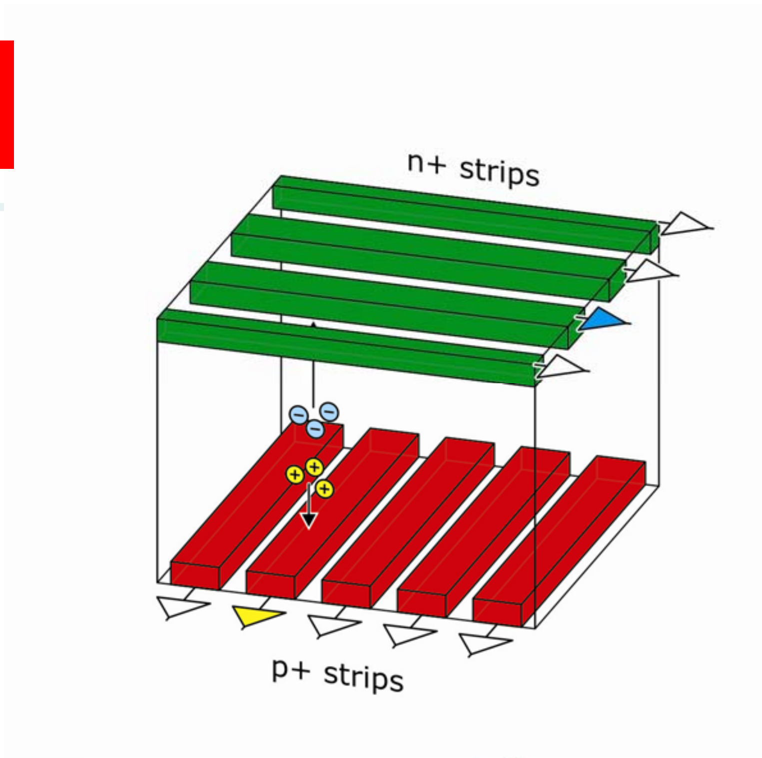

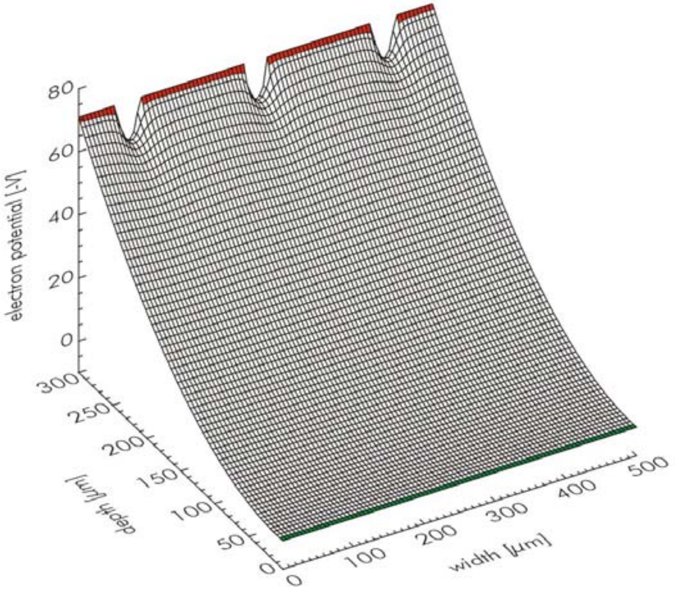

Detector Structures

- **double-sided strip detector**
  - advantage
    n^2 resolution elements with
    2n readout channels
  - disadvantage
    ambiguity at high occupancy

↳ **2dim pixel sensor** **??**

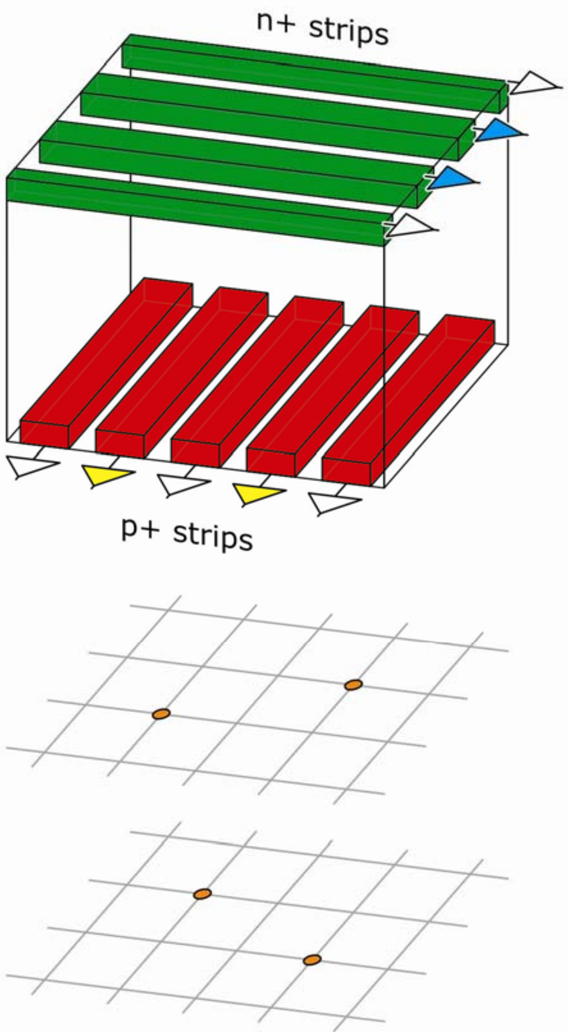

Detector Structures

♦ pad detector 'p on n'

- material silicon
  germanium
  compound semiconductors
  (GaAs, CdTe, CZT, …)
  diamond

- geometry
  - size wafer size
    typ. 6 x 6 cm^2
    10 x 10 cm^2
  - thickness 300, 500 µm
  - pixel size ≥ 50 µm

- applications
  - particle tracking
    ↳ detection of individual charged particles
  - imaging
    ↳ count / integrate particles or photons

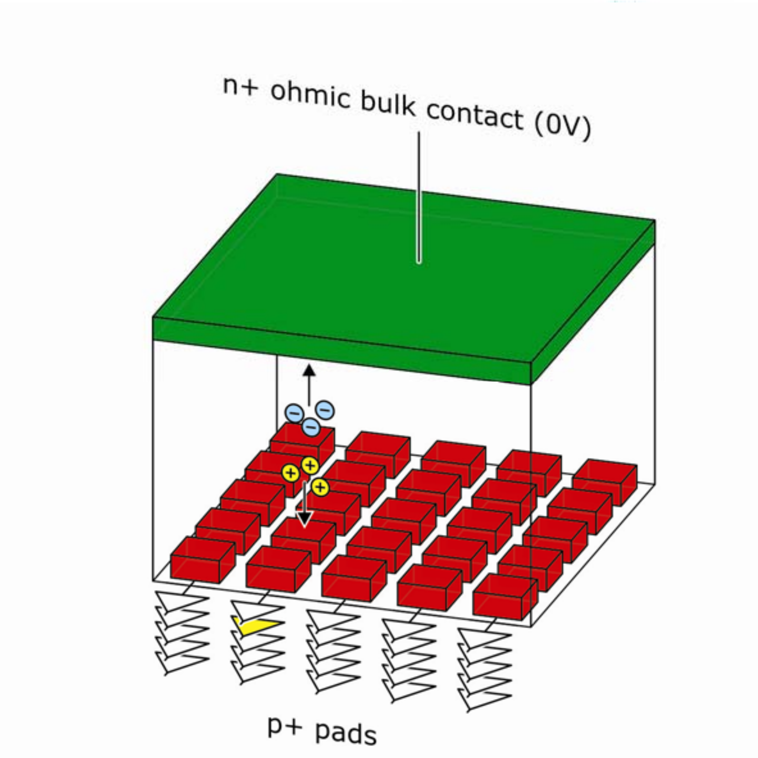

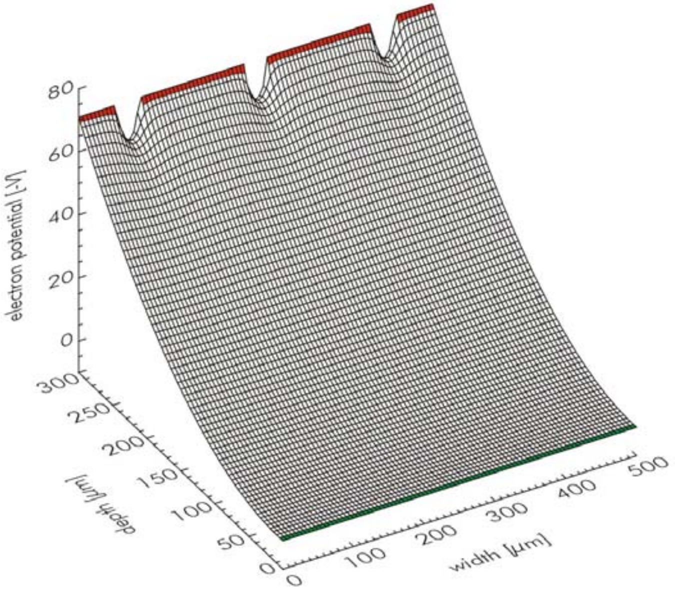

Detector Structures

♦ pad detector 'n on n'

- material — silicon
  - germanium
  - compound semiconductors (GaAs, CdTe, CZT, ...)
  - diamond
- geometry
  - size — wafer size
    - typ. — 6 x 6 cm^2
    - 10 x 10 cm^2
  - thickness — 300, 500 µm
  - pixel size — ≥ 50 µm
- applications
  - particle tracking
    - ↳ detection of individual charged particles
  - imaging
    - ↳ count / integrate particles or photons

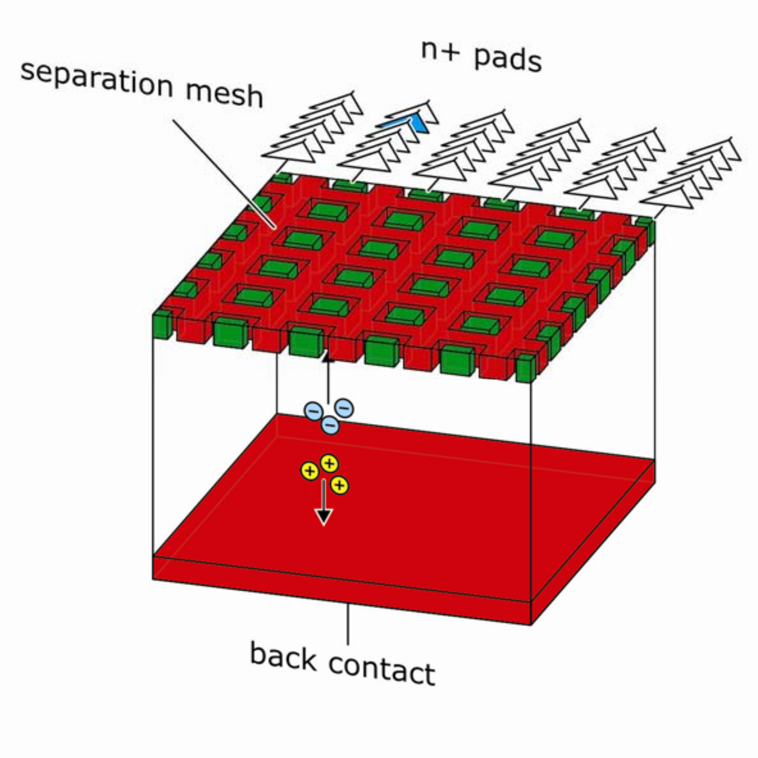

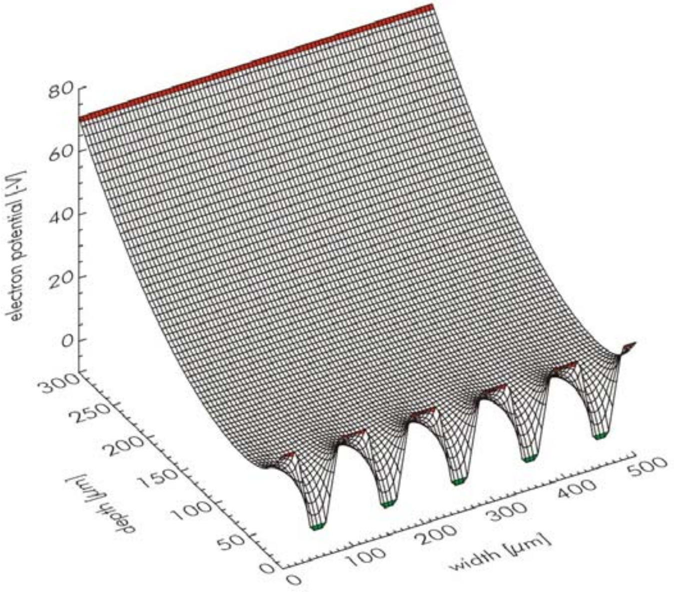

Detector Structures

♦ diode

- electronic noise

$$ENC = \sqrt{\alpha \frac{2kT}{g_m} C_{tot}^2 A_1 \frac{1}{\tau} + 2\pi a_f C_{tot}^2 A_2 + q I_L A_3 \tau}$$

- optimum shaping time

$$\tau_{opt} = \sqrt{\frac{2A_3}{A_1} \frac{kT}{q} \frac{C_{tot}^2}{I_L} \frac{2}{3g_m}}$$

↳ for

  - **good resolution**
  - **high count rate capability**

the total capacitance must be minimised!!

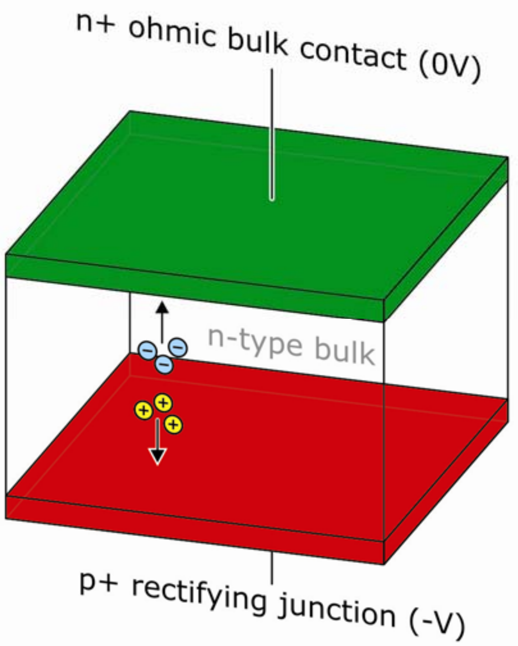

Detector Structures

◆ sideward depletion structure

Emilio Gatti & Pavel Rehak, 1983

- symmetric bias
- volume is fully depleted by reverse biased diodes on both surfaces
- minimum capacitance of bulk contact, independent of overall area
- potential minimum for majority carriers (electrons @ n-Si) in the centre plane

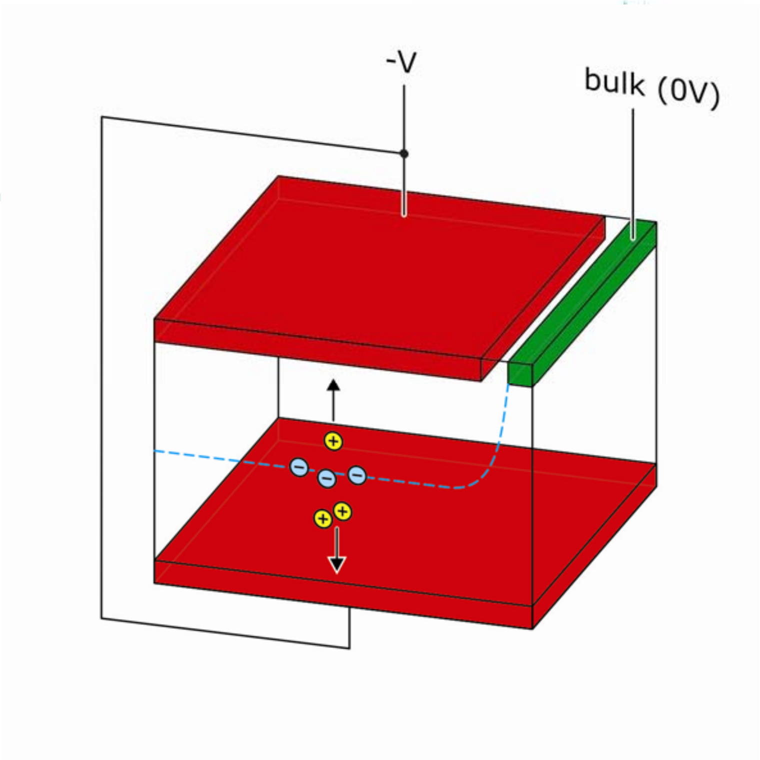

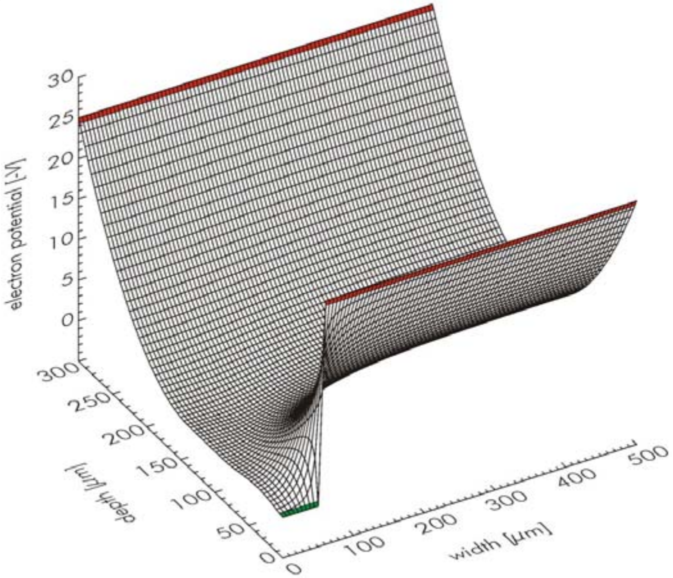

Detector Structures

♦ sideward depletion structure

asymmetric bias

- volume is fully depleted by reverse biased diodes on both surfaces
- minimum capacitance of bulk contact, independent of overall area
- vertical shift of the potential minimum

?? signal extraction ??

↳ **advanced detector concepts**

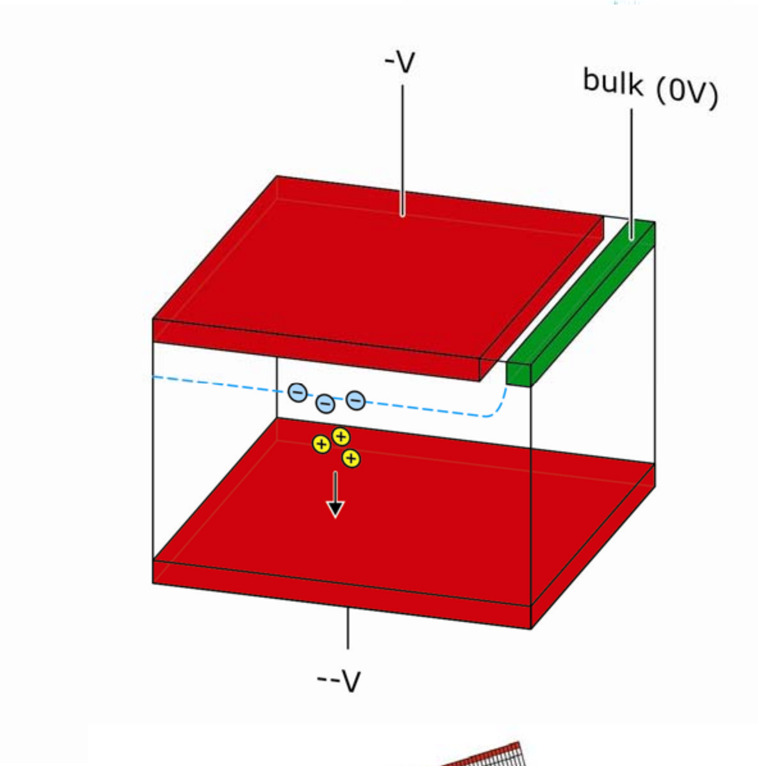

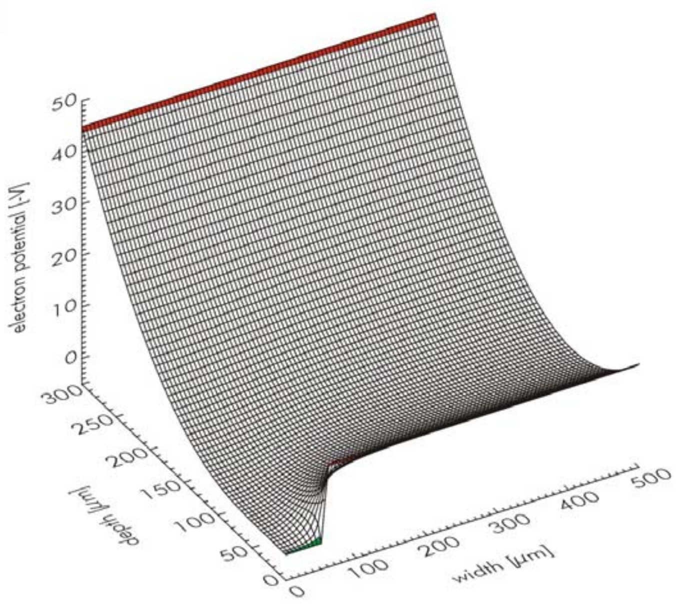

Detector Structures

♦ linear silicon drift detector (SDD)

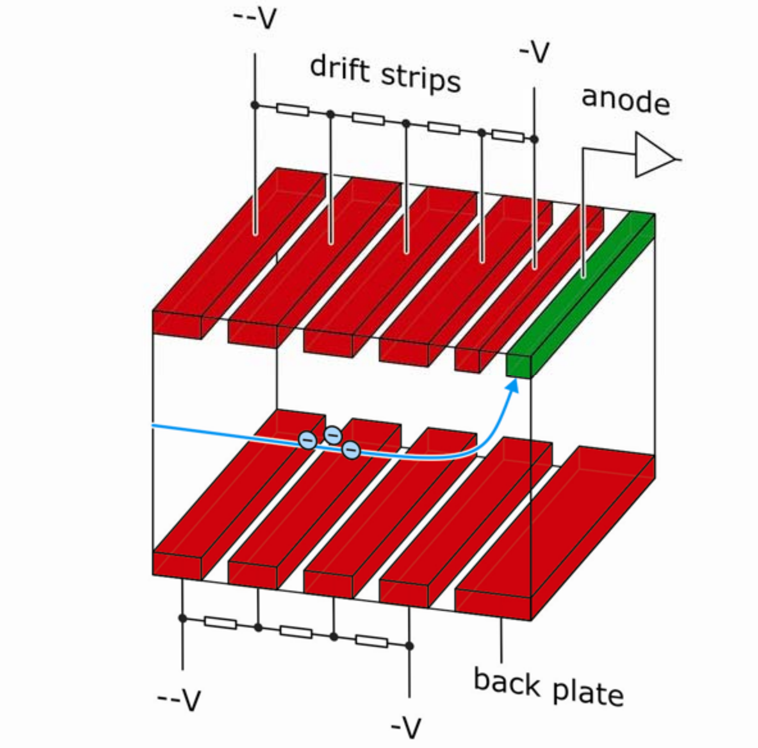

- segmentation and bias of diodes
  ↳ drift field || surface
- 1dim position resolution by drift time measurement
  start trigger required!

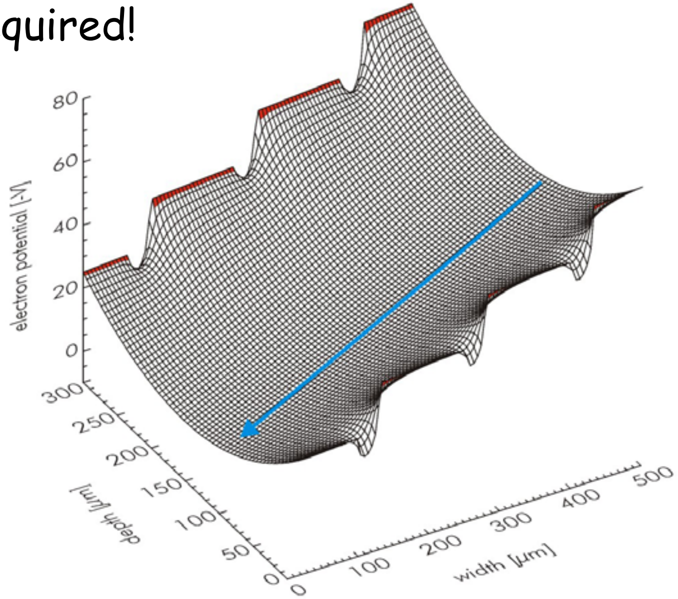

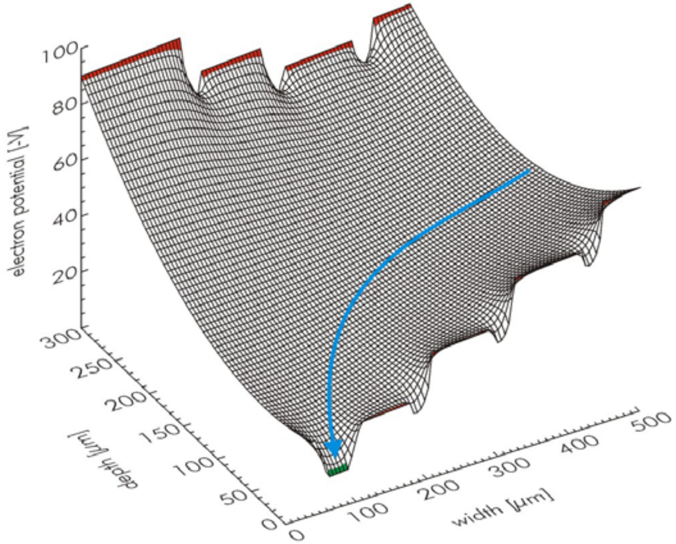

Detector Structures

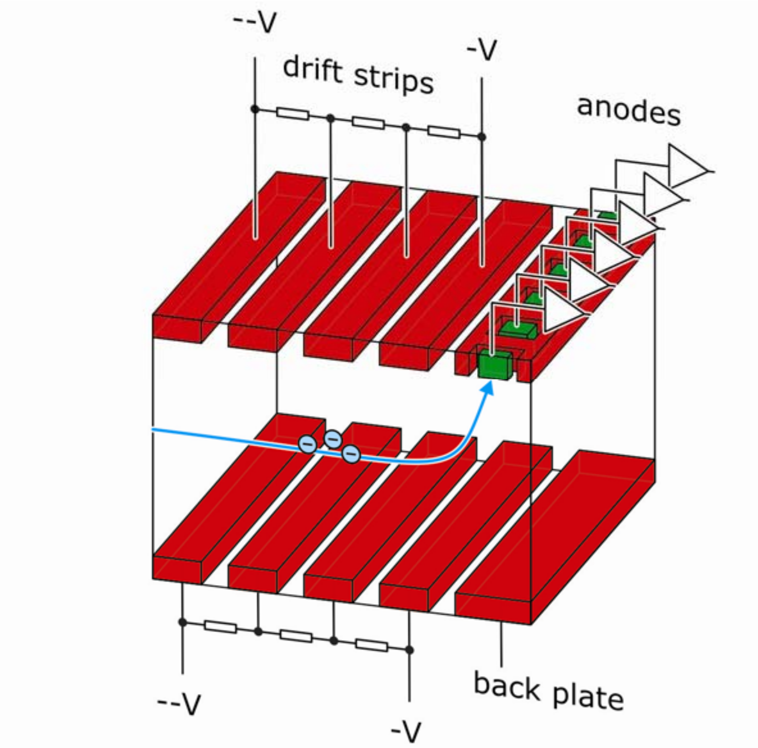

linear silicon drift detector (SDD)

- segmentation and bias of diodes
  ↳ drift field || surface
- 2dim position resolution by
  - drift time measurement (trigger!)
  - segmentation of the anode
- application: particle tracking

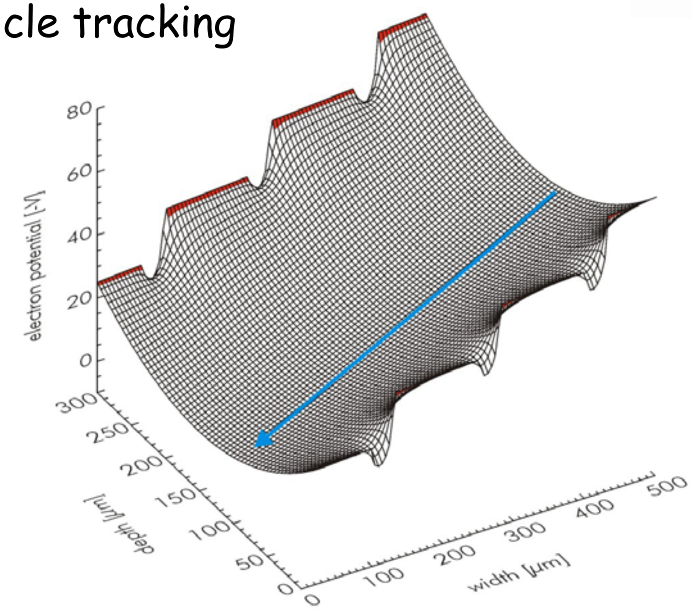

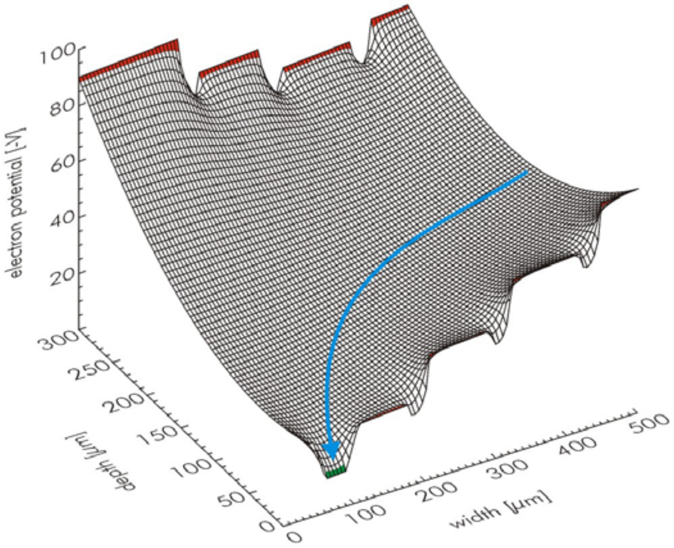

Detector Structures

♦ SDD with on-chip FET

- one-sided field strip system
- backside illuminated
- integration of 1st amplifying FET dedicated n-JFET
  - ↳ minimization of total capacitance
  - ↳ good energy resolution
  - ↳ high count rate capability
  - ↳ robust against pickup, microphony
- comparison
  - ✦ pin diode 10 mm² x 300 µm

    C_{tot} = 3.5 pF
  - ✦ SDD with FET 10 mm²

    C_{tot} = 50 fF

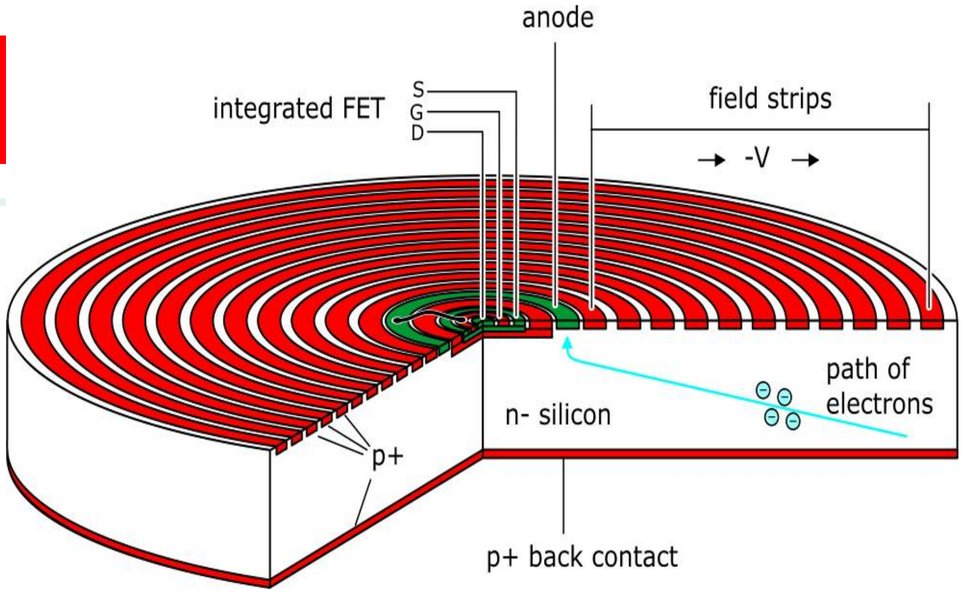

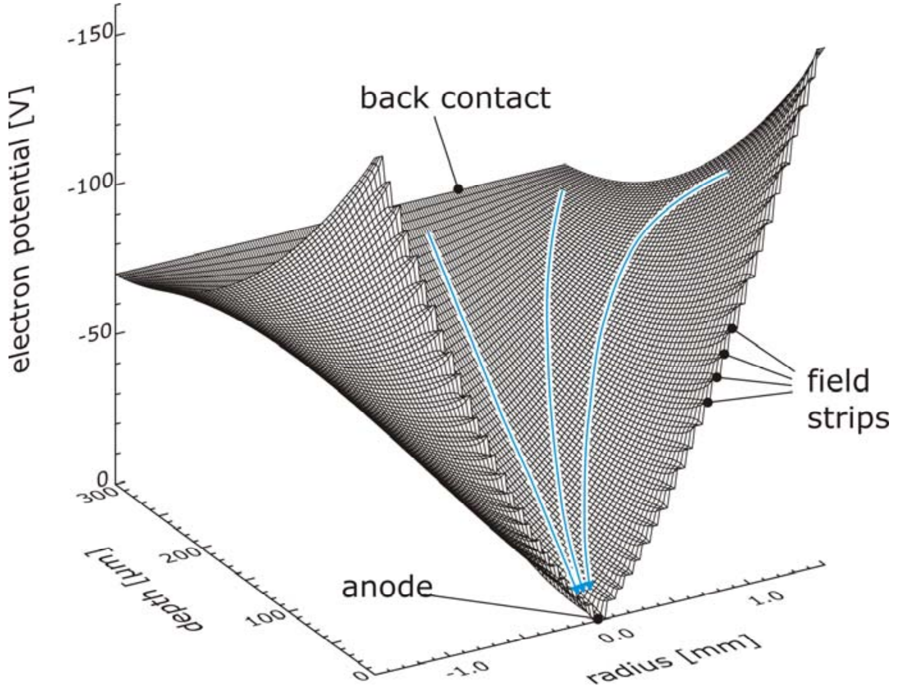

CCD basics

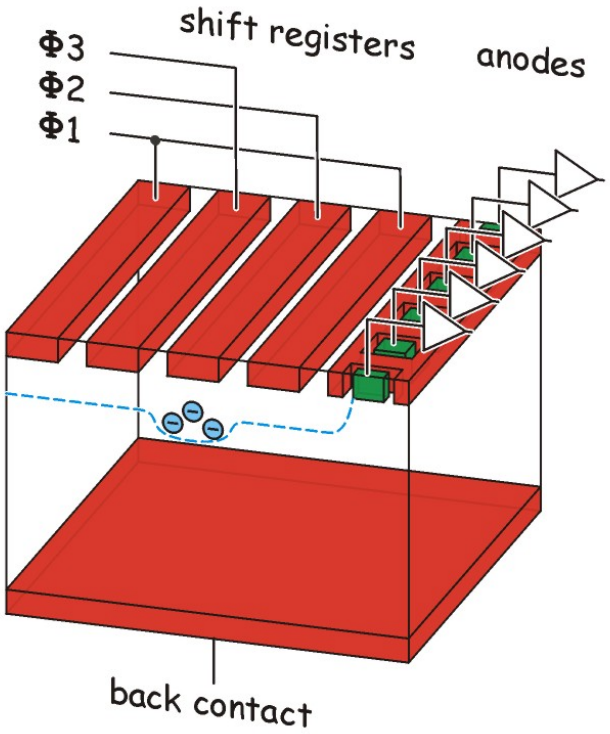

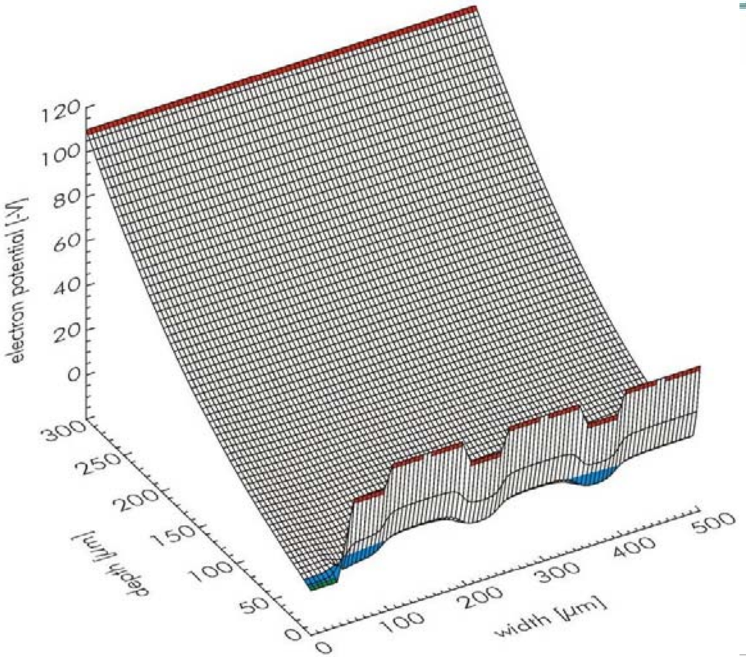

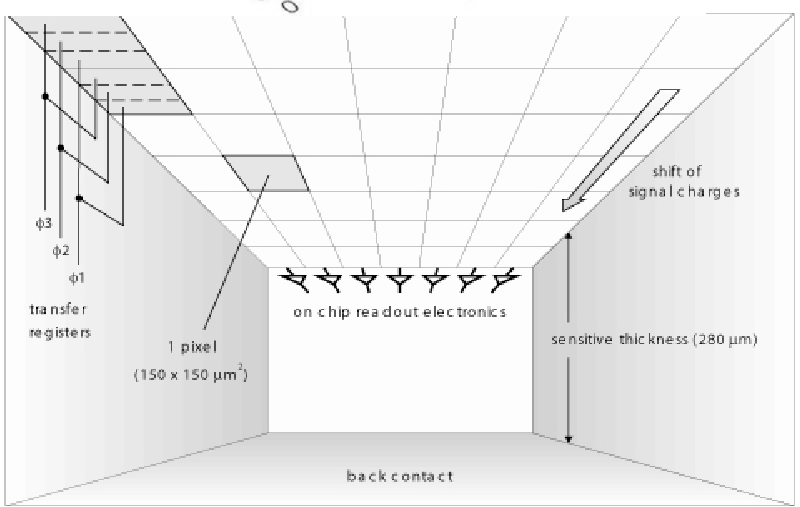

- full depletion (50 µm to 500 µm)
- back side illumination
- radiation hardness
- high readout speed
- pixel sizes from 36 µm to 650 µm
- charge handling: more than 10^6 e^-/pixel
- high quantum efficiency

How many charges can be stored in one pixel ?

What determines the charge handling capacity in a pixel ?

pixel volume:
20x40x12 μm^3 ≈ 1x10^{4}μm^3

Doping: 10^2 P per μm^3

CHC = 5 x 10^5 per pixel

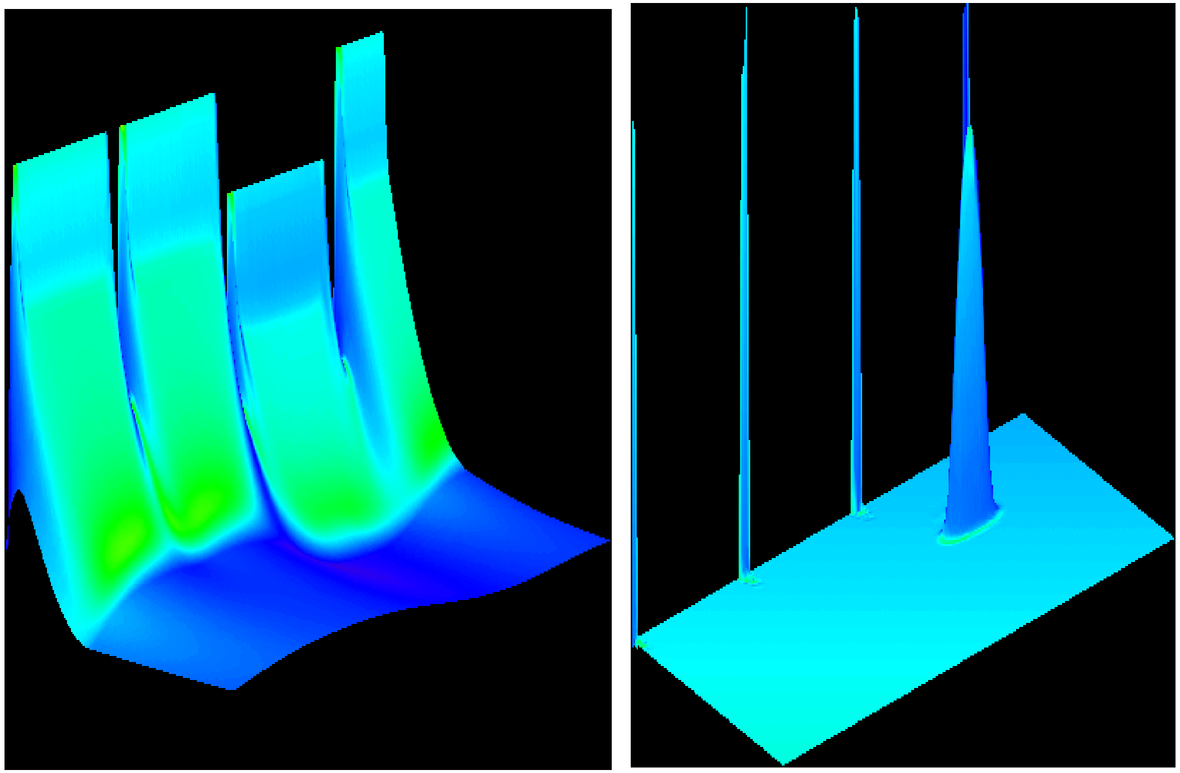

can be increased by
external voltages

can be increased by doping

Detector Structures

pnCCD vs. MOS-CCD

MOS-CCD (´video CCD´)

- MOS transfer gates

↳ implanted pn-junctions

- buried channel

↳ deep transfer

- partial depletion

↳ full depletion

- frontside illumination

↳ back entrance window

- serial readout

↳ column parallel readout
1 preamp / channel

pnCCD

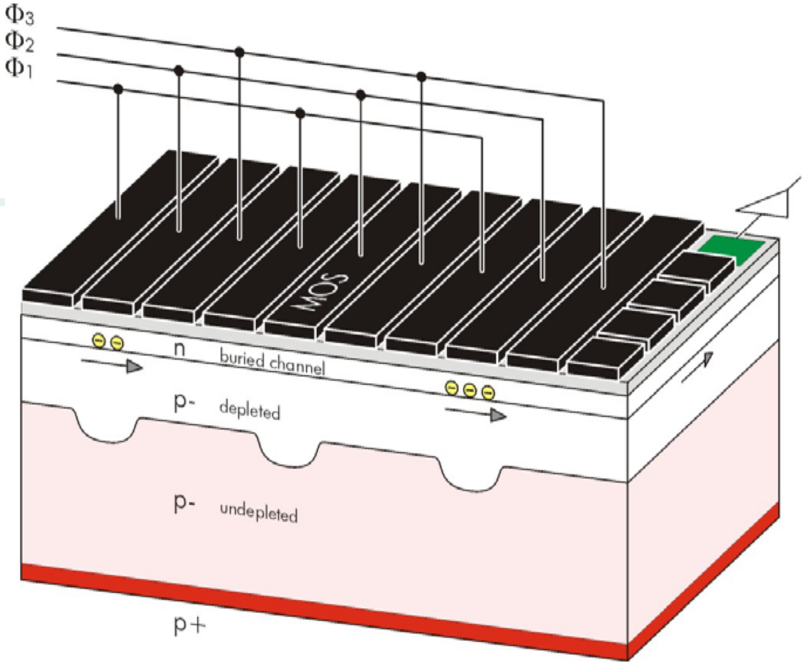

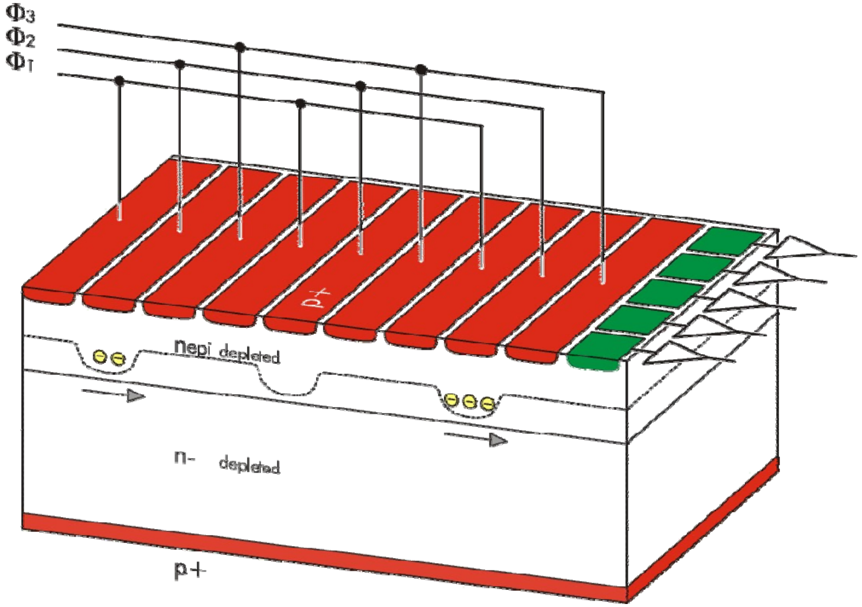

Detector Structures

DEPFET

Josef Kemmer & Gerhard Lutz, 1987

- applications
  - unit cell of active pixel sensor
    - ↳ X-ray imaging & spectroscopy
    - ↳ particle tracking
  - integrated readout device of SDD, CCD, …
- format ~ cm^2 … wafer scale
- thickness 50 … 450 µm
- pixel size 20 … 500 µm □

  … 1 cm^2 (DEPFET & SDD)
- readout time 2 µsec / row
- low noise 2 - 3 el. ENC

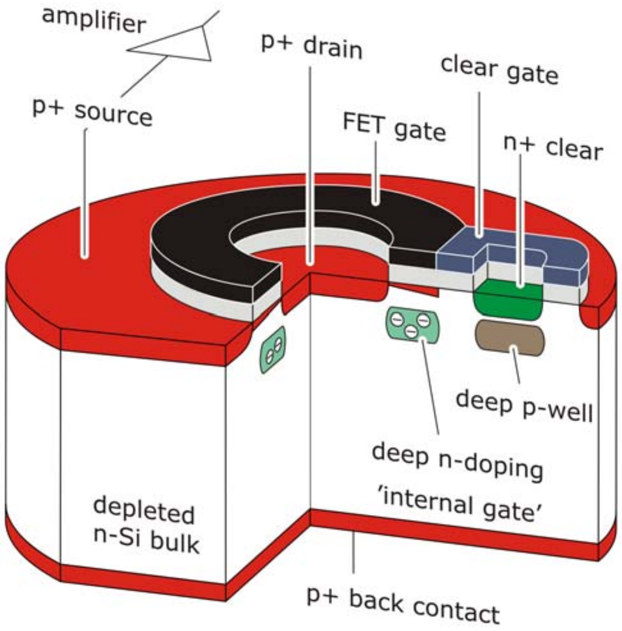

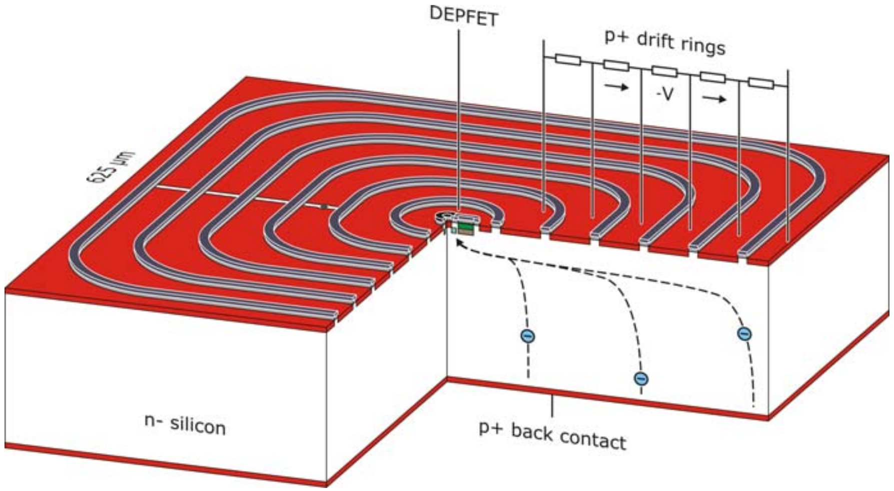

Detector Structures

♦ DEPFET

p-MOSFET on depleted n-substrate

- combined detector & amplifier function
- localized potential minimum under gate = 'internal gate'
  - ↳ modulation of FET current (300 pA/el.)
- low capacitance (20 fF) and noise
  - ↳ excellent spectroscopic performance
- charge storage capability
  - ↳ readout on demand
- non-destructive readout
  - ↳ potential of repetitive readout
- complete clearing of signal charge
  - ↳ no reset noise
- backside illuminated, fully depleted
  - ↳ quantum efficiency

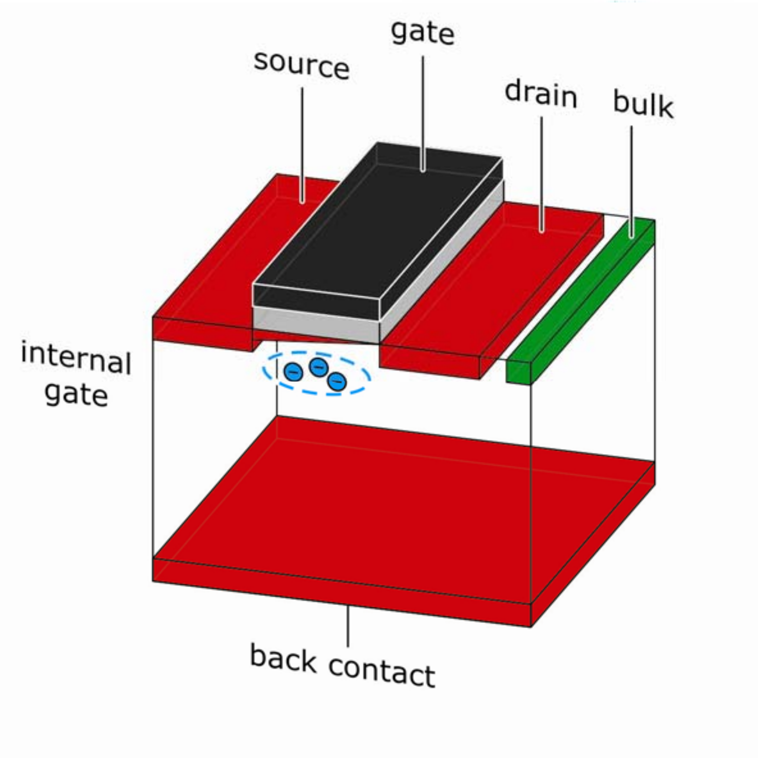

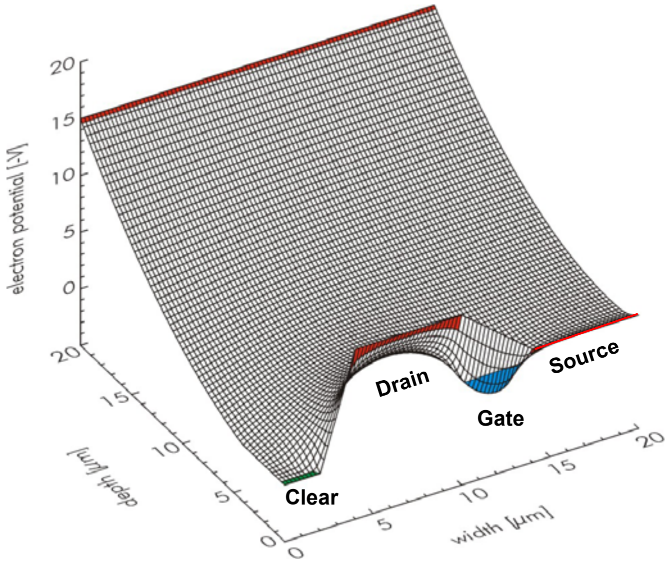

MPE-HLL projects

1. X-ray astronomy

eROSITA	2012
BepiColombo	2013
SIMBOL-X	2014 (discontinued !)
IXO	2020 + x

2. Center for Free Electron Laser Science

FLASH	2008
BESSY	2008
LCLS	2009
XFEL	2012
SCSS	2012

3. X-ray Fluorescence Physics

Mars rovers Spirit and Opportunity	now
EXOMars	2013
SIDDHARTA	2008
HICAM and DRAGO	2010

4. Optical applications

LBT, wave front sensing	2013
Avalanche pnCCDs	?
SiPMs	2012
RNDR – DePFETs	2013
IBC (BIB) detectors	?

5. Commercialization of sensors and systems

The EPIC pnCCDs on XMM-Newton

- 3 imagers
  - ▷ 2 MOS-CCD + RGS
  - ▷ 1 pnCCD
-
- energy range
  - ▷ 0.1 ... 15 keV
- Wolter-I telescopes
  - ▷ 58 nested mirror shells
  - ▷ eff. area 0,5 m² (1 keV)
  - ▷ focal length 7,5 m
  - ▷ FOV 30 arcmin
  - ▷ resolution 15 arcsec

- highly excentric orbit
  - ▷ 48 h
  - ▷ perigee: 7.000 km
  - ▷ apogee: 120.000 km

XMM EPIC pnCCD

- Device
  - ▷ Monolithic array of 12 pnCCDs
  - ▷ 200 x 64 pixels each
  - ▷ pixel size 150 x 150 μm^2
  - ▷ 6 x 6 cm^2 area
  - ▷ 4" wafer
  - ▷ 280 μm thick
  - ▷ Common entrance window

- Performance
  - ▷ 6 e- ENC
  - ▷ Readout time 4.5 ms
  - ▷ Integration time 100 ms
  - ▷ Energy resolution 150 eV FWHM @ 5.9 keV

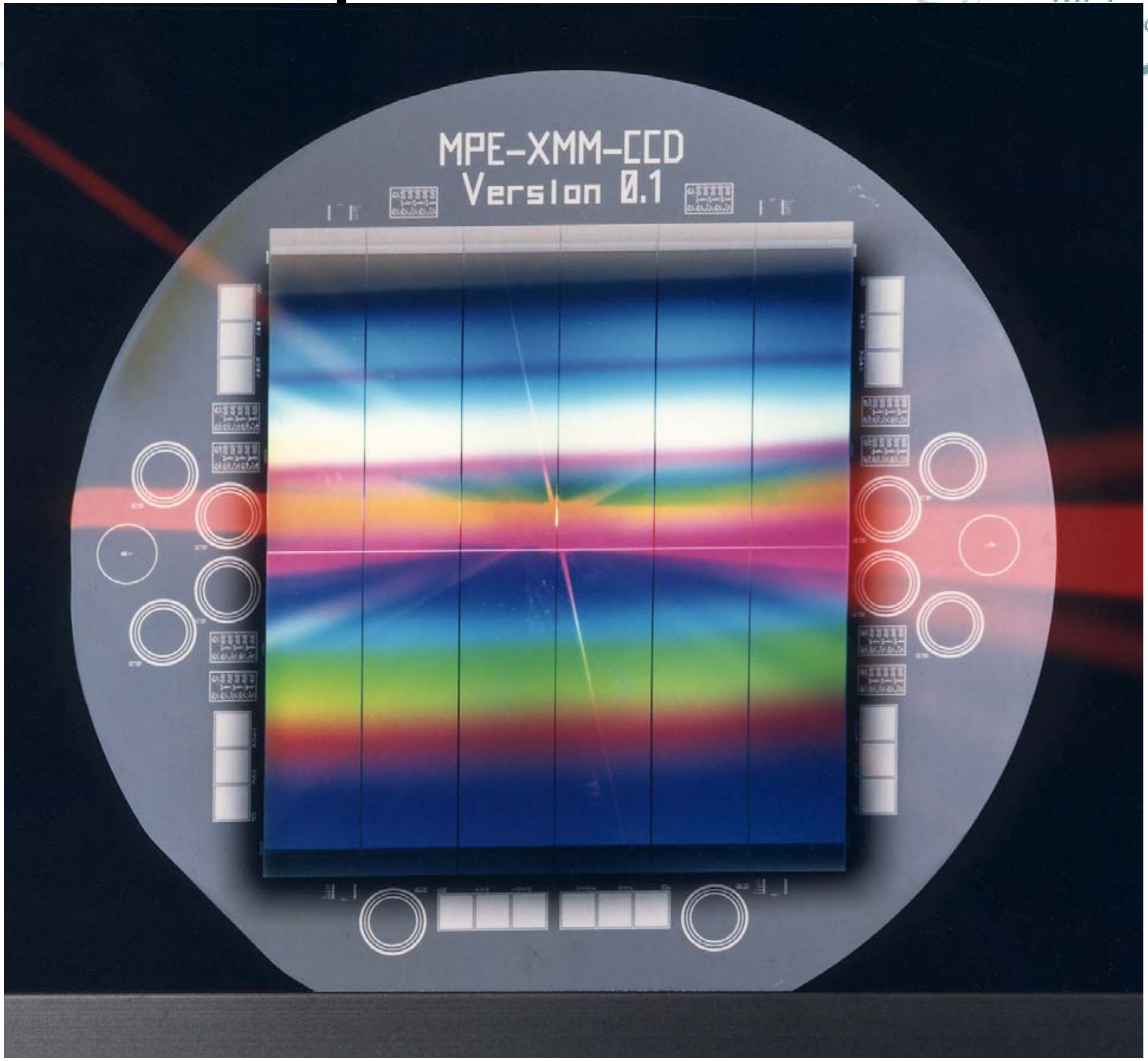

XMM-Newton observations

Tycho SNR

- Image and spectrum
- Supernova remnant
- Observed by Tycho Brahe in 1532

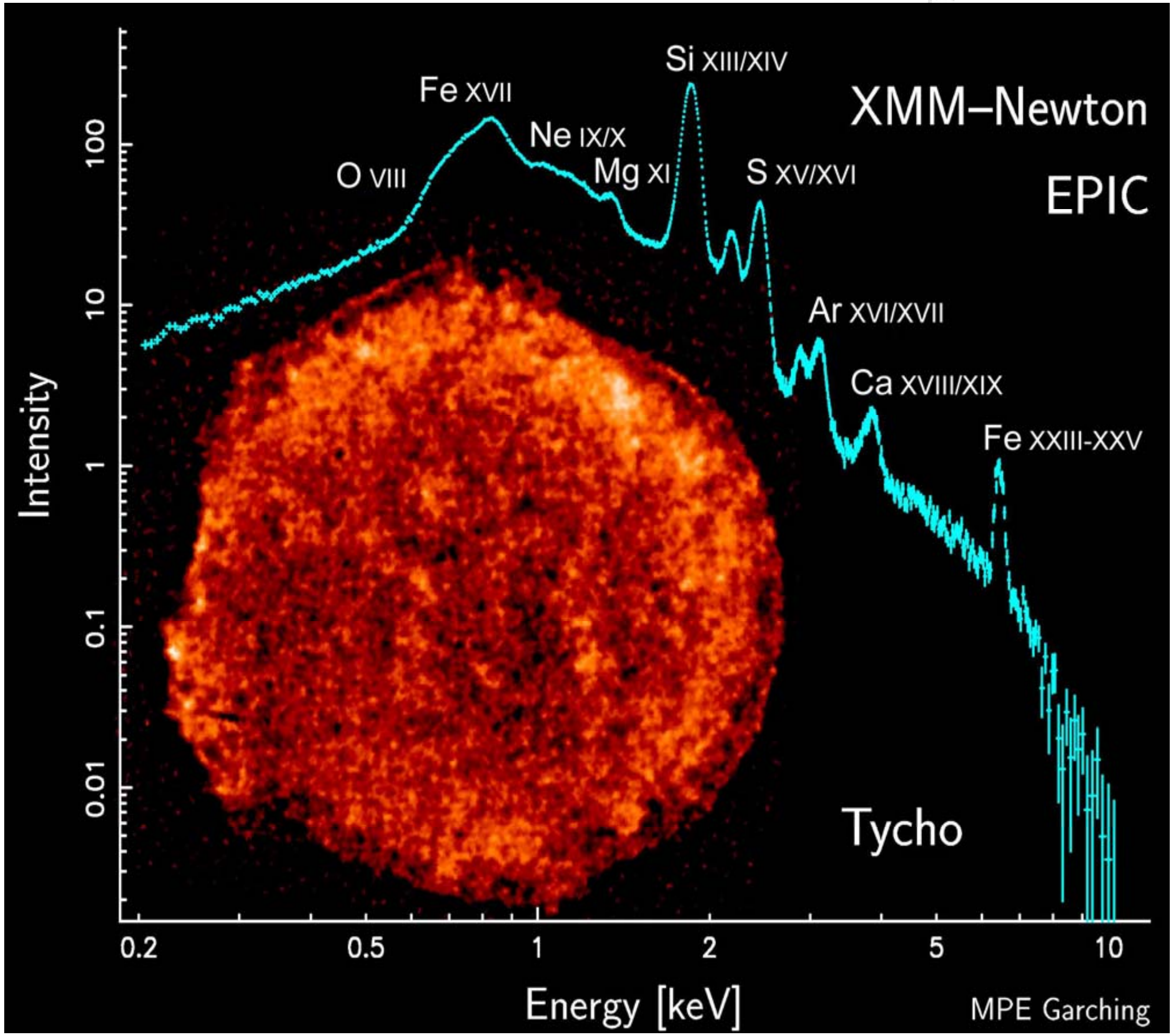

XMM Summary

- Working since launch (10. Dez. 1999) without any problem.
- The energy resolution @ the Al_K line (1.5keV) decreased since launch from 98 eV to 99 eV (FWHM).
- Since launch the operating conditions have never been changed.
- Up to now more than 20.000 observations were made with XMM – Newton.
- Up to now, > 3.000 refereed astrophysics publications have been made

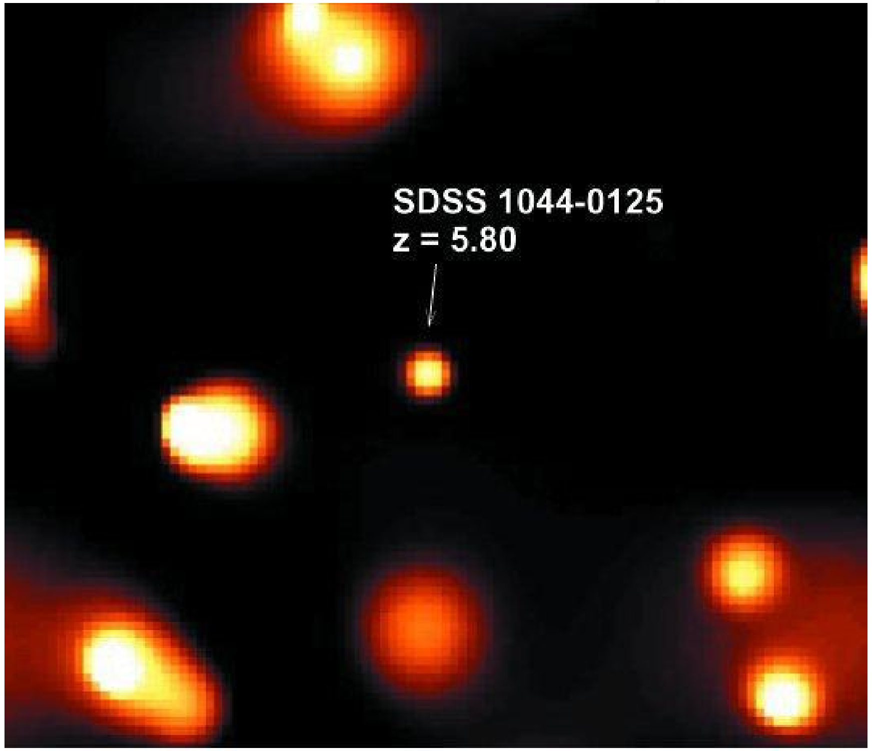

QSO SDSS 1044-0125

European Space Agency

Very high redshift QSO observed by XMM EPIC

eRosita

- ROSAT All-Sky survey (RASS)
  - ▷ Limited energy range
  - ▷ Lack in sensitivity

- All-Sky survey
  - ▷ Pathfinder for NGXT
  - ▷ Hidden population of AGN
  - ▷ **Extension of RASS towards higher energies**
  - ▷ 7 Wolter-I Mirrors
  - ▷ 54 shells each (27 before)
  - ▷ Framestore pn-CCDs
  - ▷ Focal distance ~1.6 m
  - ▷ FoV 1° diam.
  - ▷ 15`` resolution on-axis
  - ▷ 660kg / 250W

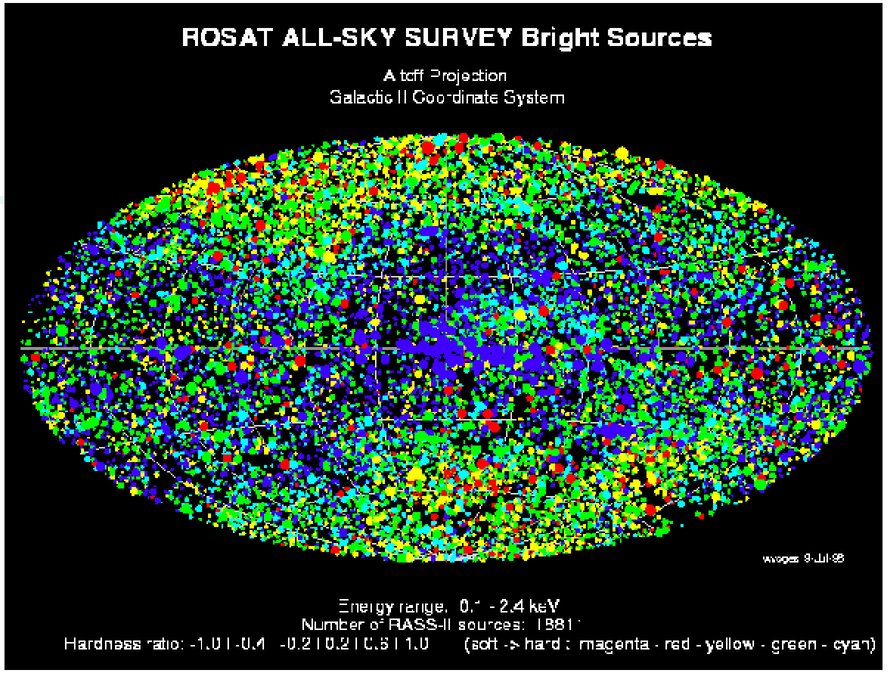

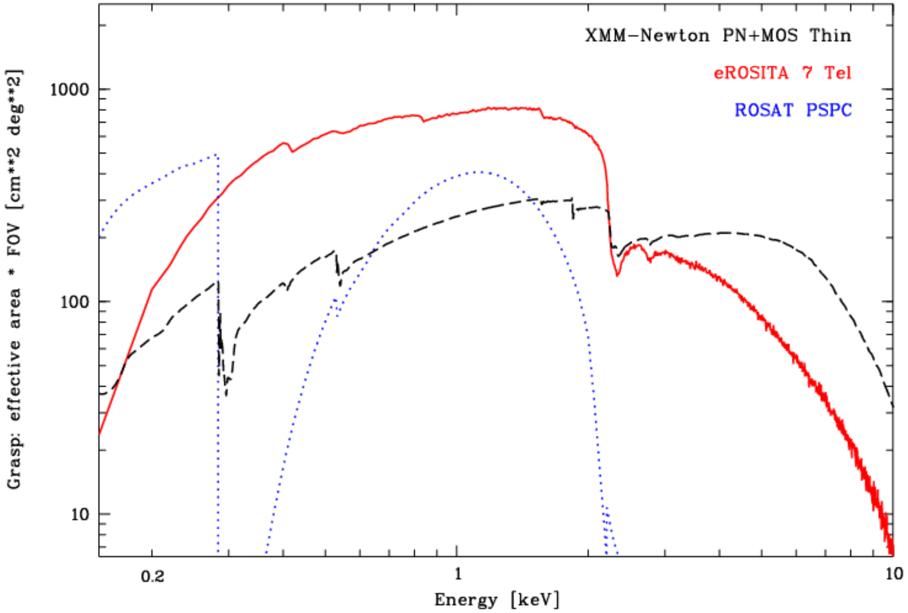

Instrument Structure

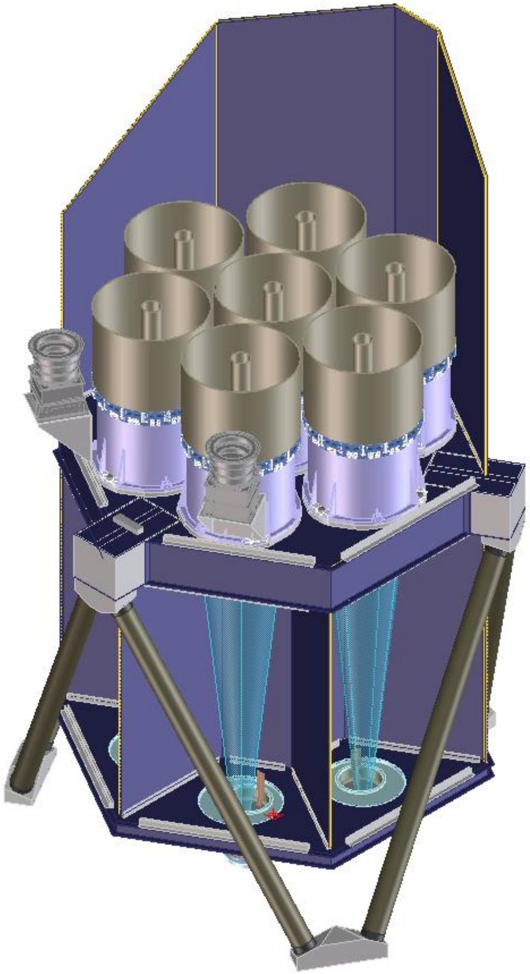

- CFRP Honeycomb Structure
  - ▷ leightweight
  - ▷ thermally stable
- Hexapod Mounting
  - ▷ no thermal/mechanical stresses induced on structure
- Sunshield
- Startracker mounted on structure

CCD-Module

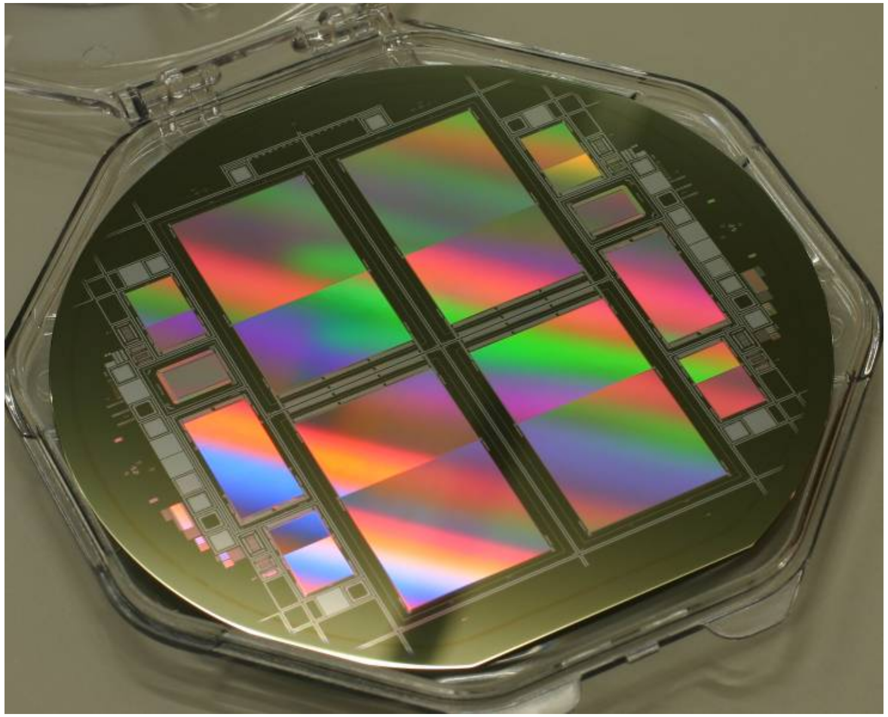

Four 3cm x 3cm CCDs still on Si-Wafer. The CCDs have 384 × 384 pixels in both image and framestore area.

Pixelsize: 75 x 75 µm^2.
Cycle time: 50 msec

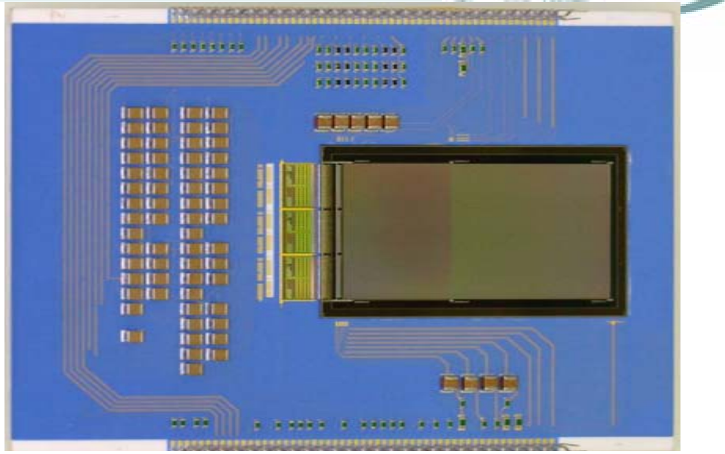

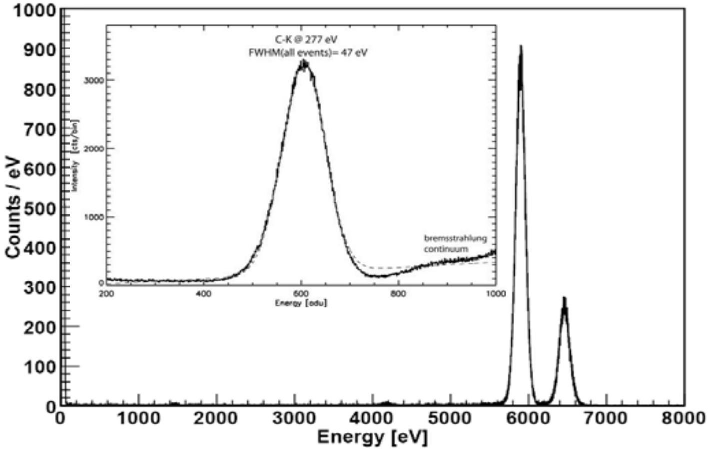

Measurements at C Ka (277eV) and Mn Ka (5,9 keV) on flight-CCDs (2cm × 2cm) show the expected energy resolution and low energy response.

Imaging

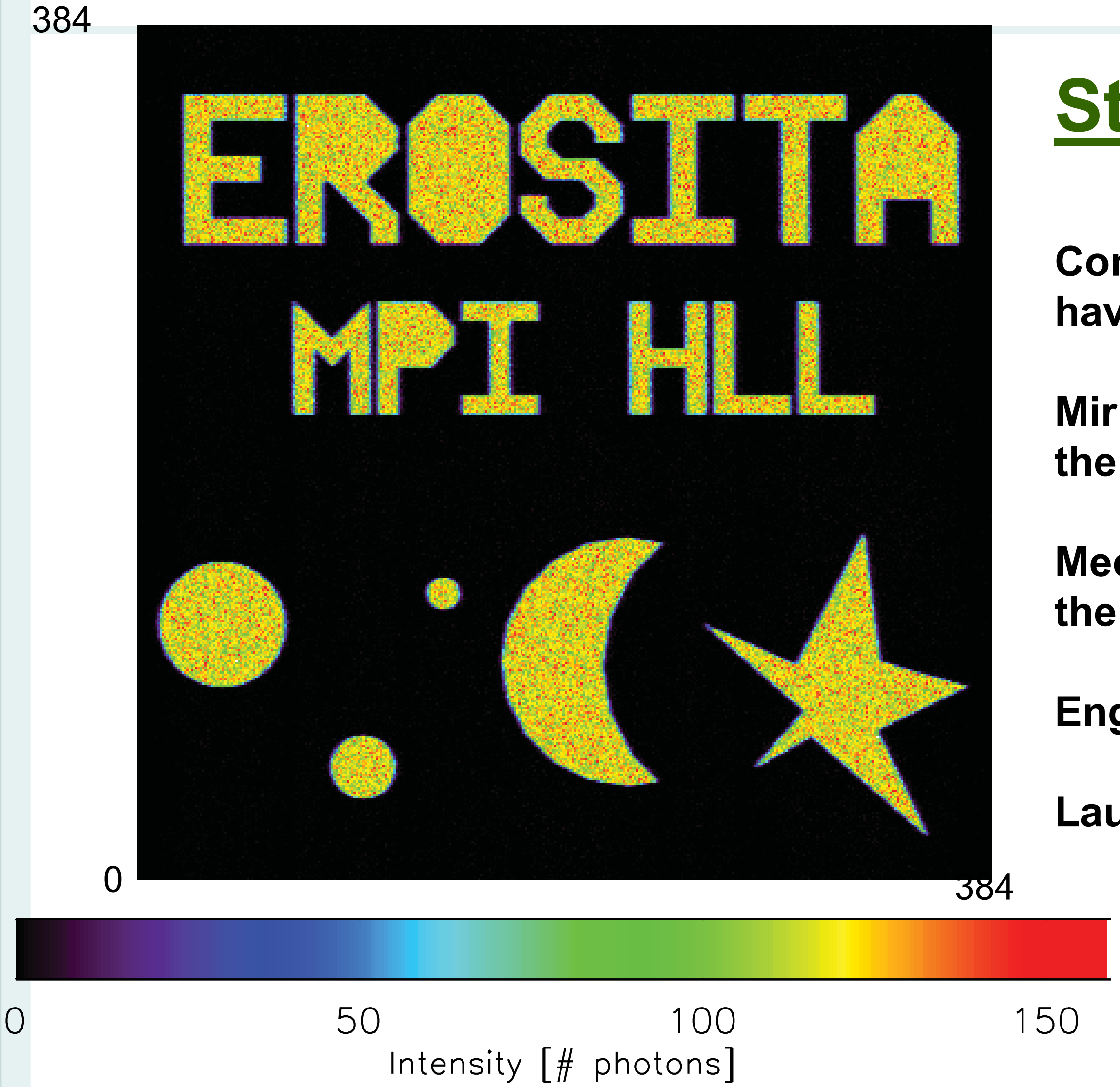

Status of eROSITA

Contracts with ROSKOSMOS have been signed

Mirror fabrication is contracted to the companies MediaLario and ZEISS

Mechanical and electrical models of the flight cameras have been built

Engineering model is in progress

Launch is expected in 2013

Time resolved structure determination with X-ray FELs

Molecules atomic resolution

J. Kirz,
Nature Physics
2, 799 (2006)

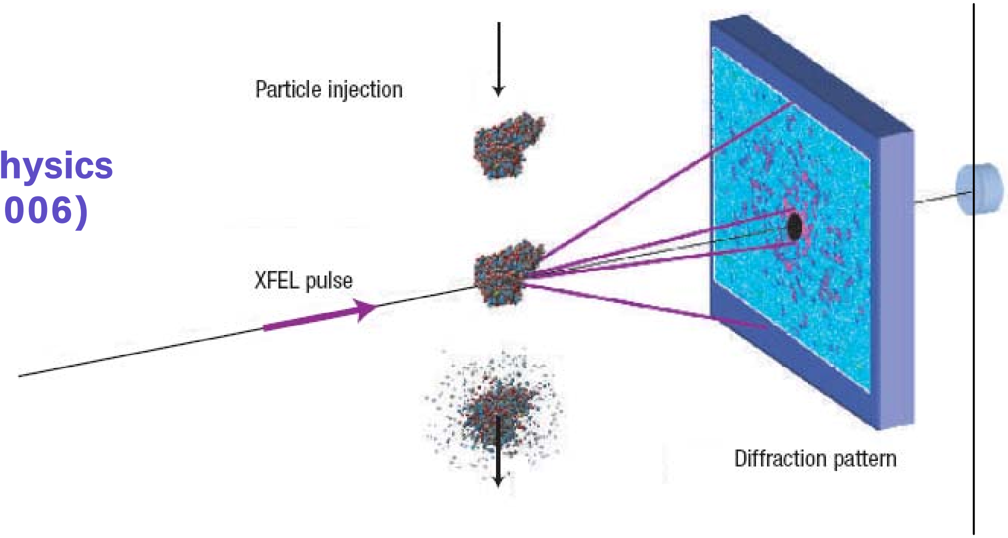

Crystal

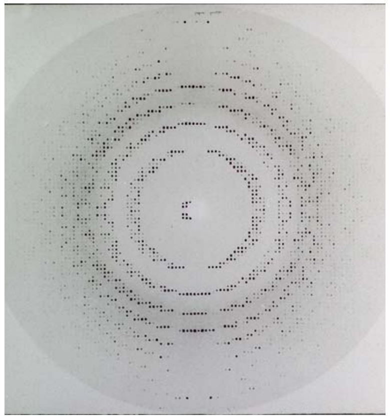

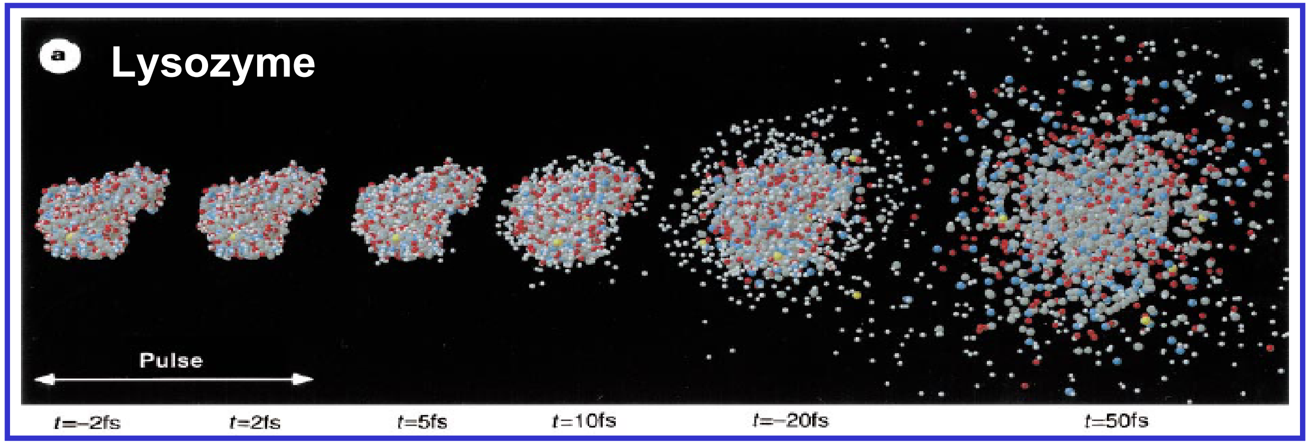

R. Neutze, J. Haidu et al., Nature 406, 752 (2000)

Radiation damage and Coulomb explosion

X-ray scattering: 30 nm Xe - Cluster

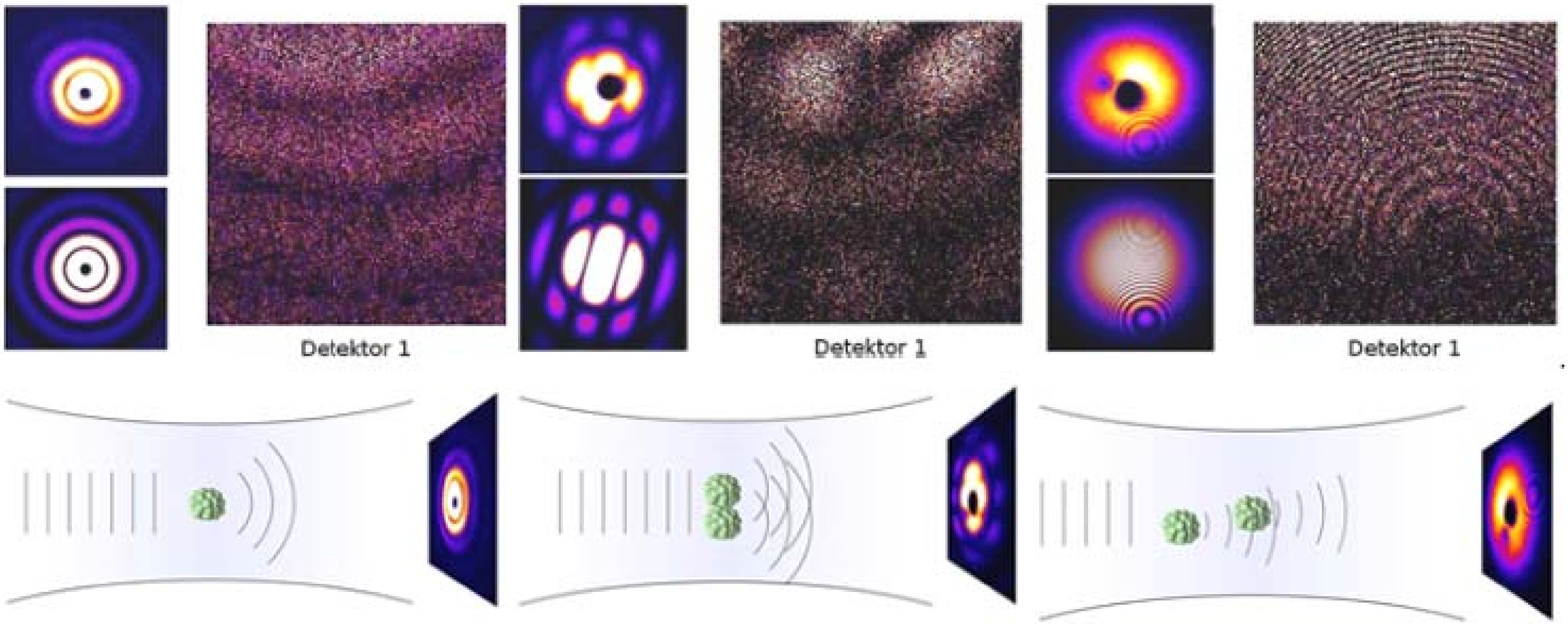

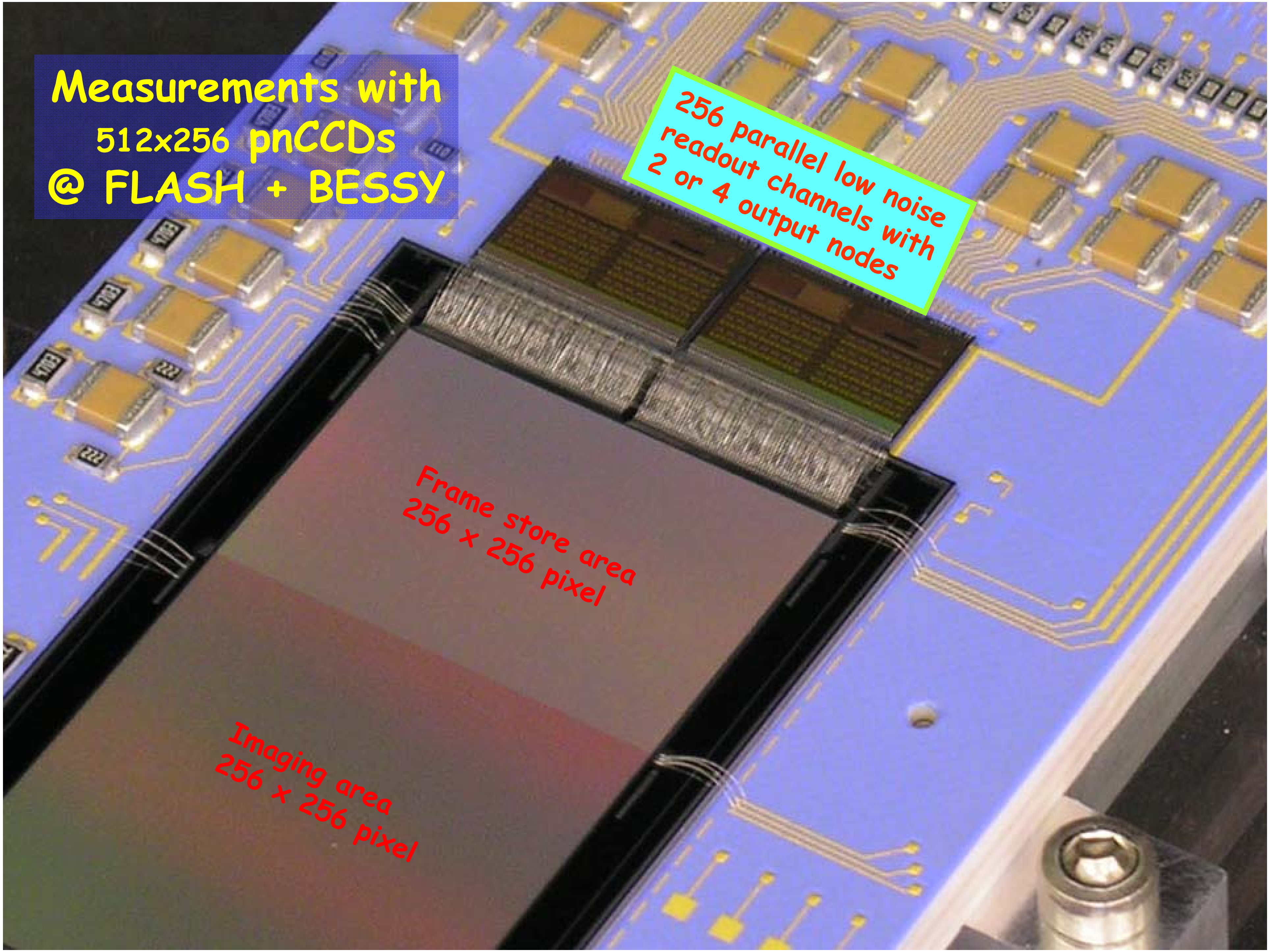

Measurements with 512x256 pnCCDs @ FLASH + BESSY

256 parallel low noise readout channels with 2 or 4 output nodes

Free Electron Lasers

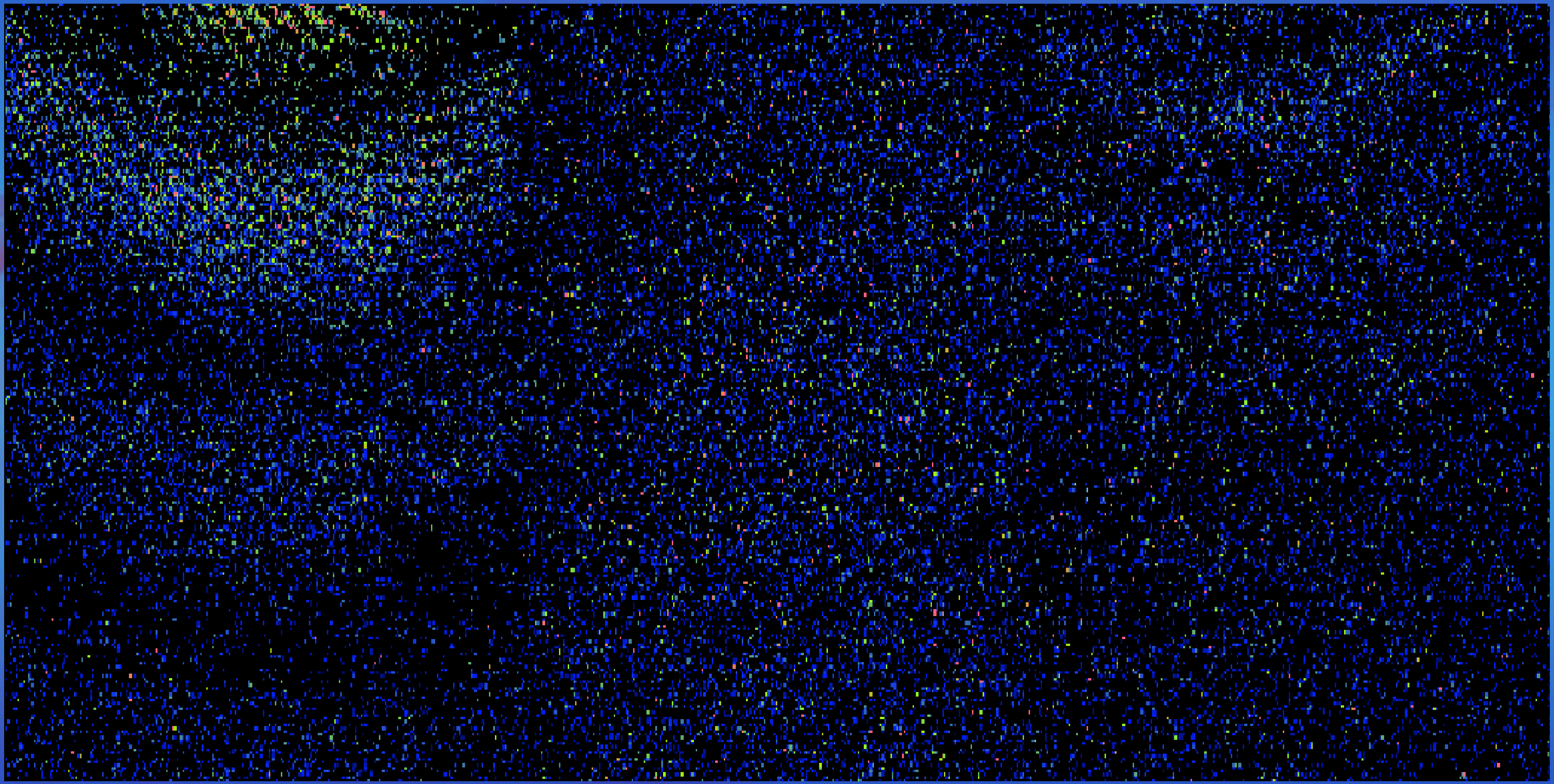

Screen-Shots: To be evaluated!

typ. 5.000 X-rays
per shot per detector,
i.e. ≈ 0.1 photon per pix.

MPI Halbleiterlabor

90 eV X-rays in single photon counting mode !!!

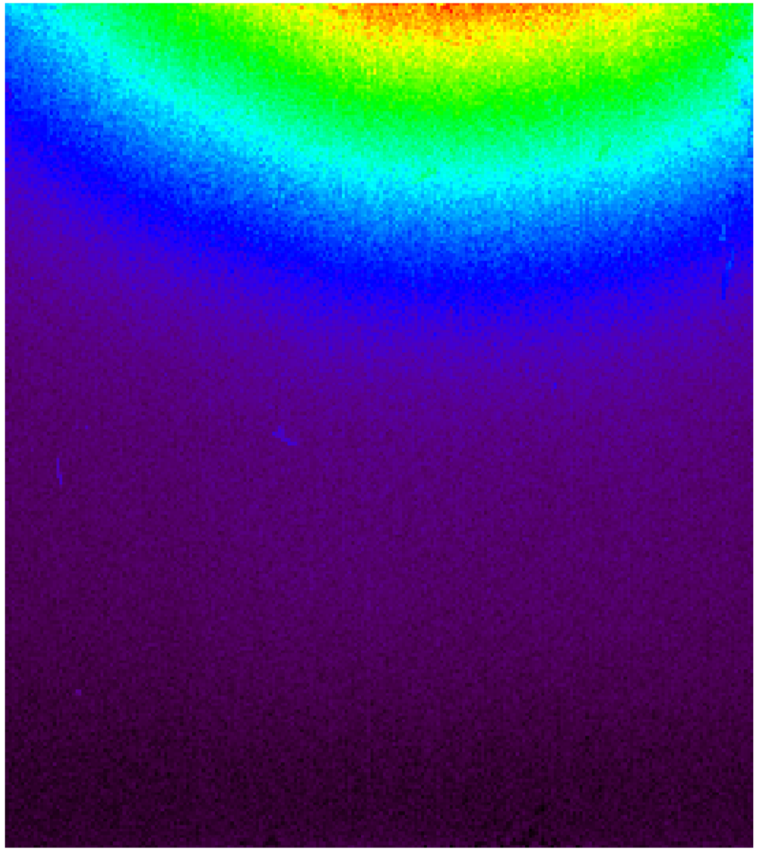

T = -50° C

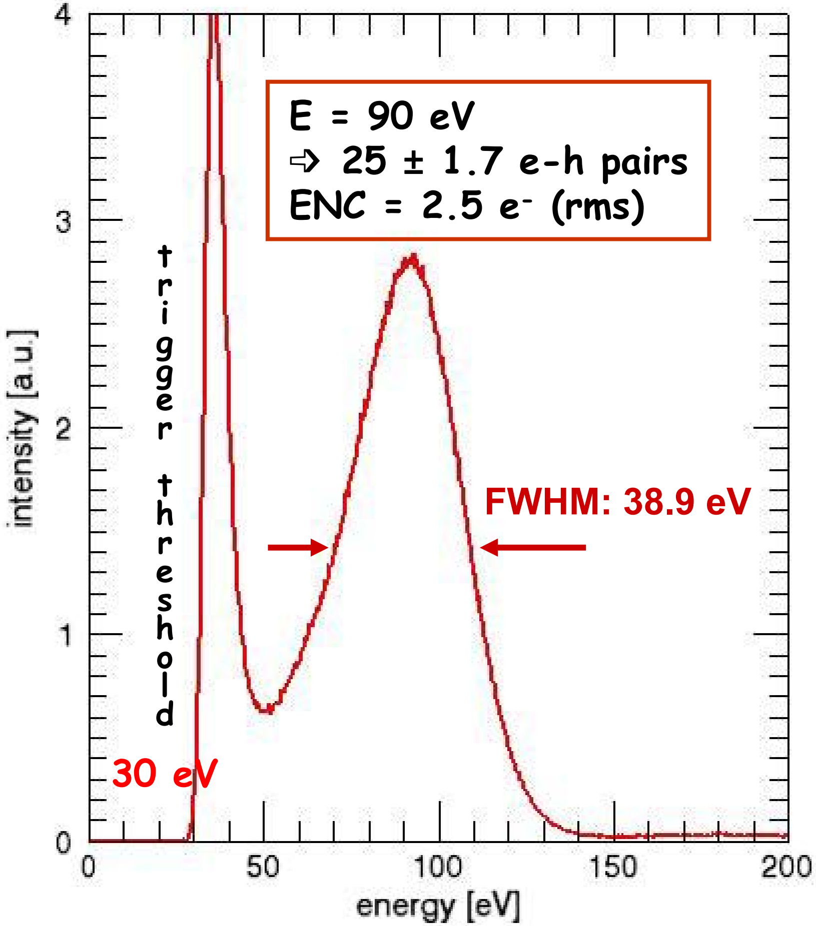

Spectrum from 4.000 frames with 0.01 photons/pixel/frame

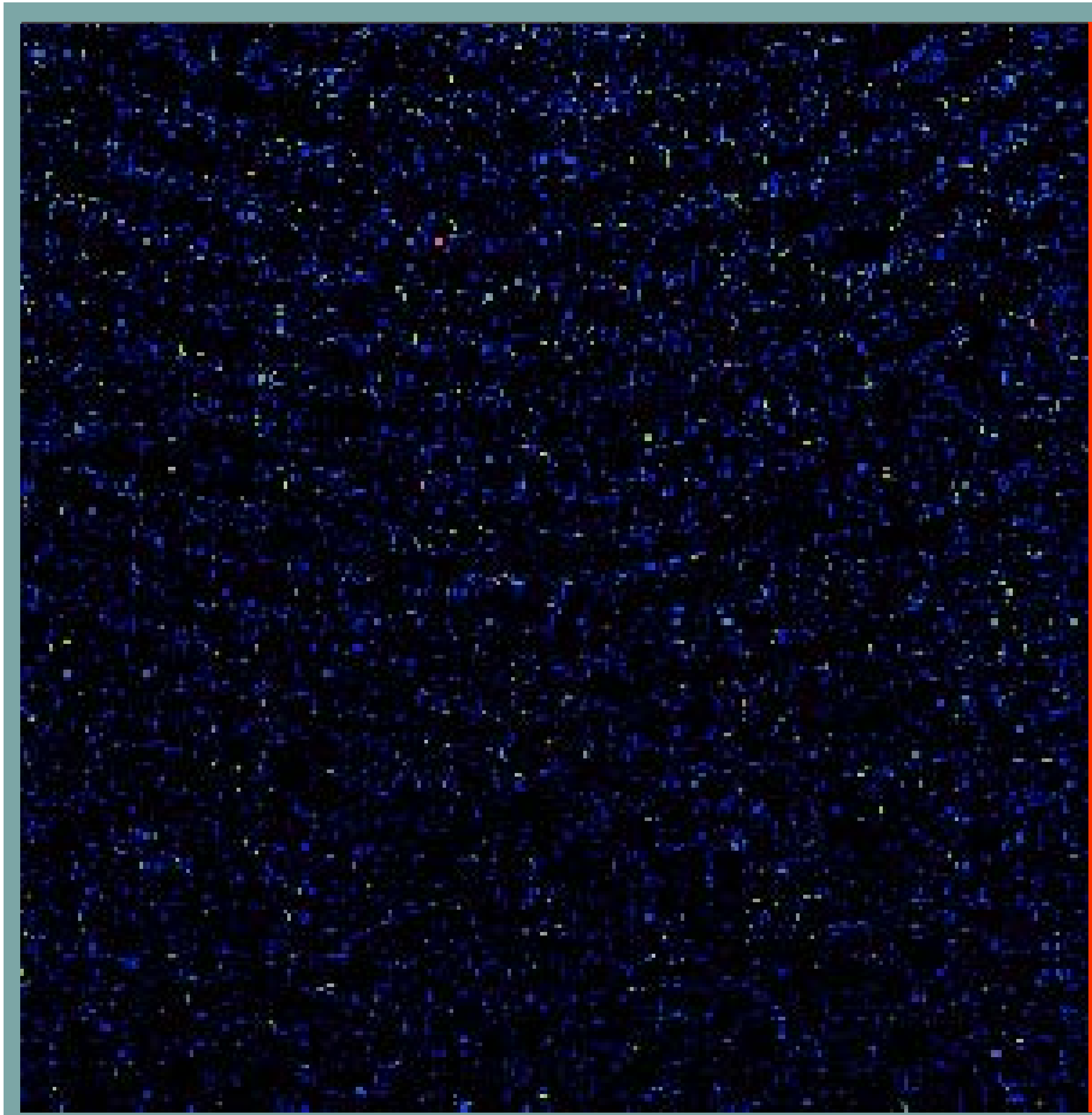

Measurement @ FLASH
λ ≈ 40 nm
on Xe clusters

E = 30 eV

i.e. 8.1 e/h pairs

ENC = 2.7 el. (rms)

ASG

Max-Planck
Advanced Study
Group

Electron Imaging with pnCCDs

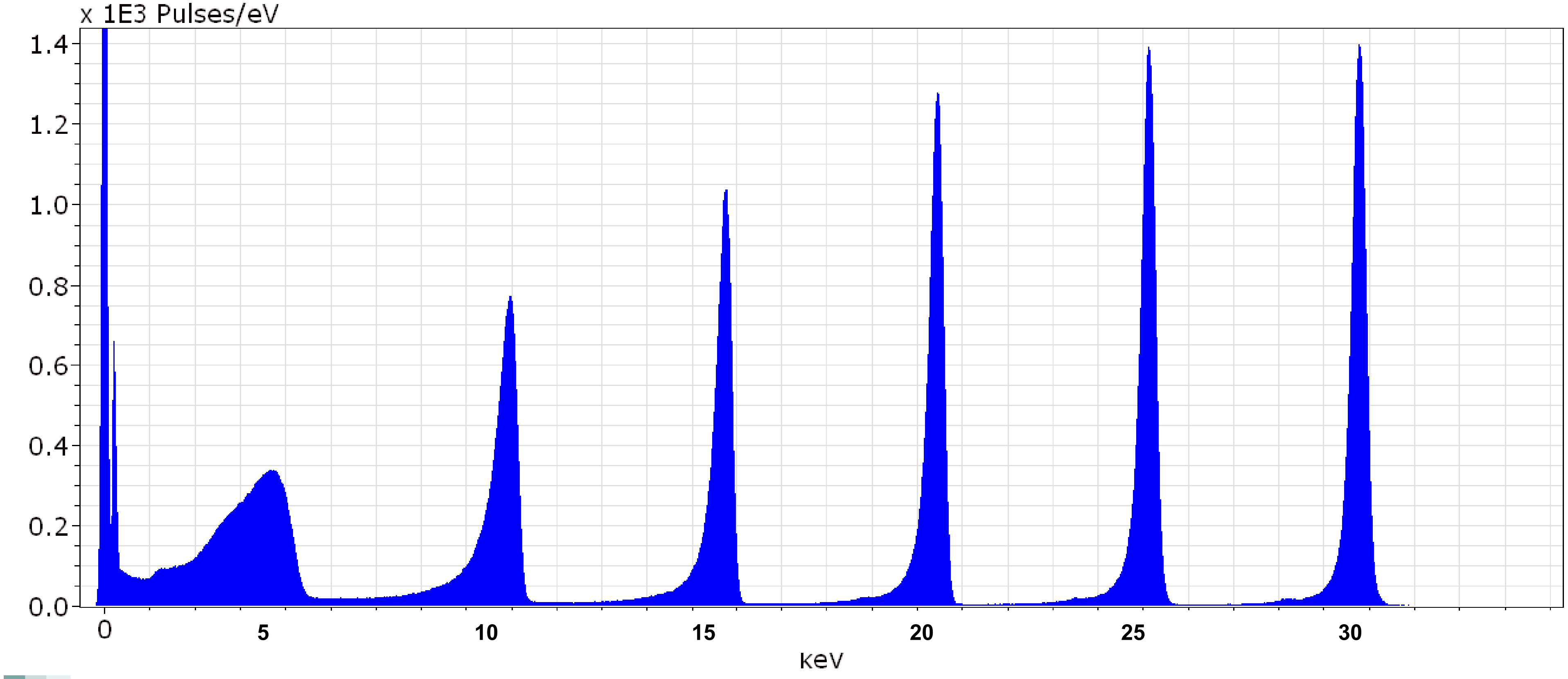

Electrons through: x nm of SiO_2

y nm of Al

TEM Detectors: Imaging

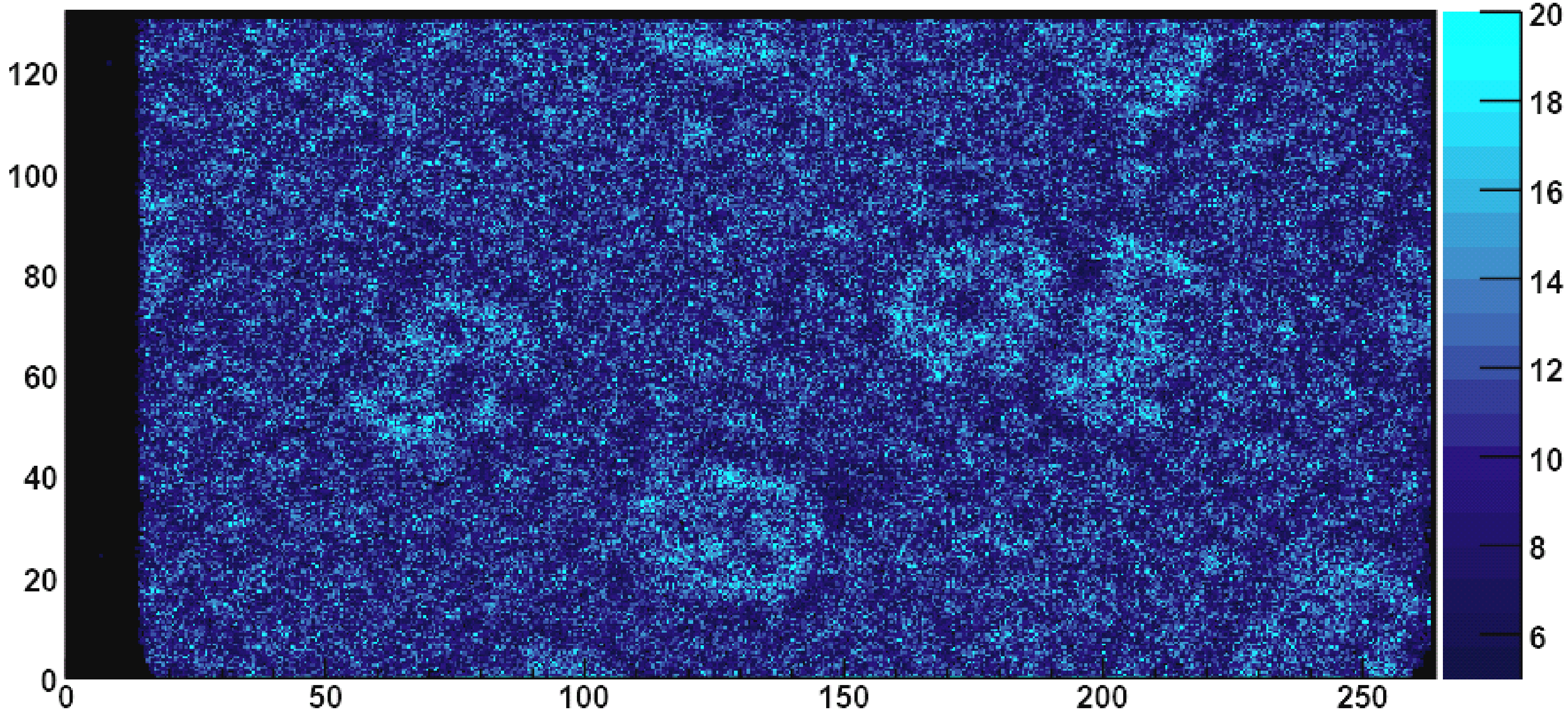

- Ultra low-dose illumination ! (mag. 110k, 1 pixel corresp. to 5Å)
- No visible image on EM fluorescence screen to be seen !

Sample: Proteason (P20S)

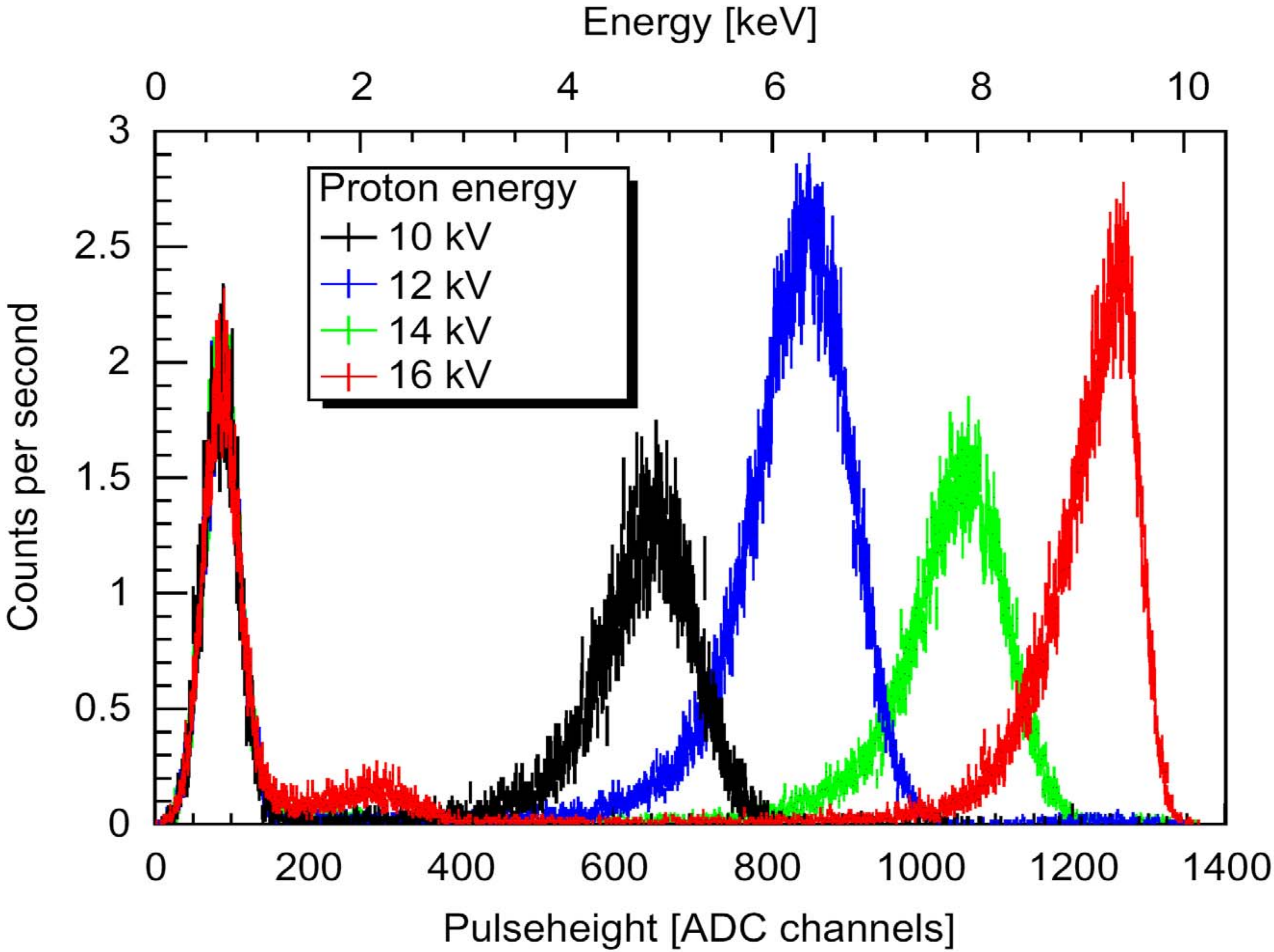
Energy [keV]
0
2
4
6
8
10
3
2.5
2
1.5
1
0.5
0
Counts per second
Proton energy
10 kV
12 kV
14 kV
16 kV
0
200
400
600
800
1000
1200
1400
Pulseheight [ADC channels]

Achievements of the FLASH, LCLS and XFEL

Photon Counting and Integrating X-ray Imaging Detectors

	FLASH, LCLS + XFEL	pnCCD system
single photon resolution	yes	yes
energy range	0.05 < E < 24 (keV)	0.05 < E < 25 [keV]
pixel size (μm)	100	75
sig.rate/pixel/bunch	10^3 (10^5)	10^3 - 10^4
quantum efficiency	> 0.8	> 0.8 from 0.6 to 12 keV
number of pixels	512 x 512 (min.)	1024 x 1024 and 2048 x 2048
frame rate/repetition rate	10 Hz - 120 Hz	up to 250 Hz
Readout noise	< 50 e^- (rms)	< 5 e^- (rms) (2 e^- possible)
cooling	possible	around - 40° C room temperature possible
vacuum compatibility	yes	yes
preprocessing	no (yes) ?	possible upon request

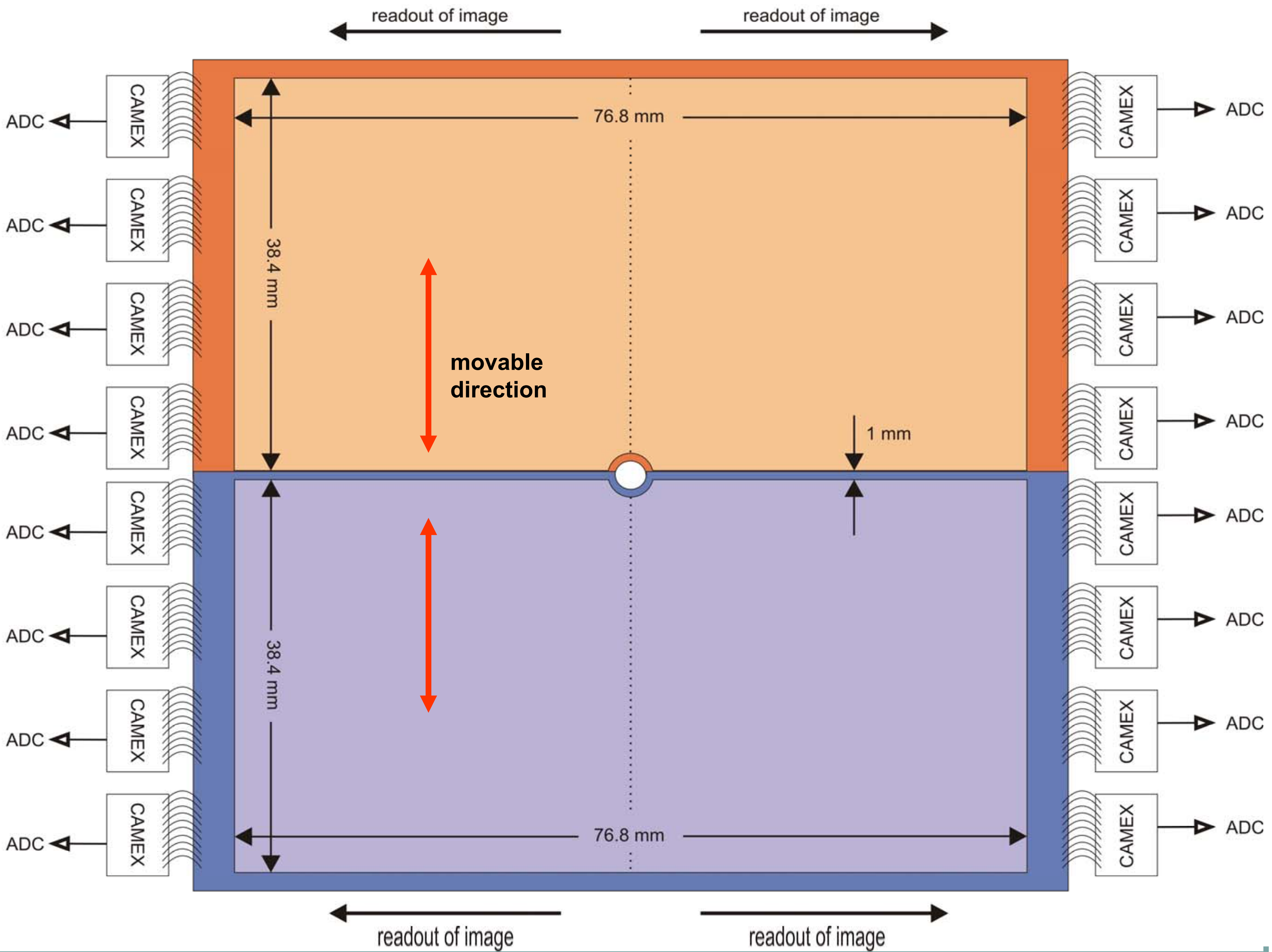
readout of image
readout of image
ADC
CAMEX
76.8 mm
38.4 mm
movable direction
1 mm
38.4 mm
76.8 mm
readout of image
readout of image

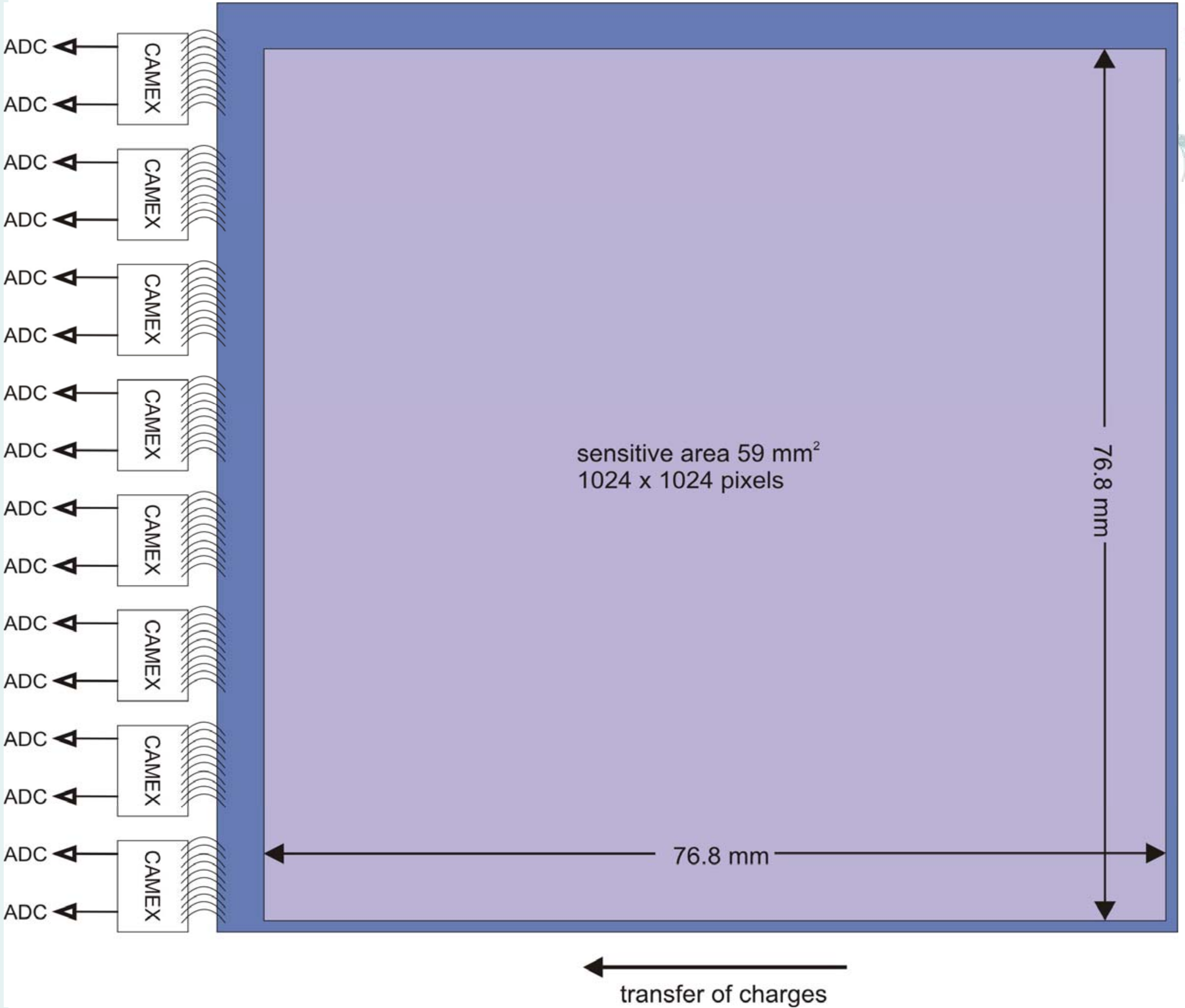

sensitive area 59 mm²
1024 x 1024 pixels

transfer of charges

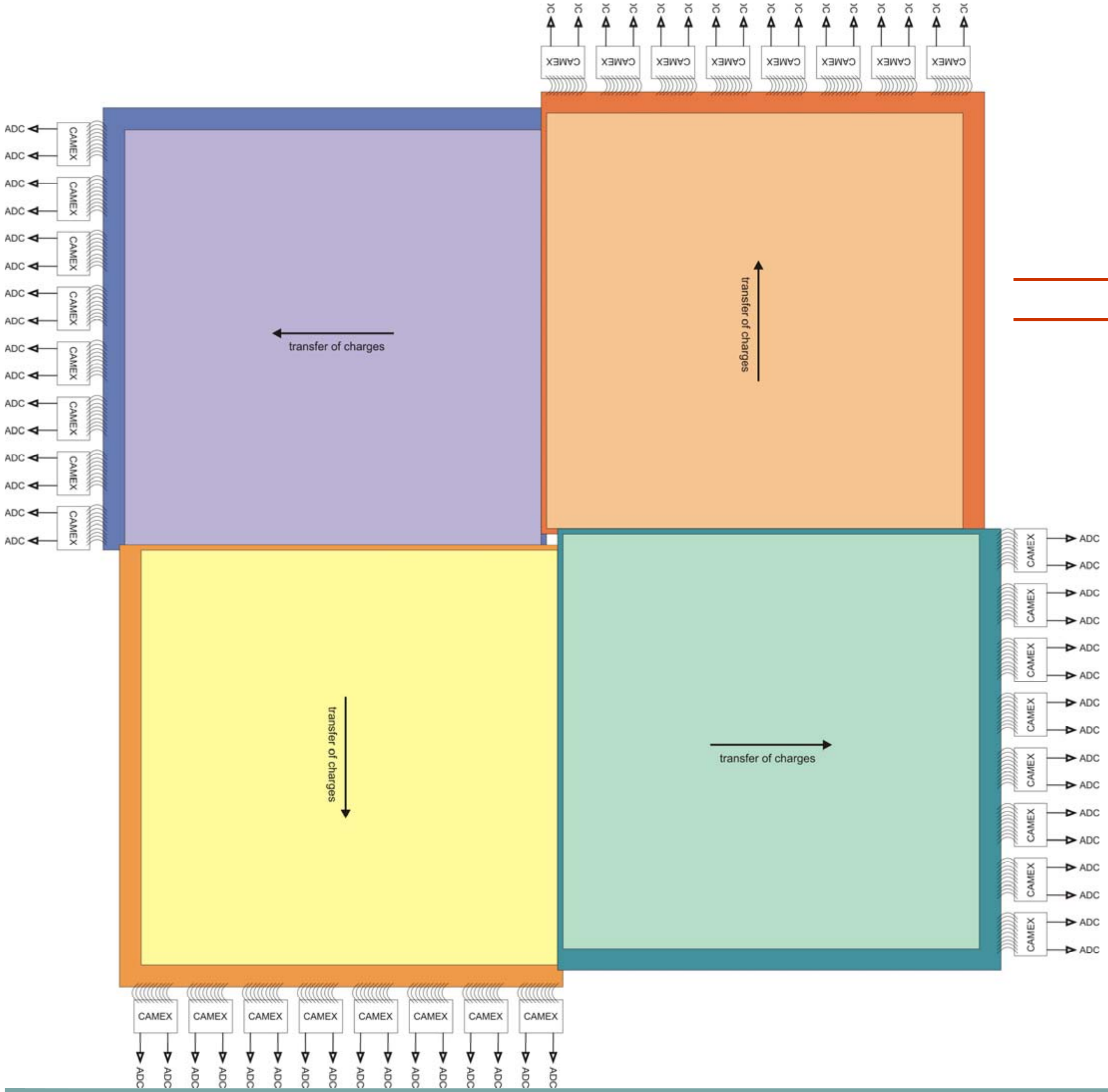

Expected system properties

pixel size: 50 x 50 μm^2
or 75 x 75 μm^2
resolution: $\sigma_{x,y} \le 10\ \mu m$
frame rate: 150 Hz
noise: 5 el. (rms)
CHC: 500.000 el.
PSF: typ. 3x3
EDpP: 20 MeV
thickness: 450 μm

pnCCD: 1024 x 512, 30 cm^2

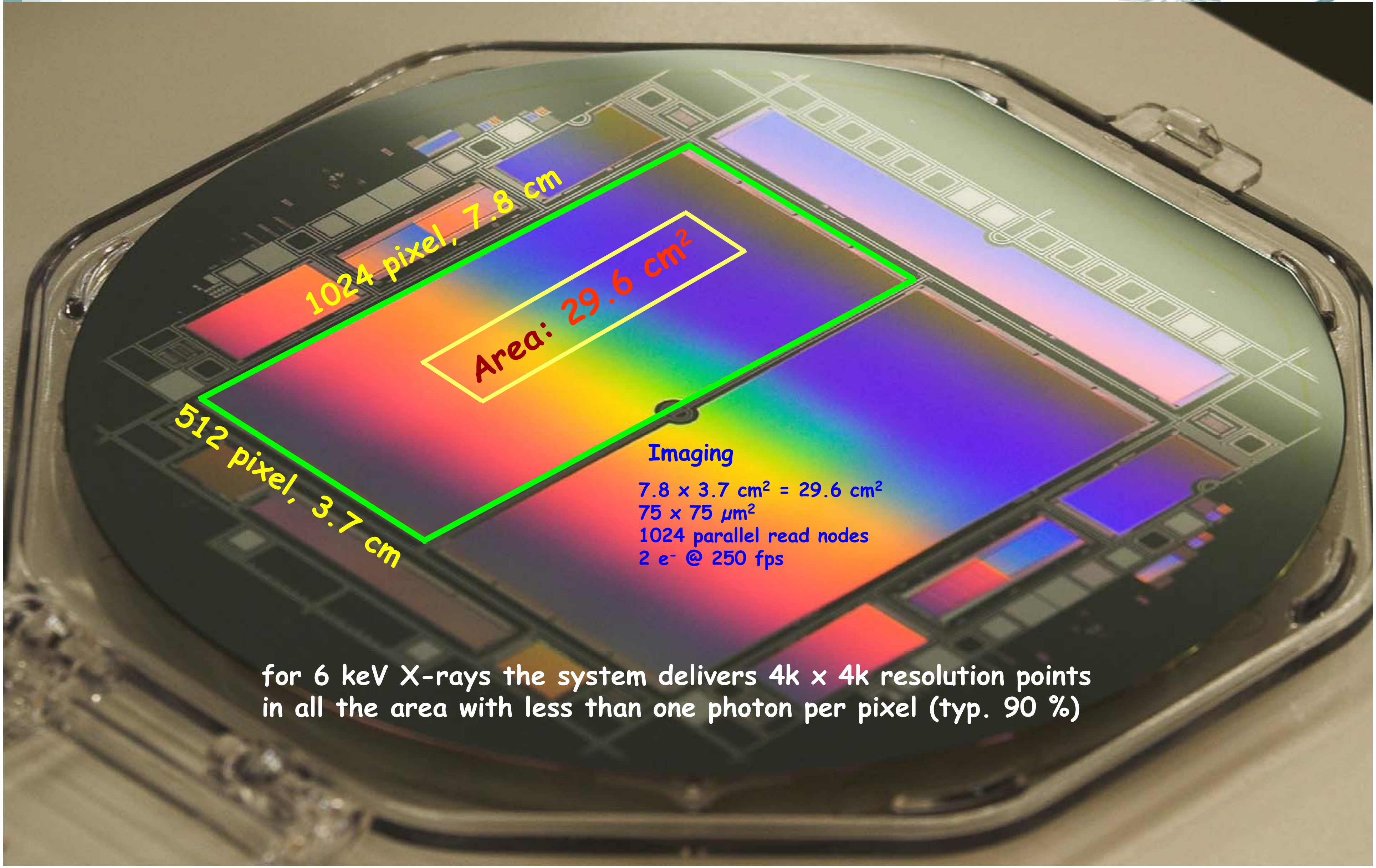

Imaging

7.8 x 3.7 cm^2 = 29.6 cm^2
75 x 75 μm^2
1024 parallel read nodes
2 e$^-$ @ 250 fps

for 6 keV X-rays the system delivers 4k x 4k resolution points in all the area with less than one photon per pixel (typ. 90 %)

CFEL-ASG MultiPurpose Chamber

Integrated Reaction Microscope

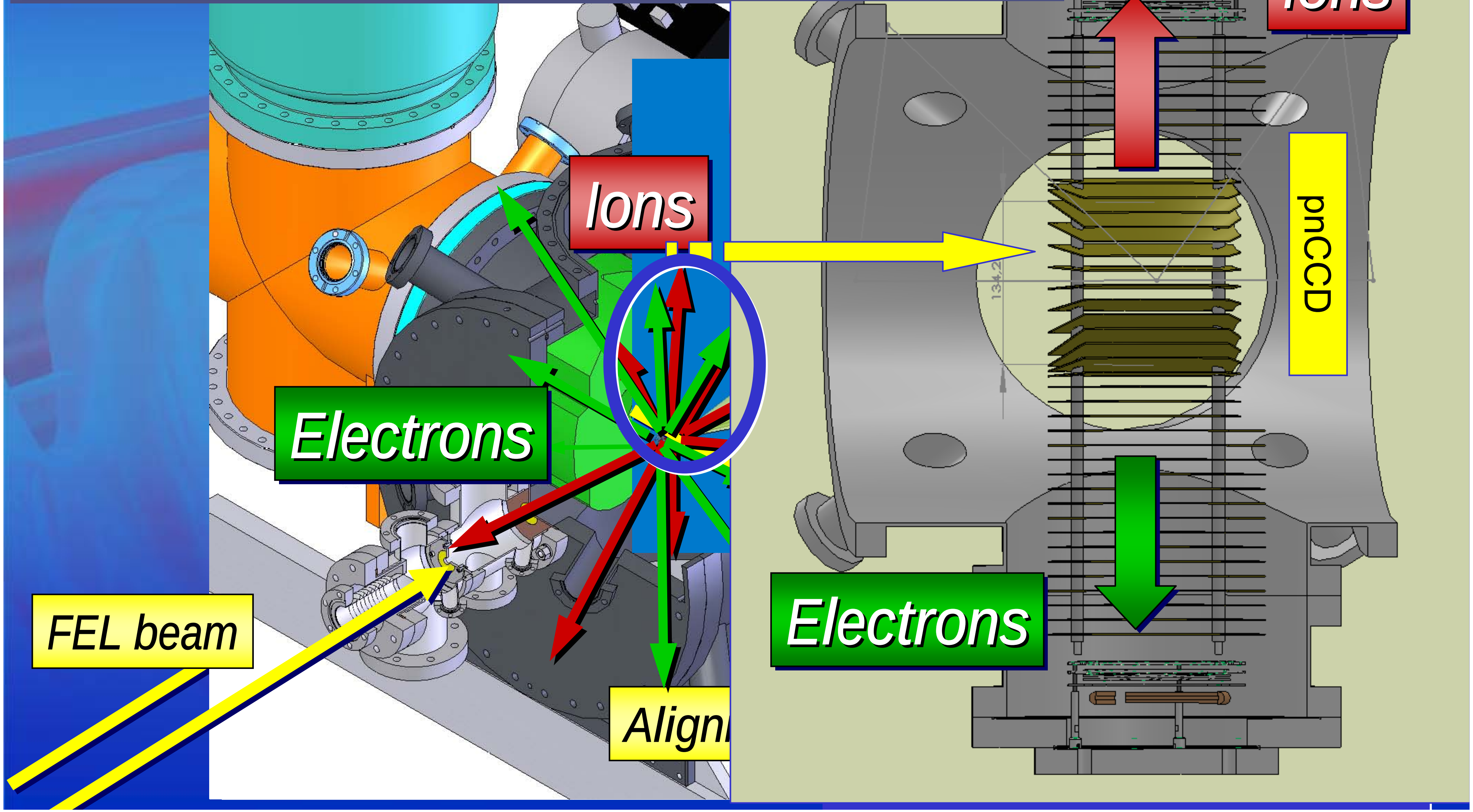

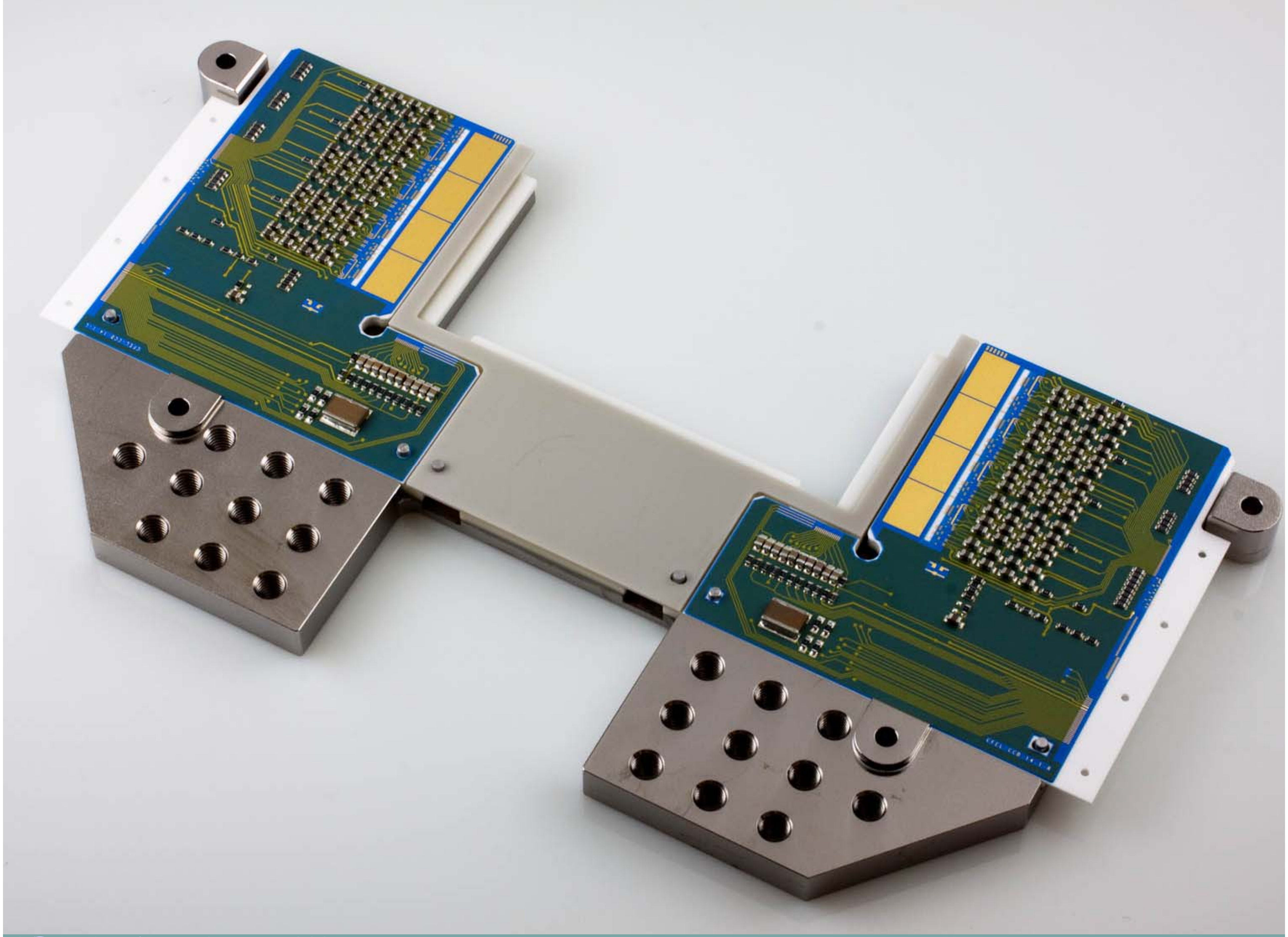


Innenplatine,
C14
P/N112-13500
S/N 09/00002
LP Innenplatine C14
P/N 112-13510/C
1
TOP
2609

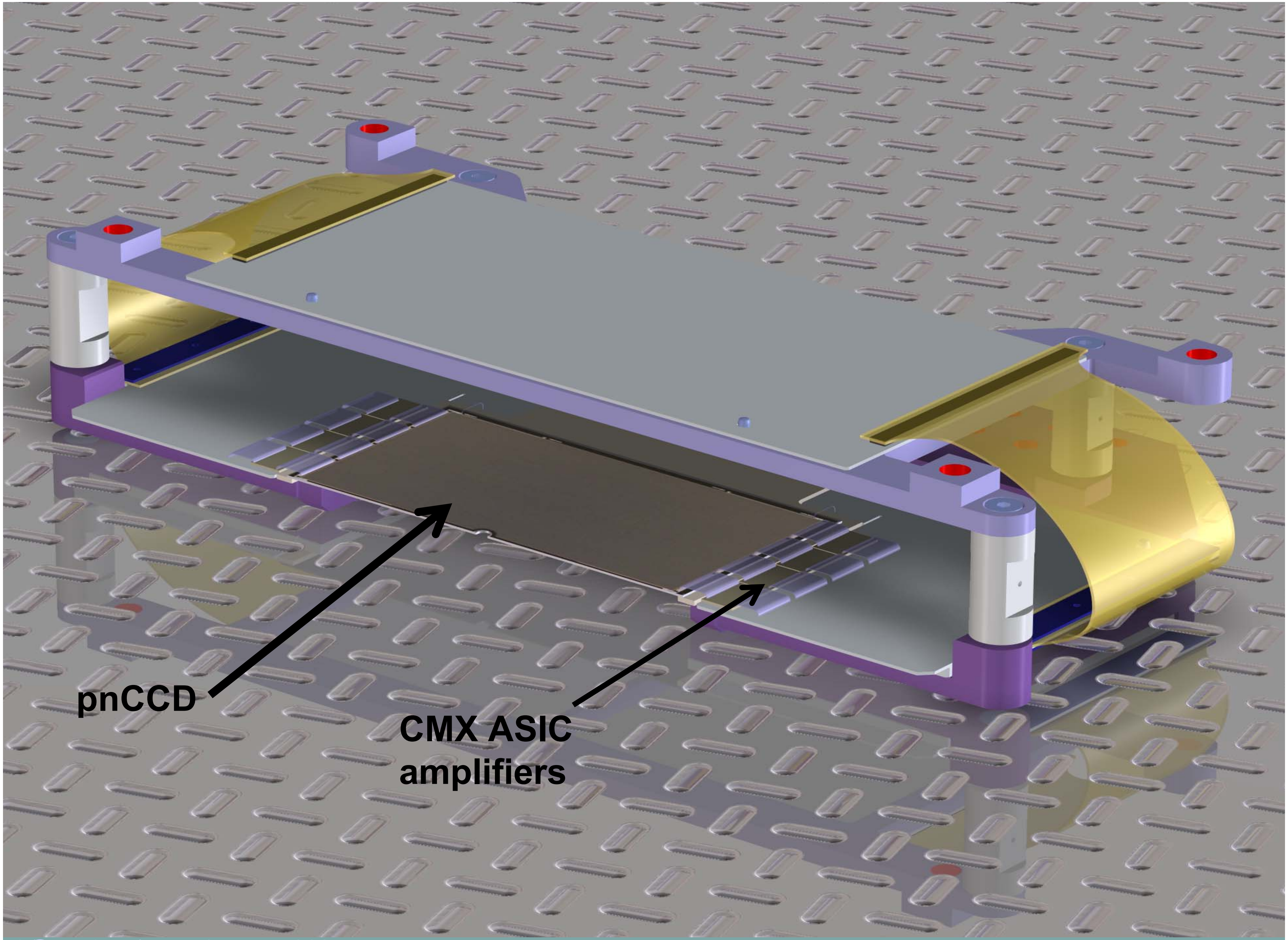
pnCCD
CMX ASIC amplifiers

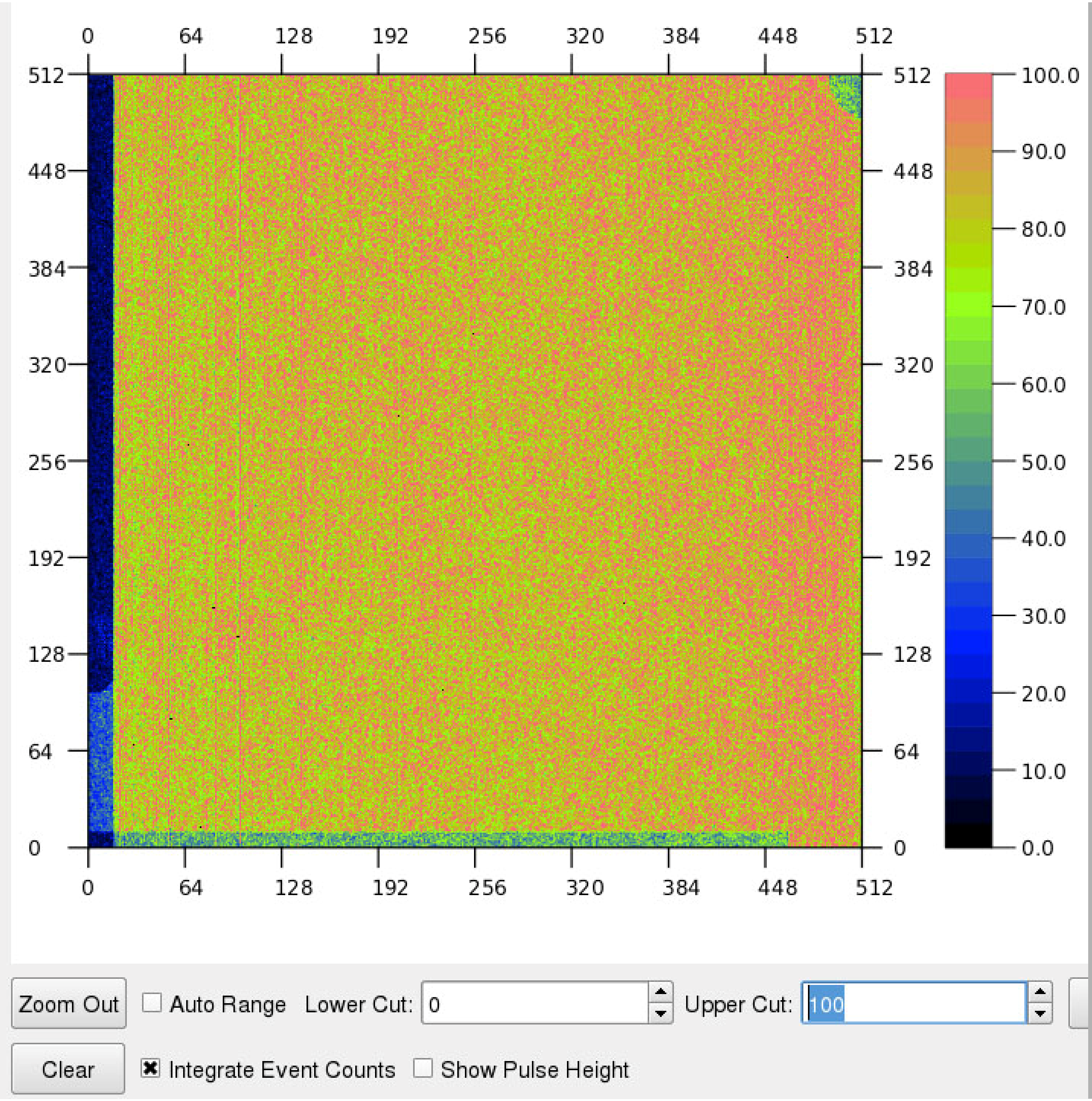

☐ Auto Range Lower Cut: 0 Upper Cut: 100

☒ Integrate Event Counts ☐ Show Pulse Height

4 "halves" (1024x1024) were sucessfully tested

operation in the coherence experiments starts on August – 5, 7 am (CET)

noise floor at – 40 ° C
ENC = 3.3 el. (rms)

in the CAMP set-up with reset per line and a lower gain by a factor of 4-16:
ENC ≈ 10 el. (rms)

QE @ 2 keV = 98 %

Frame rate: up to 150 Hz

CAMP pnCCD module performance

(typical module)

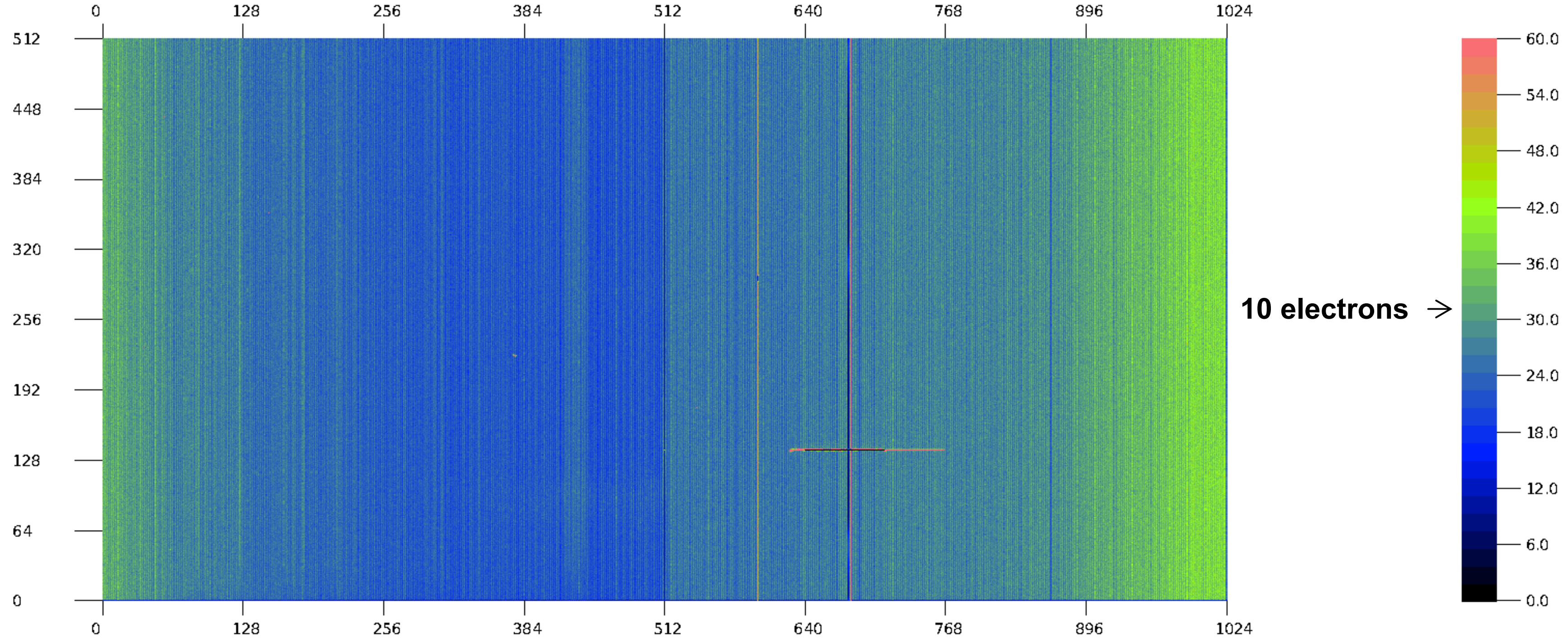

- → **588 noisy or bad pixel out of 524.288 pixel**
- → **average noise is 8 electrons (rms) at – 40 ° C, frame rate up to 120 Hz**
- → **min. X-ray energy: 850 eV, i.e. 240 electrons. S/N = 30/1**

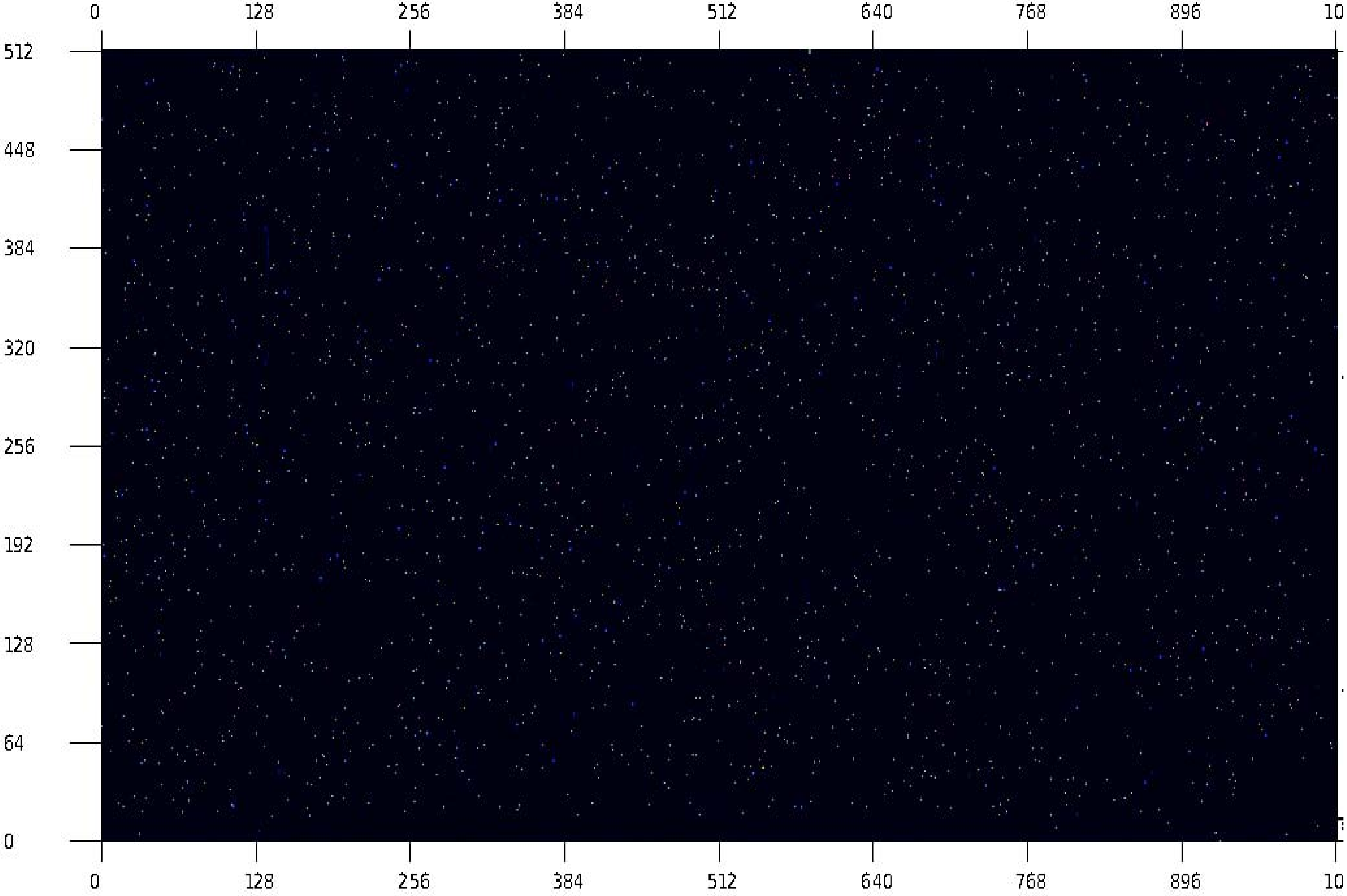
0
128
256
384
512
640
768
896
10
512
448
384
320
256
192
128
64
0

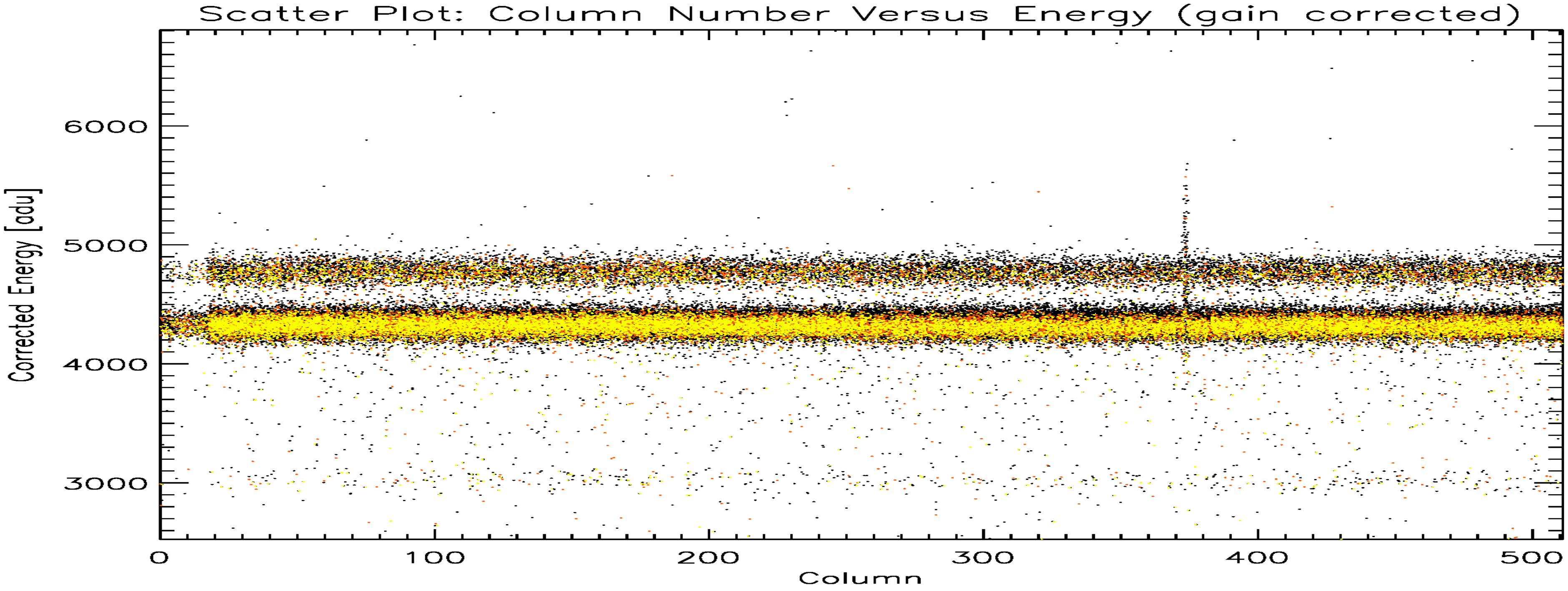
Scatter Plot: Column Number Versus Energy (gain corrected)
Corrected Energy [adu]
6000
5000
4000
3000
0
100
200
300
400
500
Column

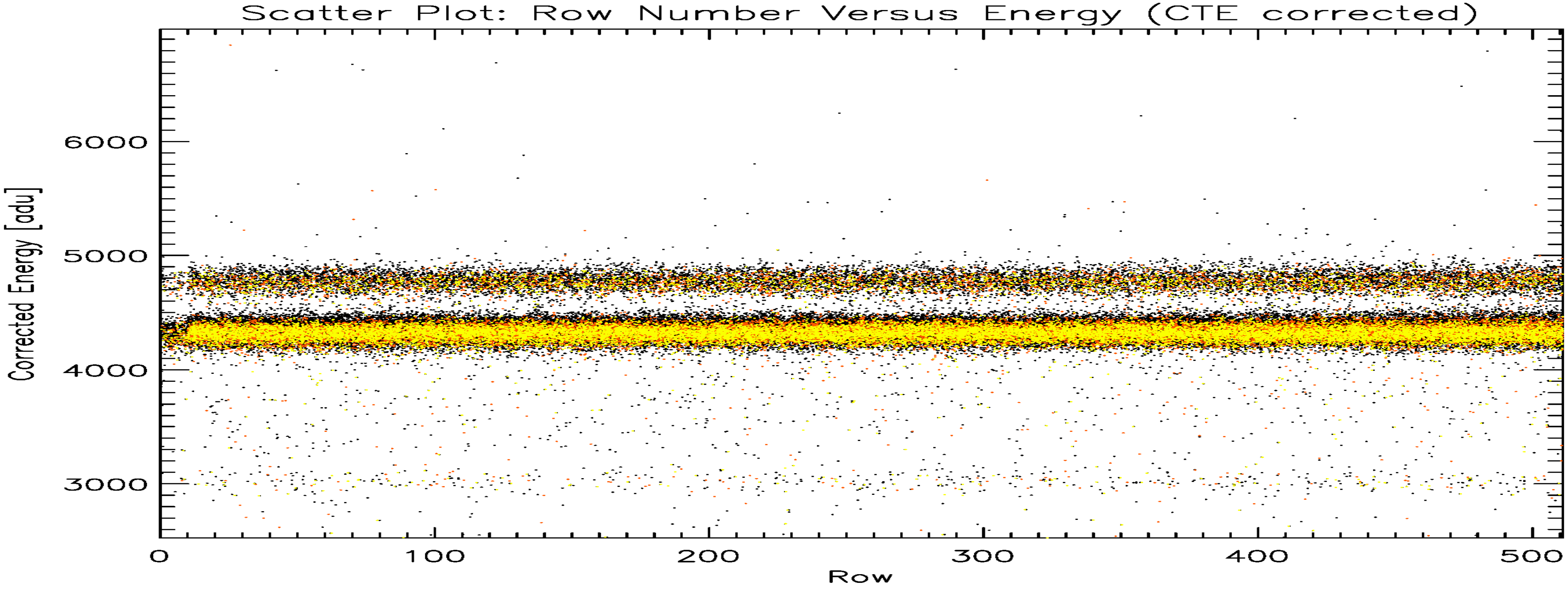
Scatter Plot: Row Number Versus Energy (CTE corrected)
Corrected Energy [adu]
6000
5000
4000
3000
0
100
200
300
400
500
Row

CAMP pnCCD module performance

(typical module)

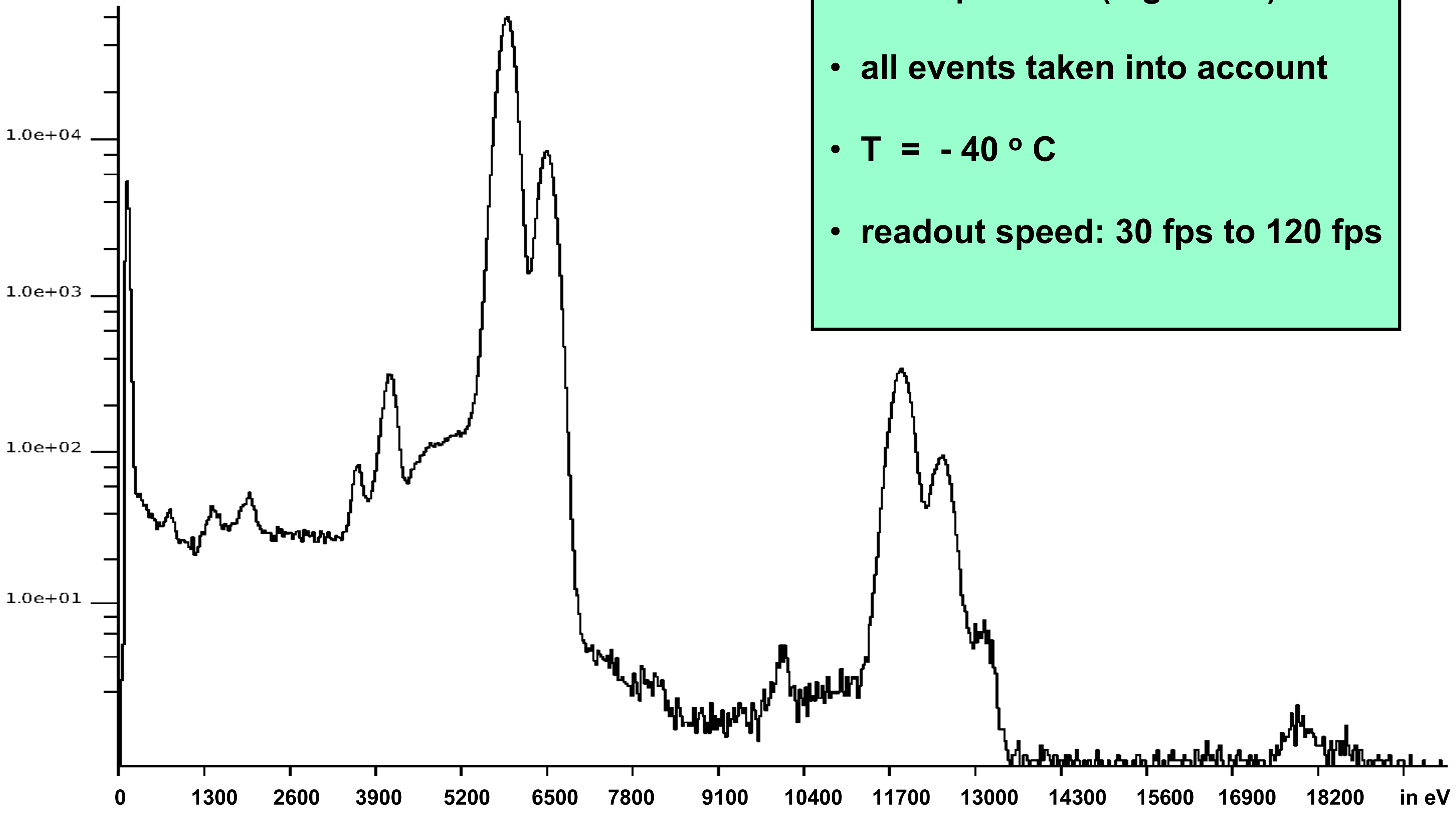

- ^{55}Fe spectrum (log. scale)
- all events taken into account
- T = - 40 ° C
- readout speed: 30 fps to 120 fps

First Experiments at LCLS

- Fluorescence (PI: Daniel Rolles)
- Cluster (PI: Christoph Bostedt)
- Imaging (PI: Henry Chapman)

- Molecule alignment (PI: HC and Jochen Küpper)

  (was cancelled because of safety issues,

  will be carried out in May 2010)

Fluorescence Spectroscopy @ LCLS

Daniel Rolles experiment

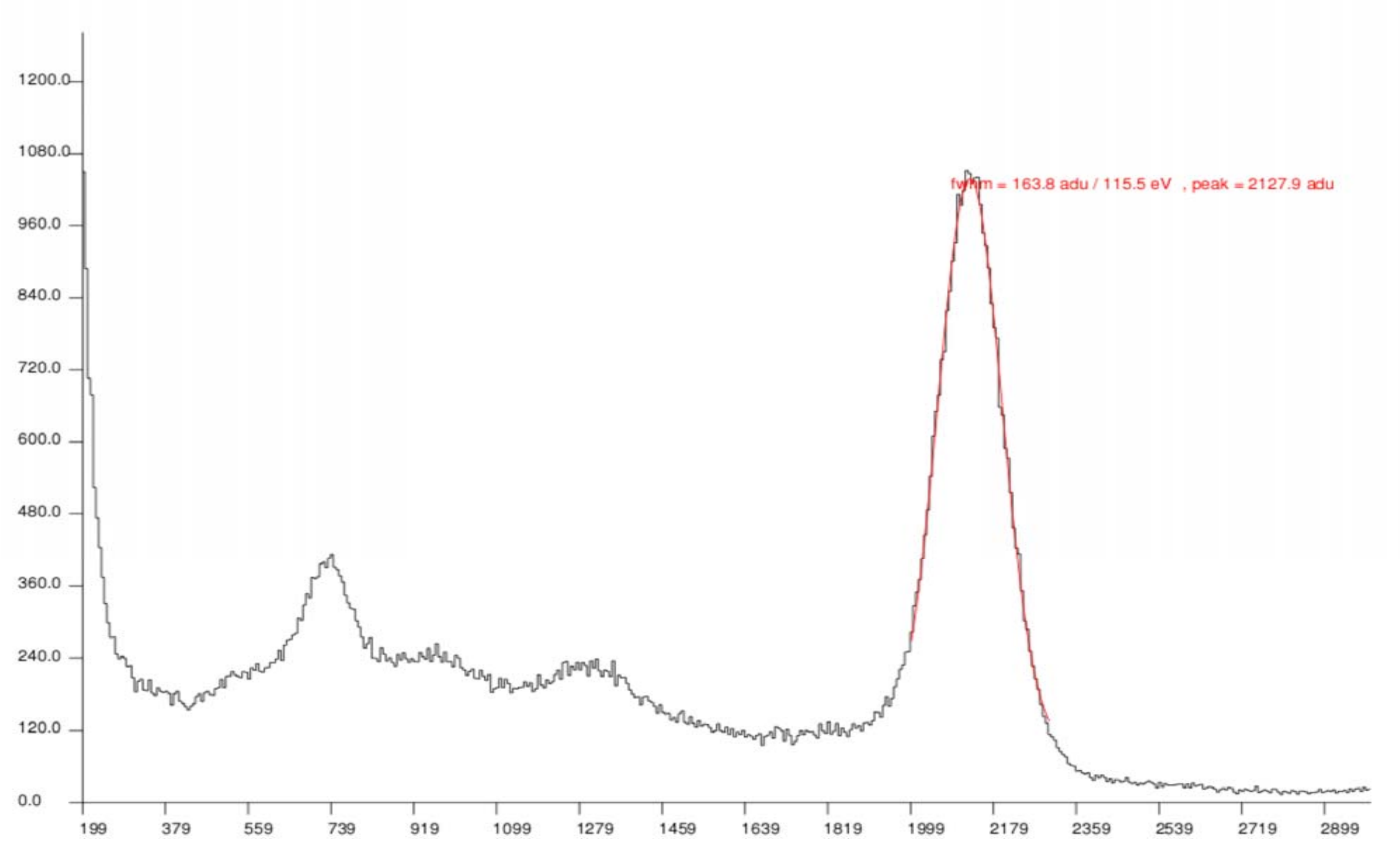

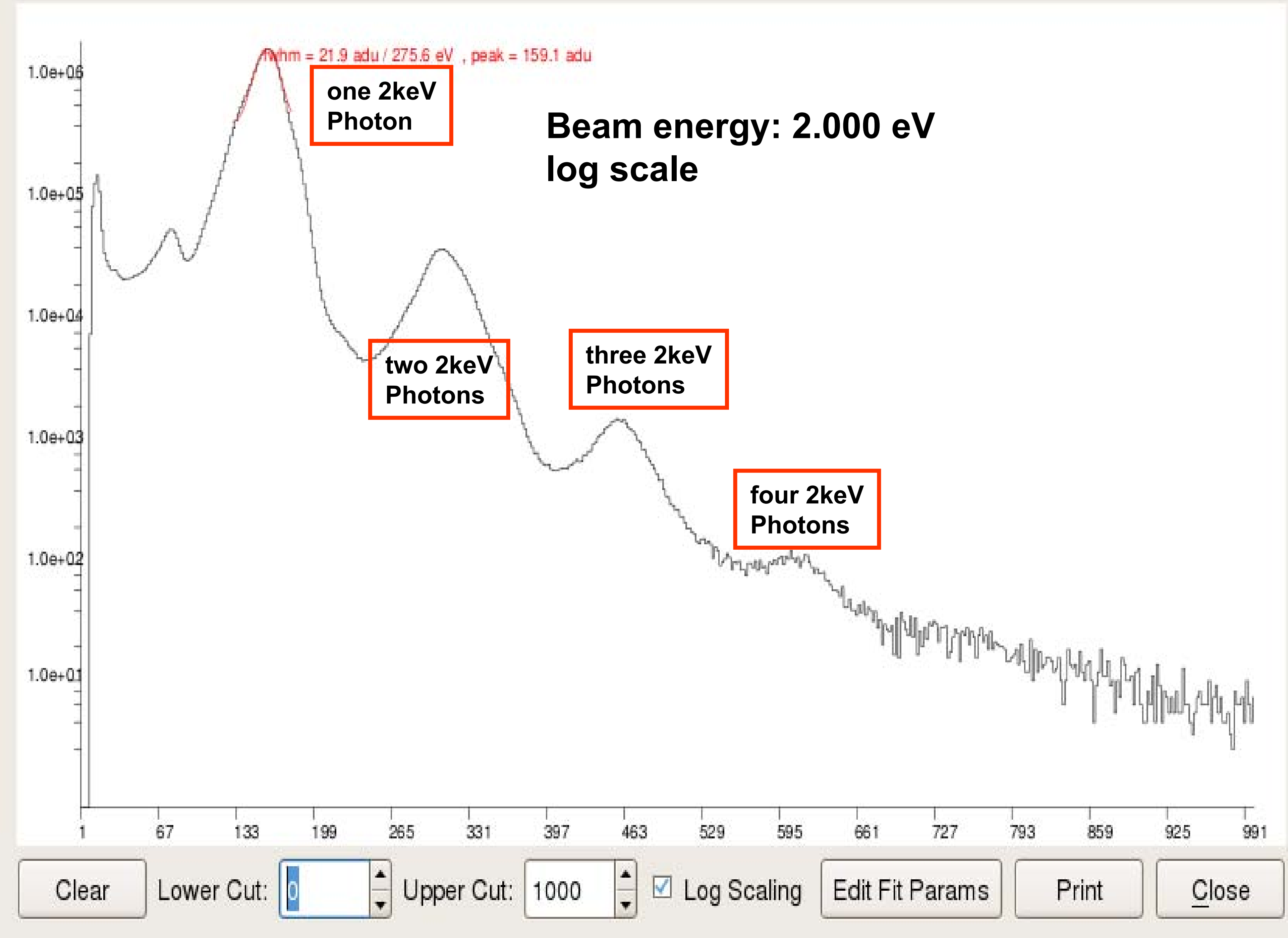

fwhm = 21.9 adu / 275.6 eV , peak = 159.1 adu

Lower Cut: 0

Upper Cut: 1000

☑ Log Scaling

one 2keV Photon

two 2keV Photons

three 2keV Photons

four 2keV Photons

Beam energy: 2.000 eV
log scale

Achievements with pnCCDs at FLASH and LCLS

Photon Counting and Integrating X-ray Imaging Detectors

	FLASH, LCLS	pnCCD system
single photon resolution	yes	yes
energy range	0.05 < E < 24 (keV)	0.05 < E < 25 [keV]
pixel size (µm)	100	75
sig.rate/pixel/bunch	10^3 (10^5)	10^3 - 10^4
quantum efficiency	> 0.8	> 0.8 from 0.8 to 12 keV
number of pixels	512 x 512 (min.)	2 times 1024 x 1024
frame rate/repetition rate	10 Hz - 120 Hz	up to 120 Hz
Readout noise	< 50 e^- (rms)	< 5 e^- (rms) (up to 20 e^- in low gain)
cooling	possible	around - 40° C room temperature possible
vacuum compatibility	yes	yes
preprocessing	no (yes) ?	possible upon request


GORBEL
COFFING

DEPFET readout

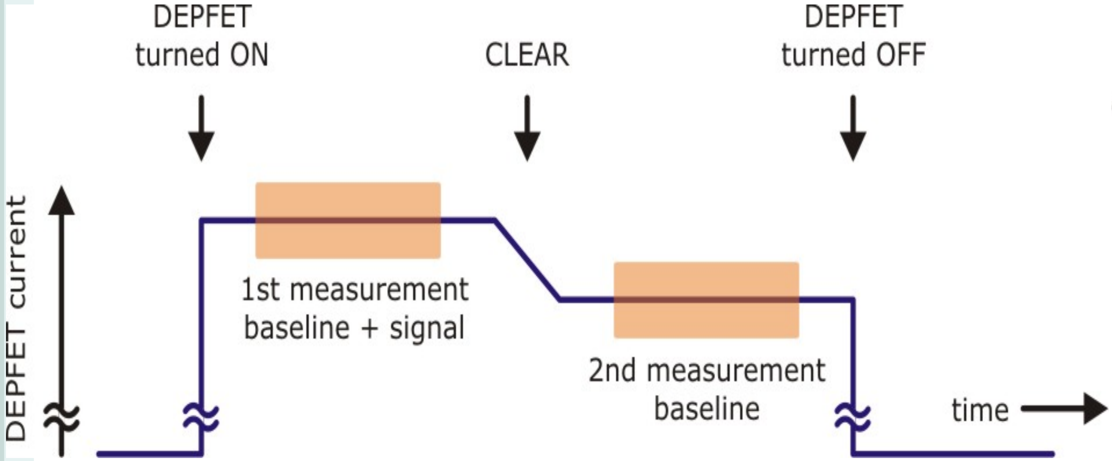

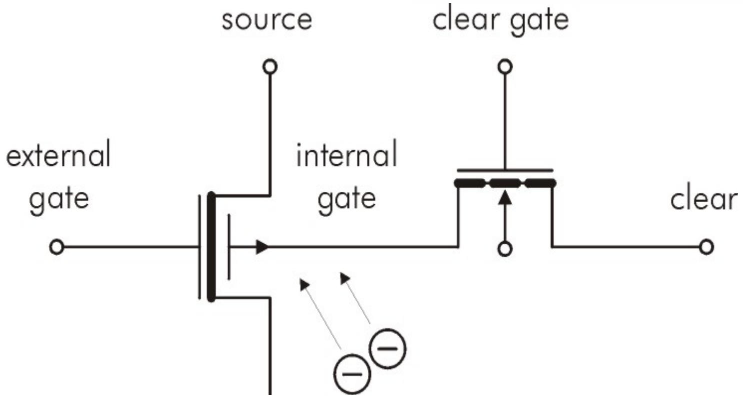

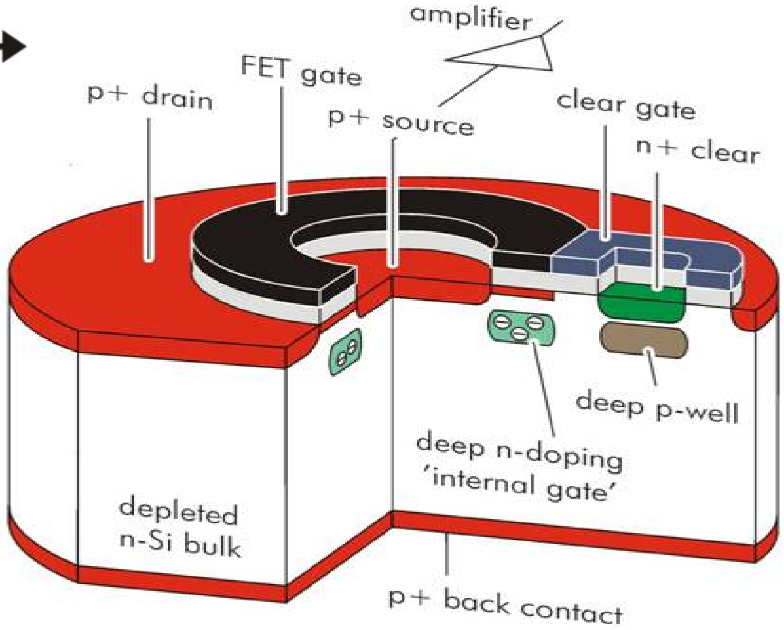

- ***Measurement of signal***
  - **Measure signal levels**
    - **source potential / drain current**
  - **Measure both before and after clear**
  - **Calculate the difference**
    - **correlated double sampling (CDS)**

DEPFET matrix devices

- *Readout scheme*
  - ▷ Global drain contact
  - ▷ Gate,Clear and Cleargate connected row-wise
  - ▷ Sources connected column-wise
  - ▷ Only one row is turned on and read out
- *Source follower readout*
  - ▷ Column bias by current source
  - ▷ Alternatively: Conversion of drain current
- *Target:*
  - ▷ Framerate 1 kHz
  - ▷ Array dimension 1024 x 1024
  - ▷ Energy resolution < 125 eV FWHM @ 5.9 keV
- *2 ASICS required:*
  - ▷ Analog Amplifier ASIC
  - ▷ Switcher ASIC

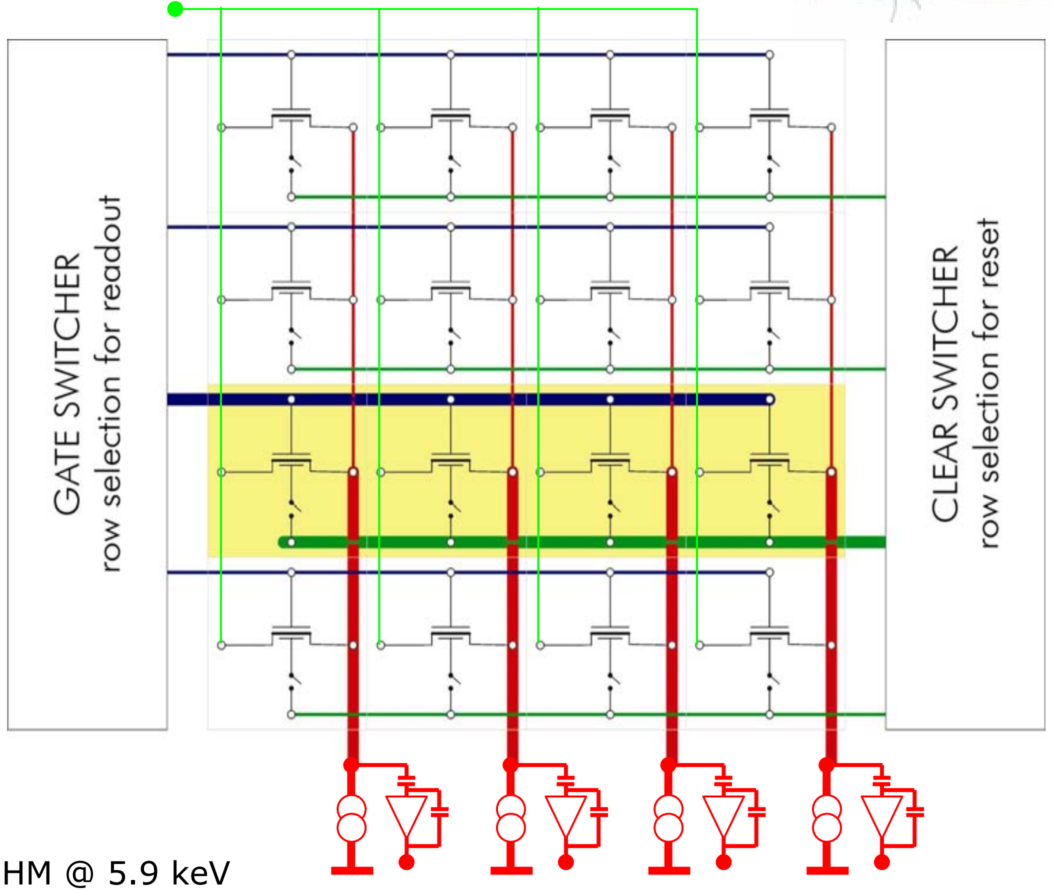

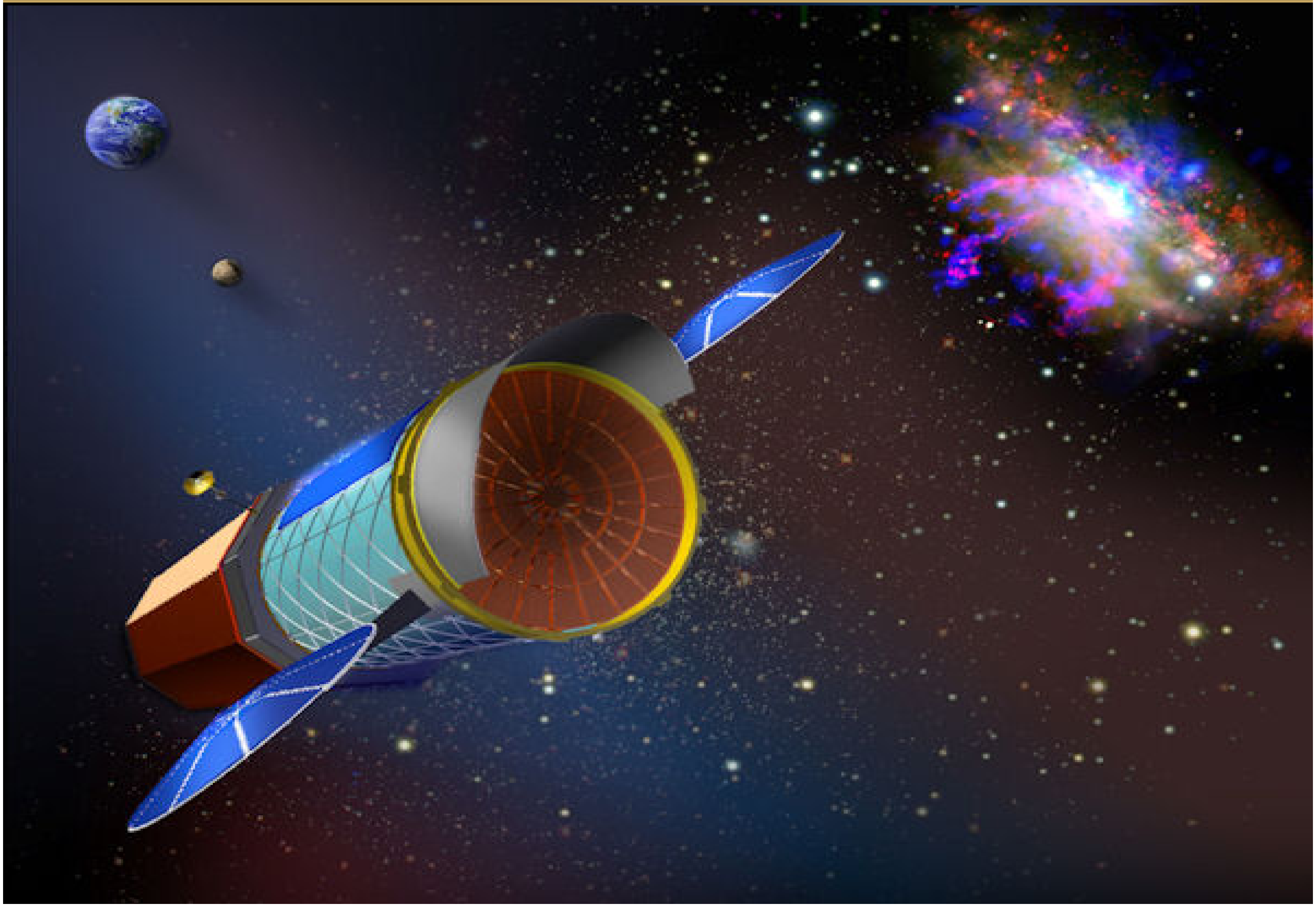

DEPFETs for the XEUS WFI

1. Flexible operating modes
2. low power dissipation (less than 2 W in 100 cm^2, DePFETs only)
3. Fano limited energy resolution from 0.5 keV to 30 keV
4. Spatial resolution better than 20 µm @ 100 µm pixel size
5. Homogeneous radiation entrance window
6. Intrinsic radiation hardness, no charge transfer needed
7. ENC was lowered to 0.2 e$^-$ rms with RNDR
8. Thin optical ``Blocking Filter´´ can be directly integrated
9. Operation at ``warm temperatures´´, e.g. – 40 ° C

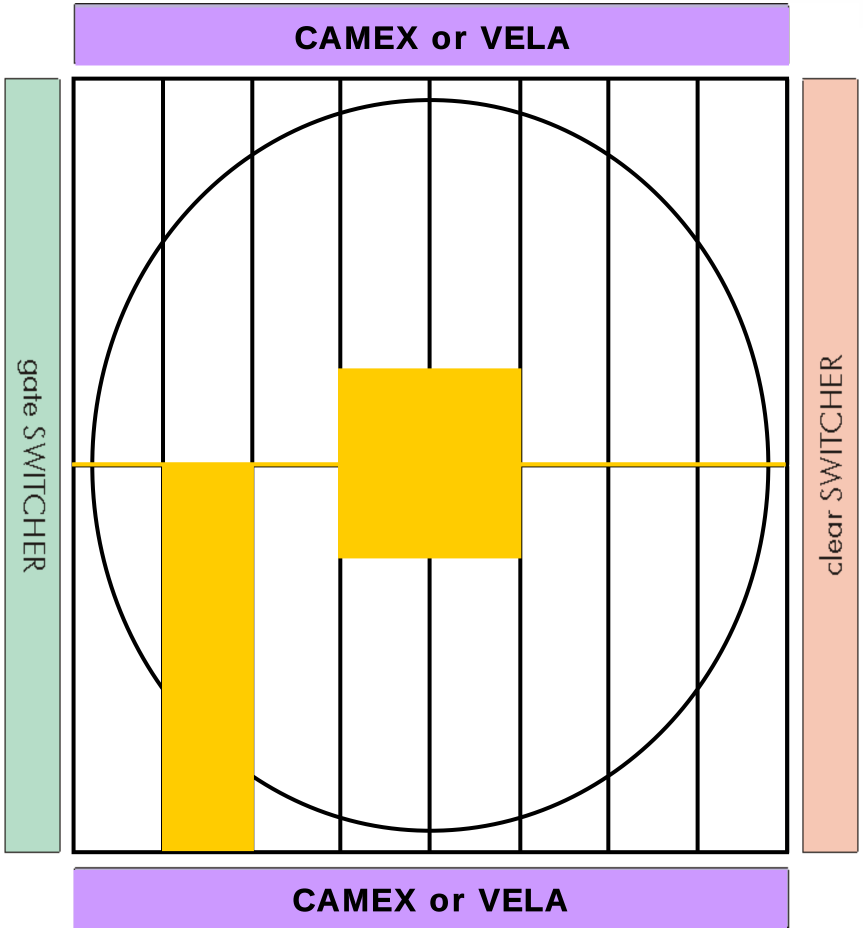

"Backside" illumination: Source on top of entrance window

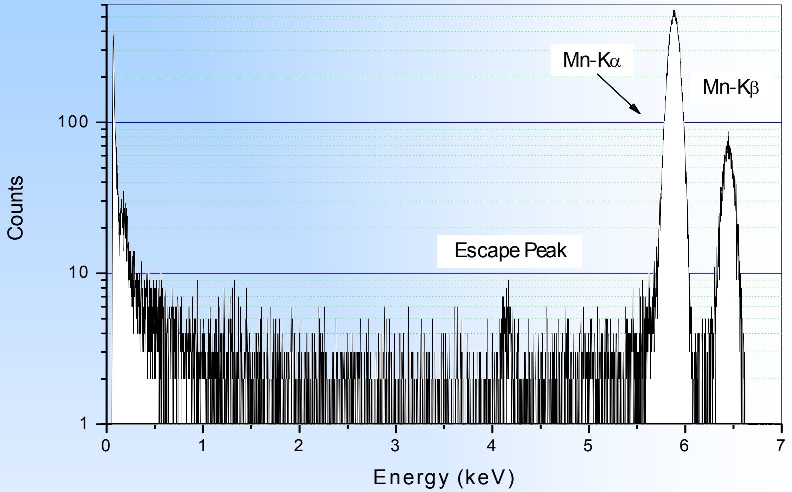

- timing

  2 µsec/row <-> 32 µsec/32x512 sensor

- room temperature

  220 eV FWHM @ 5.9 keV **(singles)**

- moderate cooling -40 °C

  127 eV FWHM @ 5.9 keV **(singles)**

  132 eV FWHM @ 5.9 keV **(all events)**

- extrinsic speed & resolution limitations

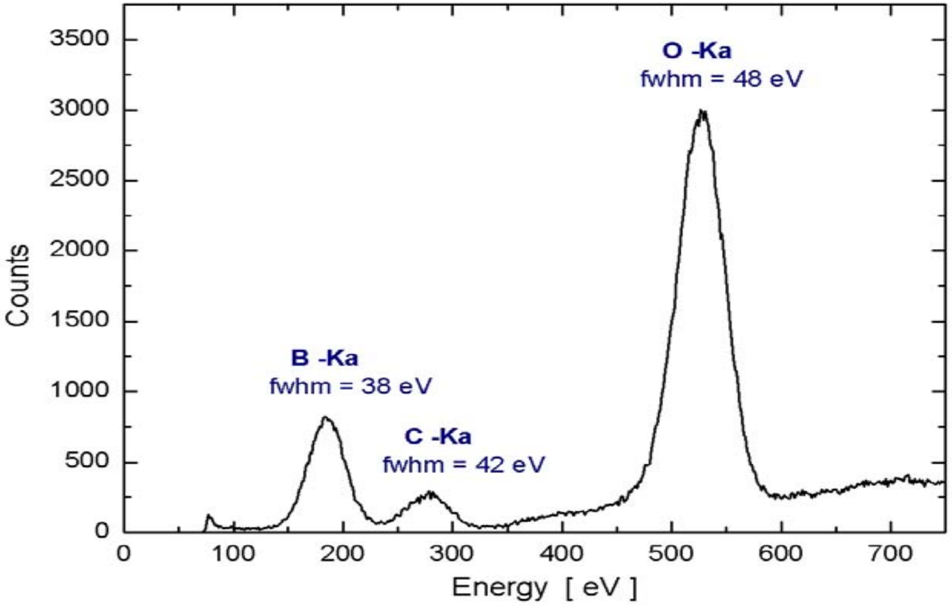

♦ **yield & homogeneity**

- defect pixels

  2 in 45 devices (> 10^6 pixels)

  pixel yield > 0.99999

- dispersions

  offset < 2 % (of Mn-Kα)

  gain < 5 %

  noise < 10 %

DEPFET APS – mesh experiment

◆ **method**

- irradiation through tilted periodic mesh
- Moire pattern
- X-ray interaction position with subpixel resolution

◆ **setup**

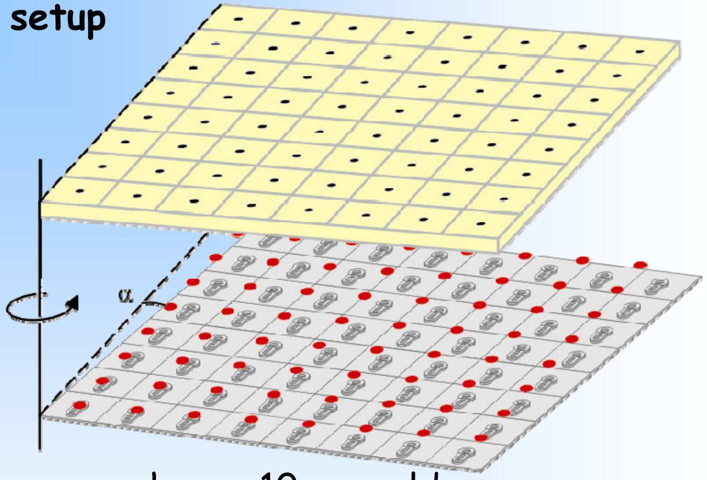

• mesh	10 µm gold 5 µm holes 150 µm pitch
• X-rays	Cr-K_α (5.4 keV)

◆ **example**

- variation of multiple pixel hit patterns with back contact voltage
- V_back =

-400 V

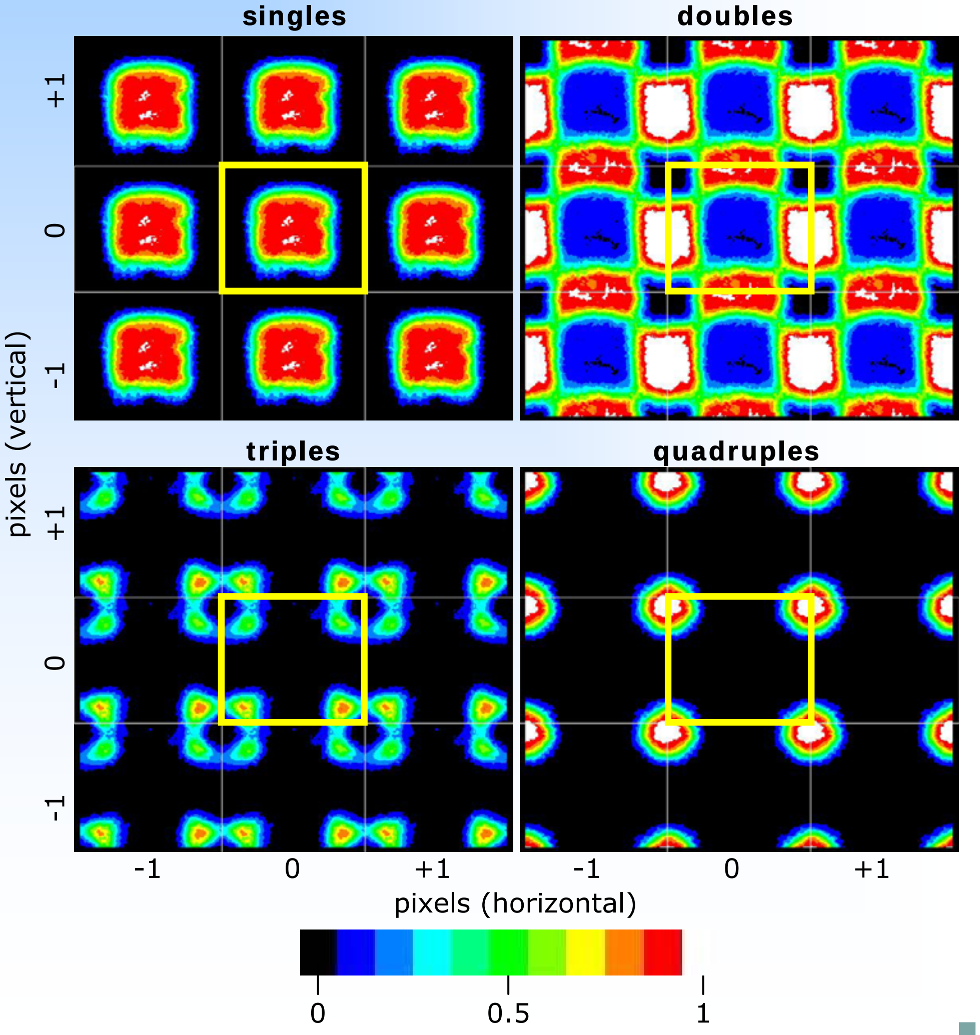

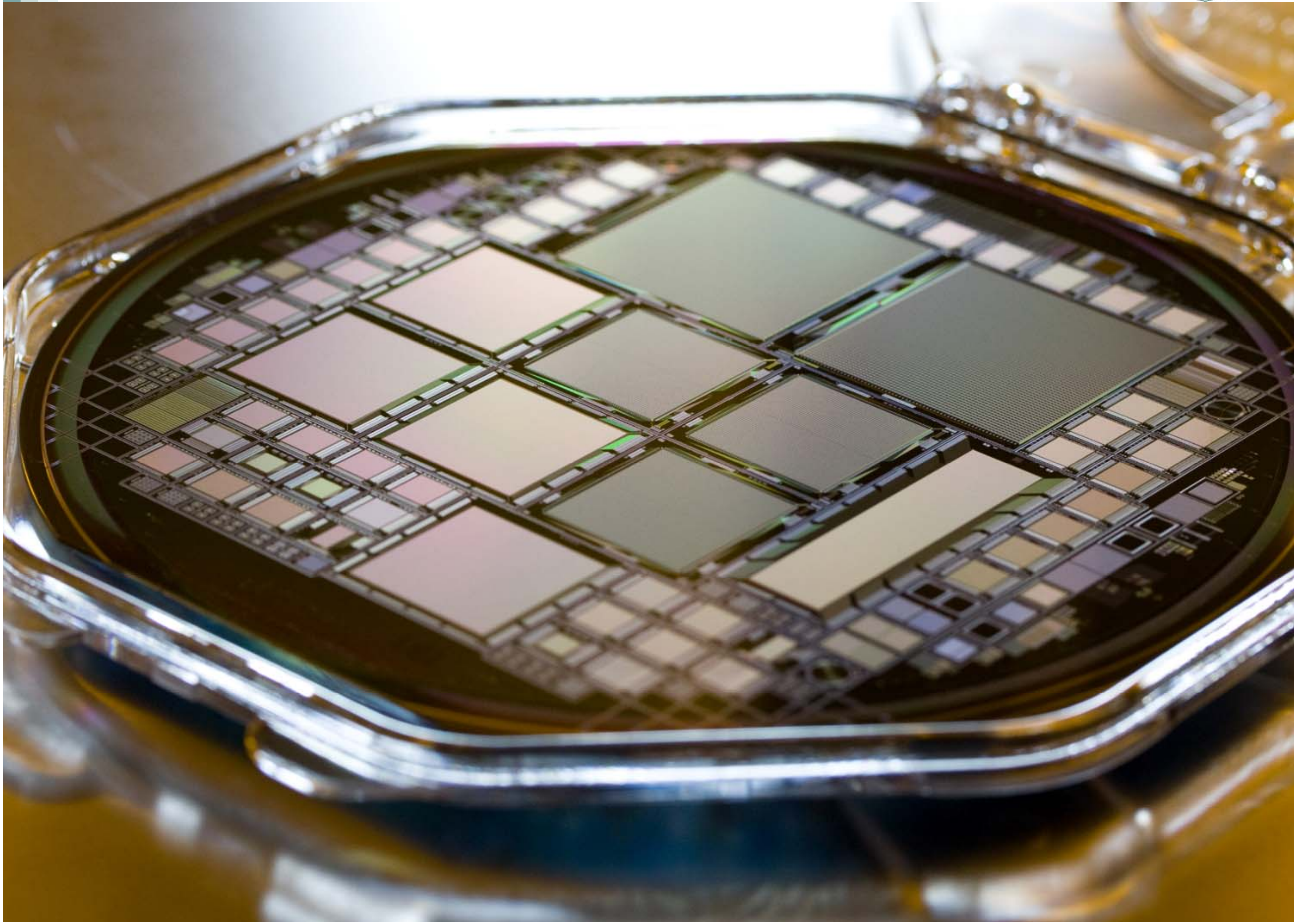

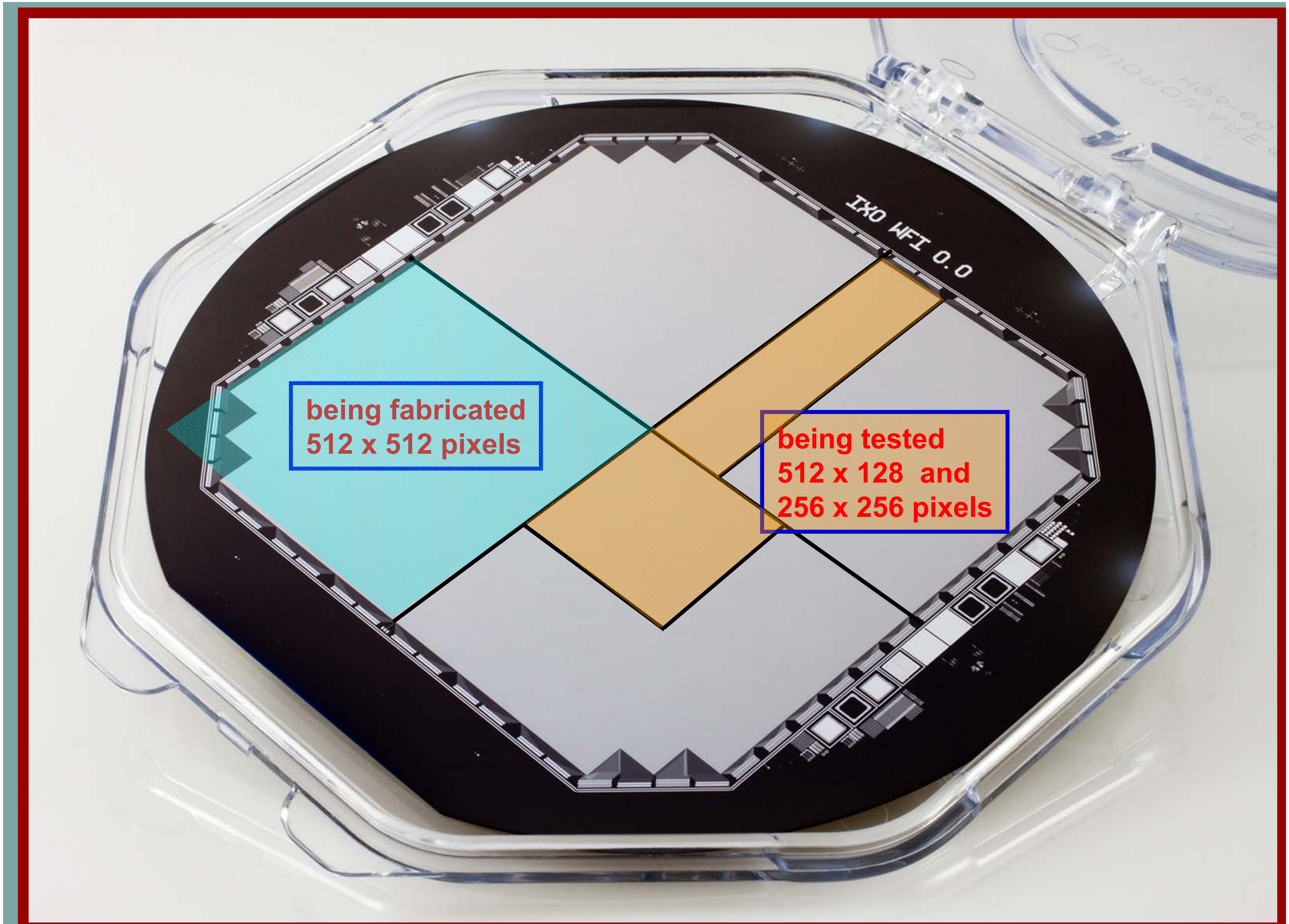

being fabricated
512 x 512 pixels

being tested
512 x 128 and
256 x 256 pixels

What is the challenge for Detectors @ XFEL

Time structure: difference with "others"

Electron bunch trains; up to 3000 bunches in 600 μsec, repeated 10 times per second.
Producing 100 fsec X-ray pulses (up to 30 000 bunches per second).

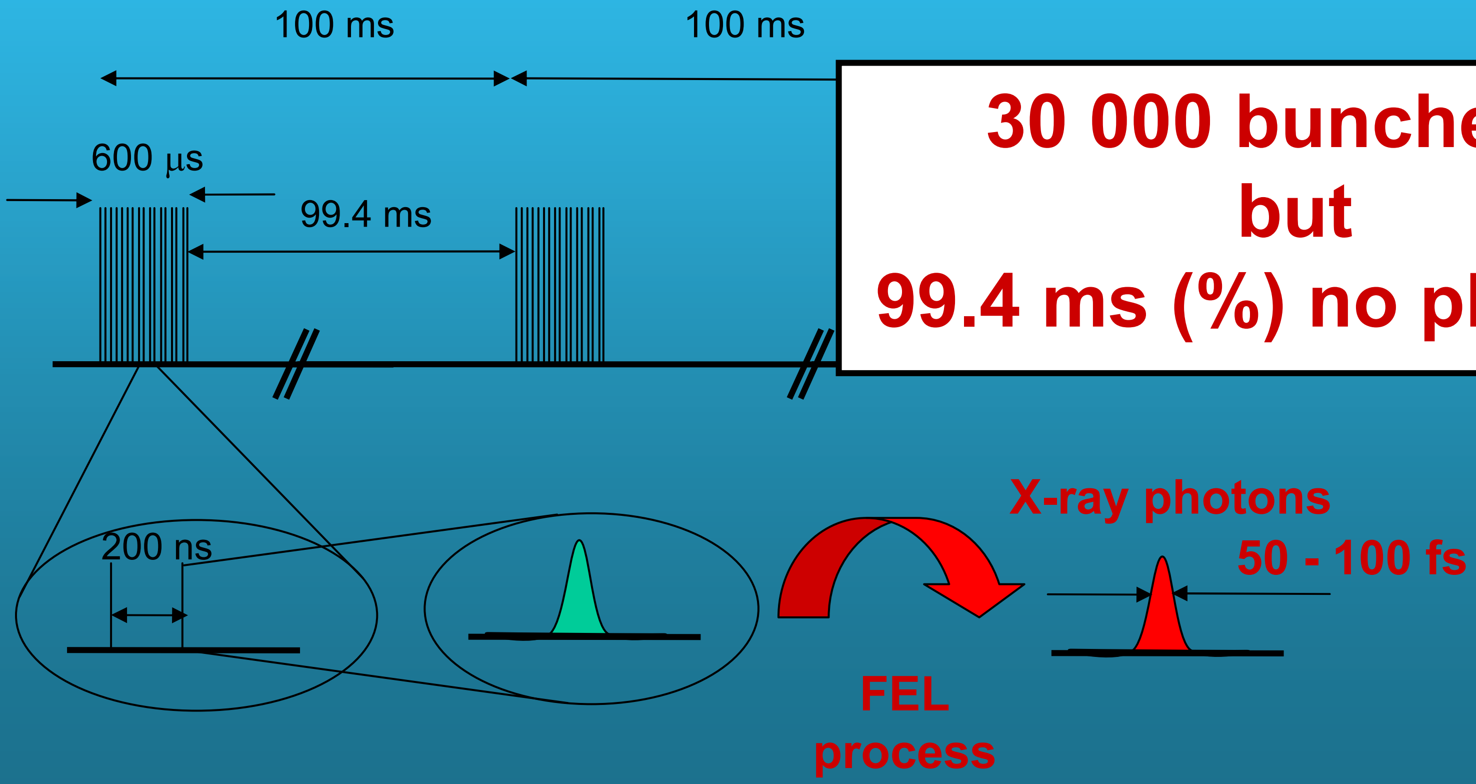

30 000 bunches/s
but
99.4 ms (%) no photons

DSSC - Expected Performance

Parameter	Expected DSSC performance
Energy range	0.5 … 25 keV (optimized for 0.5 … 4 keV)
Number of pixels	1024 x 1024
Sensor Pixel Shape	Hexagonal
Sensor Pixel pitch	~ 204 x 236 µm^2
Dynamic range / pixel / pulse	> 10.000 photons @1 keV
Resolution (S/N >5:1)	Single photon @ 1 keV (5 MHz) Single photon @ 0.5 keV (≤ 2.5 MHz)
Electronics noise	< 25 electrons r.m.s.
Frame rate	1-5 MHz
Stored frames per Macro bunch	≥ 512
Operating temperature	-10˚C optimum, RT possible

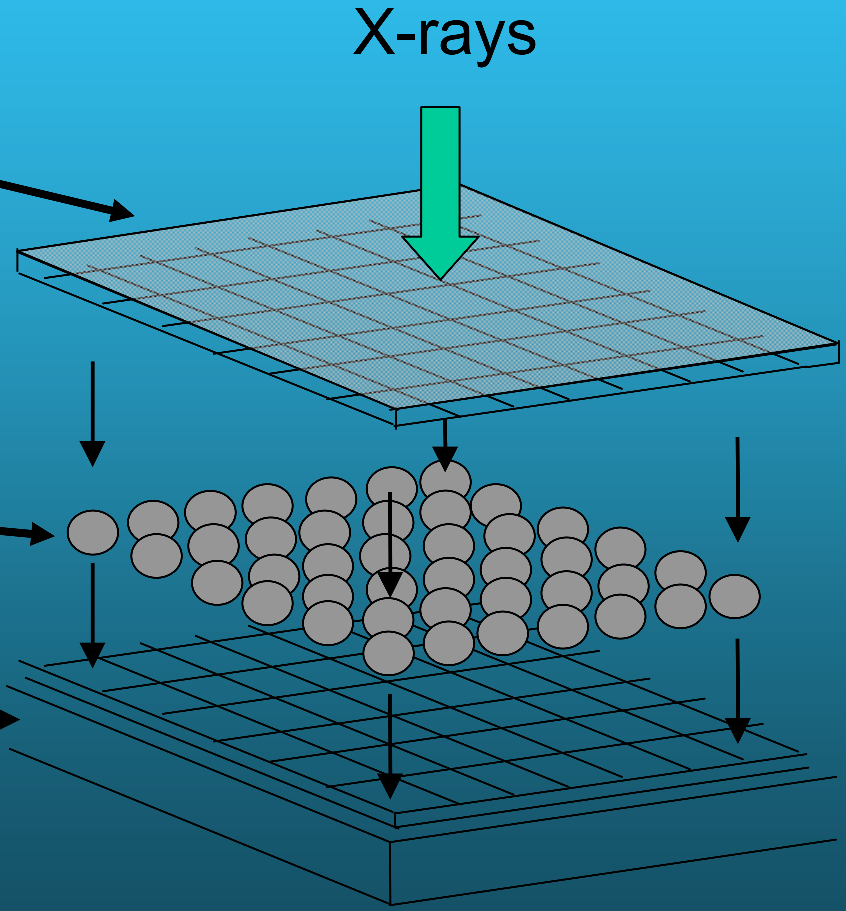

DePMOS Active Pixel Sensor

Connecting Bumps

- **1 per pixel**

CMOS Layer

- **Signal processing**
- **Signal storage & output**

DSSC - Concept

- DEPFET Active Pixel Sensor
- Every DEPFET pixel provides detection and amplification with:
  - **Low noise**
  - **Signal compression at the sensor level**
  - **High speed** (fully parallel readout at 1-5 MHz)

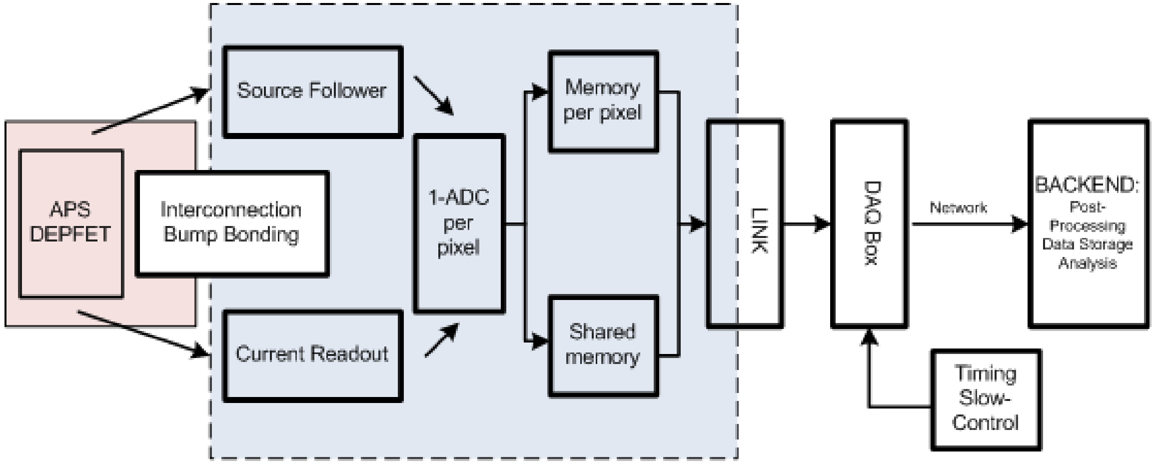

Non-Linear DEPFET Working Principle

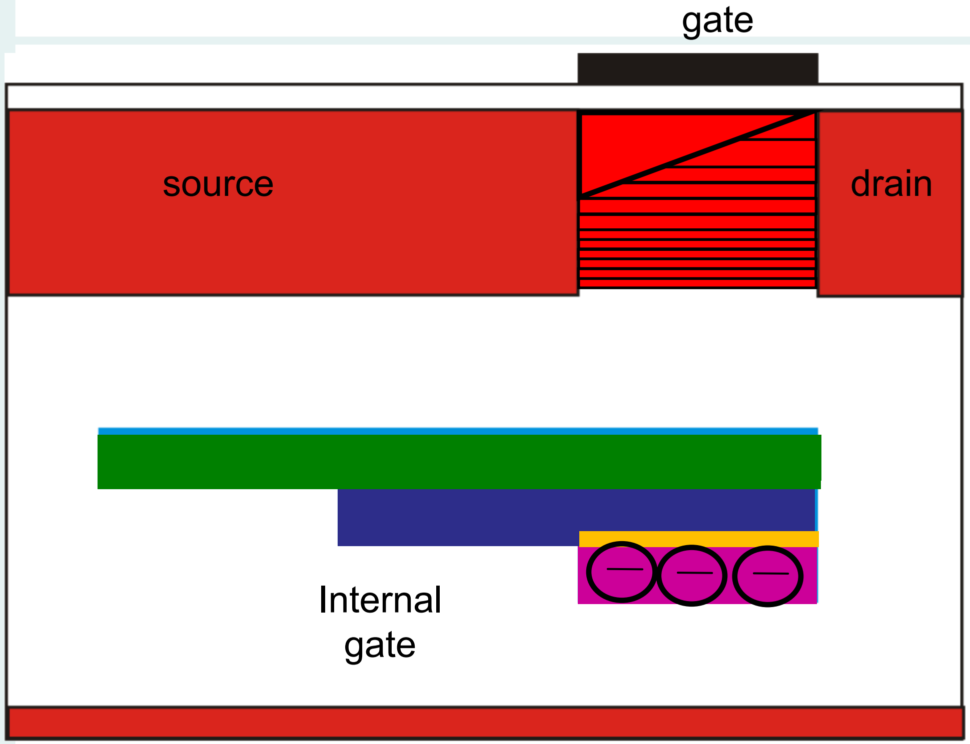

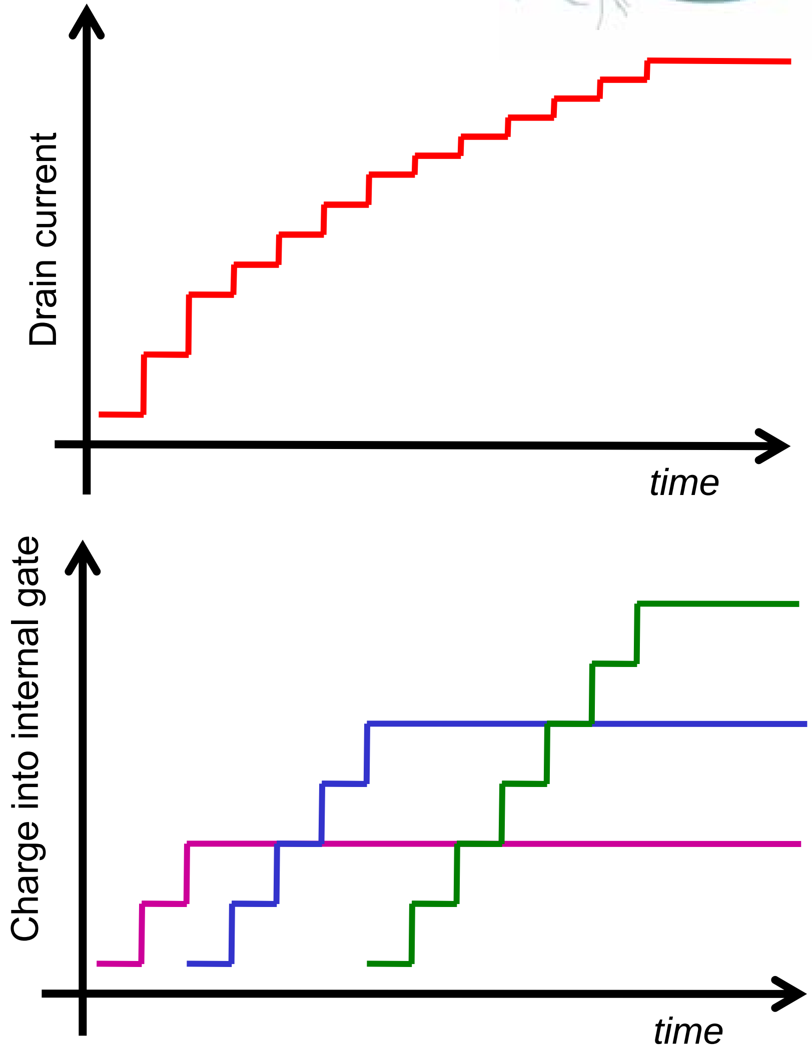

- The internal gate extends into the region below the source
- Small signals assemble below the channel, being fully effective in steering the transistor current
- Large signals spill over into the region below the source. They are less effective in steering the transistor current.

Mechanics - Focal Plane Overview

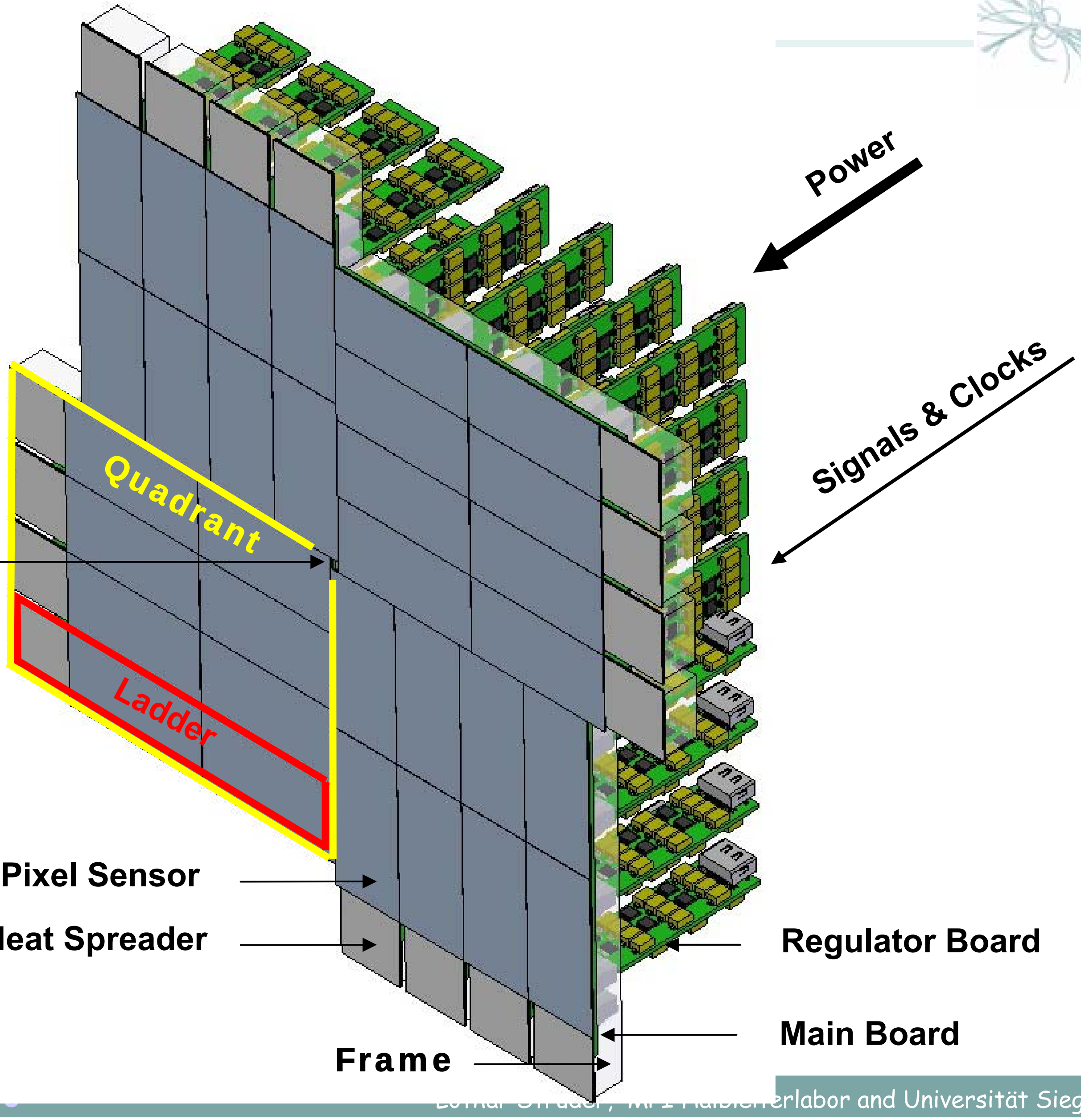

Power

Signals & Clocks

x-y Gap

128 x 256 Pixel Sensor

Heat Spreader

Regulator Board

Main Board

Frame

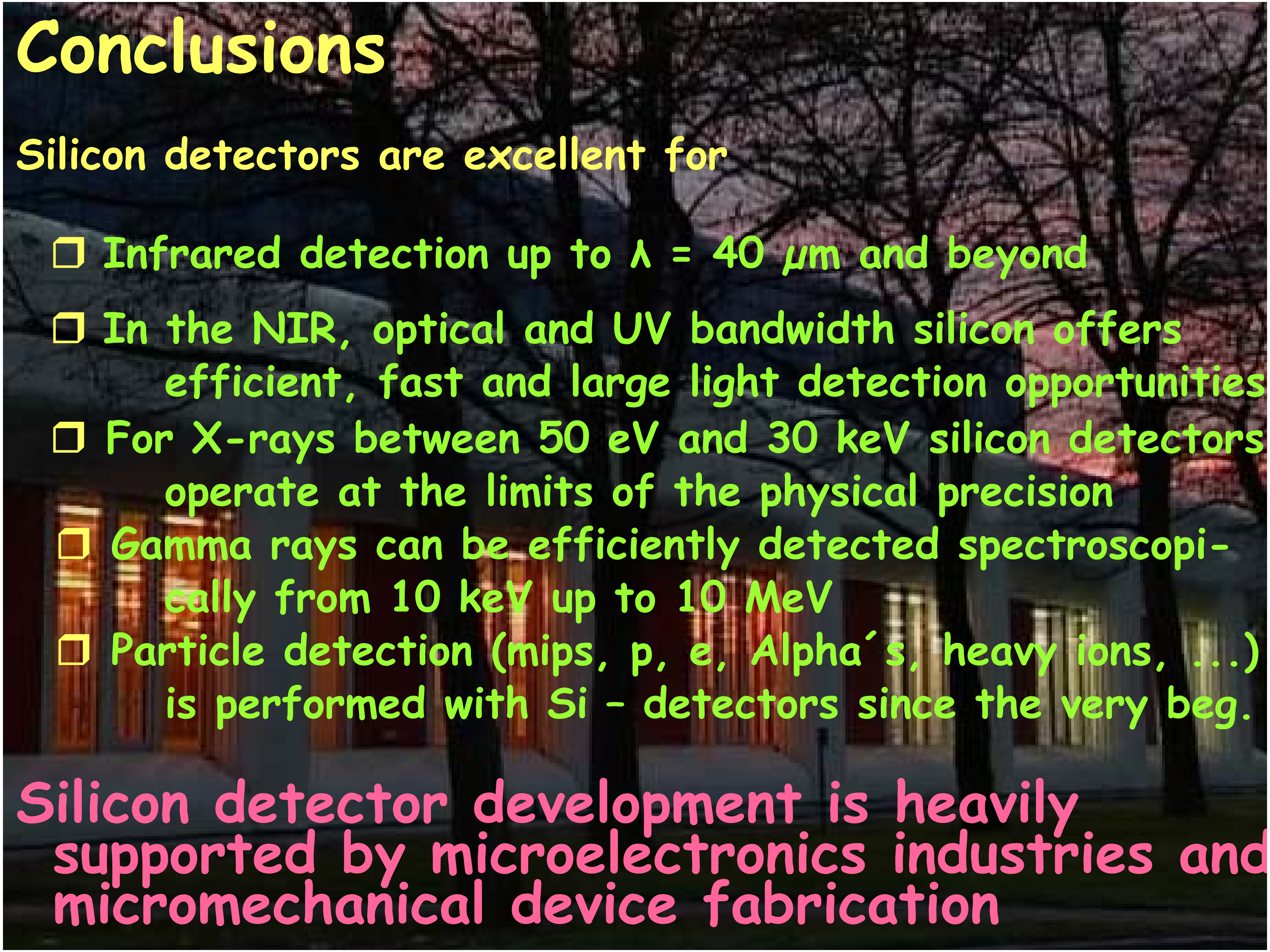

Conclusions

Silicon detectors are excellent for

- Infrared detection up to λ = 40 μm and beyond
- In the NIR, optical and UV bandwidth silicon offers efficient, fast and large light detection opportunities
- For X-rays between 50 eV and 30 keV silicon detectors operate at the limits of the physical precision
- Gamma rays can be efficiently detected spectroscopically from 10 keV up to 10 MeV
- Particle detection (mips, p, e, Alpha´s, heavy ions, ...) is performed with Si - detectors since the very beg.

Silicon detector development is heavily supported by microelectronics industries and micromechanical device fabrication

The MPI Semiconductor laboratory* at the SIEMENS Research Campus in Munich


*Halbleiterlabor

(Not) The End